

# Morphodynamics of estuarine navigation channel

Student: J.P. Tamboezer

Date: December 2002

Committee: prof.dr.ir. M.J.F. Stive (TU Delft, Section of Hydraulic Engineering)  
prof.ir. H. Ligteringen (TU Delft, Section of Hydraulic Engineering)  
dr.ir. J.A. Roelvink (WL I Delft Hydraulics)  
ir M.D. Groenewoud (Civil Engineering Division, Directorate-General of  
Public Works and Water Management)  
drs. P.J.T. Dankers (TU Delft, Section of Fluid Mechanics)

Education: Delft University of Technology  
Faculty of Civil Engineering and Geosciences  
Section of Hydraulic Engineering

picture front page: major and intermediate ports of India, [[www.mapsofindia.com](http://www.mapsofindia.com)].

## **Preface**

This study has been performed as a final thesis for the faculty of Civil Engineering and Geosciences at the Technical University of Delft. Research has been done into the morphological development of the Port of Kandla, India. A mathematical model was used to obtain insight into the morphodynamic effects of a proposed expansion plan for the port. The outcome of the study primarily deals with maintenance dredging in the approach channel to the port.

I would like to thank all the members of the graduation committee for their guidance and support. A special thanks goes out to Dano Roelvink for helping with the set up of the mathematical computational model Delft3D and professor Ligteringen for his expertise on the field of ports. Finally I would like to thank Martin Groenwoud, who kept a daily eye on the process in Utrecht.

Jasper Tamboezer  
December 2002

## Summary

The port of Kandla, which is situated in the north west of India and is subject to a large tidal variation of about 5 metres, is preparing a major expansion plan. The capacity of the harbour will be increased in two ways. Firstly the construction of several berths and jetties will allow more ships to be handled on a yearly basis. Secondly deepening of the harbour and its approaches will allow ships with a larger draught to call upon the port. It is this deepening that causes concern. The Kandla Port Trust (KPT) and the Central Water and Power Research Station (CWPRS) have calculated the amounts of cubic metres that will have to be dredged in order to raise the permissible draught from 10.7 to 14 metres. Especially the maintenance dredging poses a problem. KPT and CWPRS have calculated that between 90 and 111 million  $\text{m}^3$  have to be dredged annually to maintain the required depths. This is an increase by a factor 20 from the present 5 million  $\text{m}^3$ . The costs that accompany this huge increase of dredging exceeds the extra generated income by large.

As no details are known about the calculation methods of both KPT and CWPRS and the expected dredging amounts seem unrealistically high, a goal of this study is to simulate the future situation and determine the dredging amounts that will arise. A second goal is to determine the effects of training walls on the sedimentation in the approach channel, where the largest increase in maintenance dredging is expected. A process-based software package, Delft3D, developed by WLI Delft Hydraulics will be used to simulate the reality.

The set up and calibration of the model has led to mixed results. In Kandla Creek, where the port is situated, the flow velocities calculated by the model resemble the measured data quite good. In the area around the approach channel (Sogal Channel), the flow velocities are too low in comparison with reality. This has consequences for the morphodynamics in the region. The morphological development in Kandla Creek shows better results than the morphological activity in the shallower vicinity of the approach channel, where little to no morphological change has occurred.

The simulation of the future situation has led to the calculation of a significantly lower increase in maintenance dredging than found by KPT and CWPRS. Even though assumptions have been made the increase amounted to a more realistic magnitude of a factor 3. The costs that accompany this increase are significantly smaller than the extra income generated by the expansion. Implementing training walls to divert or contract the flow in order to decrease sedimentation by means of natural flushing of Sogal Channel will not be necessary from an economical point of view. The simulation of a few training wall layouts however has been done to obtain insight in the morphological development of the approach channel.

The first concept consists of a wall in line with the main flow direction. The idea is to guide the flow more into the main channel creating more natural flushing and stabilising the channel in its present position. The effect of this proposal however is negligible, as the main flow isn't deflected enough. The flow velocity in the bend of the channel is increased only marginally, especially in the creek outfall. The extra erosion in that area isn't beneficial as the depth is large enough already. In order for this concept to be more effective a larger portion of the flow (both ebb and flood) needs to be directed into the channel and therefore the training wall has to be less in line with the existing flow direction. The model has to be adjusted to create a different alignment of the wall.

The other two concepts block a part of the flow and only allow water to flow through the channel. This is done by implementing training walls perpendicular to the flow direction. The first of these concepts consists of a staggered wall, which does not block the flow completely. Water is able to flow through the wall, albeit that the flow is severely hindered. The second

layout blocks the flow completely and all of the water is directed through the channel. Both concepts have a favourable effect on the morphological development of the bend in the channel, which becomes subject to erosion. The problem however is shifted towards other parts of the approach channel, which become subject to sedimentation. The effect is roughly twice as large in case of total blockage than in case of the staggered training wall. The impact of these proposals is very severe. The rate of morphological change is very high as the present hydrodynamic situation is gravely affected. It is not clear what the effect will be in the long run.

The results of the simulations have to be interpreted cautiously. In the process of modelling assumptions have been made. A few of these assumptions had to be made due to a shortage of data, while others have been made in order to simplify the problem so that it could be dealt within the scope of this study. The quantitative results cannot serve as a basis on which conclusions are formulated. A qualitative analysis however is possible, which can be found in this report.

The overall conclusion of this study is that the best way to enlarge and maintain the maximum permissible draught is to increase dredging. The extra costs of the increase in maintenance dredging weighs up to the extra-generated income. Furthermore the impact of the different training walls is too severe and the uncertainties that accompany this impact in the long run are too plentiful.



# Contents

<b>List of figures .....</b>	<b>vi</b>
<b>List of tables .....</b>	<b>viii</b>
<b>List of symbols .....</b>	<b>ix</b>
<b>Abbreviations .....</b>	<b>xi</b>
<b>1 Problem description .....</b>	<b>1</b>
1.1 Introduction.....	1
1.2 Goal of study .....	2
1.3 Structure of report .....	3
<b>2 Development of the port .....</b>	<b>5</b>
2.1 Current situation.....	5
2.2 Future situation.....	6
2.3 Outline of costs .....	8
<b>3 Sediment transport .....</b>	<b>9</b>
3.1 Introduction.....	9
3.2 Current induced transport.....	9
<b>4 Data.....</b>	<b>11</b>
4.1 Introduction.....	11
4.2 FLOW boundary conditions .....	11
4.3 Morphological development .....	12
<b>5 Description Delft3D .....</b>	<b>15</b>
5.1 Introduction.....	15
5.2 Delft3D-FLOW .....	16
5.3 Delft3D-TRAN .....	18
5.4 Delft3D-BOTT .....	20
5.5 Delft3D-MOR.....	21
<b>6 Model set-up.....</b>	<b>23</b>
6.1 Introduction.....	23
6.2 Delft-RGFGRID.....	23
6.3 Delft-QUICKIN .....	25
6.4 Delft3D-FLOW .....	26
6.5 Delft3D-TRAN/BOTT .....	29
6.6 Delft3D-MOR.....	31
<b>7 Calibration.....</b>	<b>33</b>
7.1 Introduction.....	33
7.2 Parameters.....	33
7.3 Results.....	34
7.4 Overall findings .....	44

---

<b>8</b>	<b>Simulation runs .....</b>	<b>47</b>
8.1	Introduction.....	47
8.2	Future situation.....	47
8.3	Concept 1.....	50
8.4	Concept 2.....	52
8.5	Concept 3.....	55
8.6	Overall findings .....	57
<b>9</b>	<b>Conclusions and recommendations.....</b>	<b>59</b>
	<b>References .....</b>	<b>I</b>
	<b>Annexes .....</b>	<b>II</b>
	<b>Annex A.....</b>	<b>A</b>
	<b>Annex B .....</b>	<b>B</b>
	<b>Annex C .....</b>	<b>C</b>
	<b>Annex D.....</b>	<b>D</b>
	<b>Annex E .....</b>	<b>E</b>
	<b>Annex F .....</b>	<b>F</b>
	<b>Annex G.....</b>	<b>G</b>
	<b>Annex H.....</b>	<b>H</b>
	<b>Annex I .....</b>	<b>I</b>
	<b>Annex J .....</b>	<b>J</b>

# List of figures

Figure 1-1 Geographical location.....	1
Figure 1-2 Port layout.....	2
Figure 2-1 Sogal Channel.....	5
Figure 2-2 Lateral flow.....	8
Figure 2-3 Training works.....	8
Figure 3-1 Velocity and concentration profile.....	10
Figure 4-1 Water level and velocity measurements at buoy 4 and point 3.....	11
Figure 4-2 Sedimentation/erosion.....	12
Figure 4-3 General cargo area.....	12
Figure 4-4 Jetty area.....	12
Figure 4-5 Four zones of Sogal Channel.....	13
Figure 4-6 Development Sogal Channel.....	13
Figure 5-1 Medium term morphological model.....	15
Figure 5-2 Staggered grid.....	17
Figure 5-3 Continuity correction.....	21
Figure 6-1 ASCII-type lbd-file.....	24
Figure 6-2 Landboundary.....	24
Figure 6-3 Splines drawn by user.....	24
Figure 6-4 Splines into grid.....	24
Figure 6-5 Manipulated grid.....	24
Figure 6-6 Samples.....	25
Figure 6-7 Depth points.....	25
Figure 6-8 3D view of (part of) bathymetry.....	25
Figure 6-9 Mixed tide.....	26
Figure 6-10 Measurements northern boundary.....	27
Figure 6-11 Locations in model area.....	28
Figure 6-12 Buoy 6 compared.....	28
Figure 6-13 Dredging scenario 2.....	30
Figure 6-14 Process tree Delft3D-MOR.....	31
Figure 6-15 Adaptation time.....	32
Figure 7-1 Areas of comparison.....	34
Figure 7-2 Residual bed load transport, combinations 4, 5 and 6.....	34
Figure 7-3 Residual suspended transport, combinations 4, 5 and 6.....	35
Figure 7-4 Sedimentation/erosion pattern, combinations 4, 5 and 6.....	35
Figure 7-5 Weekly sedimentation in channel area, combinations 4, 5 and 6.....	36
Figure 7-6 Areas of comparison.....	36
Figure 7-7 Sediment concentrations, combinations 19, 22 and 25.....	37
Figure 7-8 Residual suspended transport, combinations 19, 22 and 25.....	37
Figure 7-9 Weekly erosion in berths area, combinations 19, 22 and 25.....	38
Figure 7-10 Areas of comparison.....	38
Figure 7-11 Residual suspended transport, combinations 28, 31 and 34.....	39
Figure 7-12 Weekly erosion in berths area, combinations 28, 31 and 34.....	39
Figure 7-13 Sedimentation/erosion pattern and residual suspended transport, no. 22.....	40
Figure 7-14 Sedimentation/erosion pattern and residual suspended transport, no. 28.....	40
Figure 7-15 Areas of comparison.....	41
Figure 7-16 Sediment concentration 4 and 22.....	41
Figure 7-17 Sediment concentration 12 and 30.....	41
Figure 7-18 Different patterns 0.01 m, 4 and 22.....	42
Figure 7-19 Different patterns 0.05 m, 12 and 30.....	42
Figure 7-20 Monthly development, combination 26.....	42
Figure 7-21 development average depth.....	42
Figure 7-22 Initial depth jetty.....	43
Figure 7-23 Manipulated depth.....	43
Figure 7-24 Location areas.....	45

Figure 8-1 Required depth future situation.....	47
Figure 8-2 Areas of comparison .....	47
Figure 8-3 Residual transport and sed/ero pattern future situation.....	49
Figure 8-4 Training wall concept 1.....	50
Figure 8-5 Comparison flow velocity concept 1.....	50
Figure 8-6 Residual suspended transport initial situation .....	51
Figure 8-7 Sedimentation/erosion pattern concept 1 .....	51
Figure 8-8 Residual suspended transport concept 1 .....	51
Figure 8-9 Training wall concept 2.....	52
Figure 8-10 Sediment concentration initial and concept 2 .....	52
Figure 8-11 Comparison flow velocity concept 2.....	53
Figure 8-12 Areas of comparison .....	53
Figure 8-13 Residual suspended transport initial situation .....	54
Figure 8-14 Sedimentation/erosion pattern concept 2 .....	54
Figure 8-15 Residual suspended transport concept 2 .....	54
Figure 8-16 Training wall concept 3.....	55
Figure 8-17 Comparison flow velocity concept 3.....	55
Figure 8-18 Areas of comparison .....	56
Figure 8-19 Residual suspended transport initial situation .....	57
Figure 8-20 Sedimentation/erosion pattern concept 3 .....	57
Figure 8-21 Residual suspended transport concept 3 .....	57
Figure 8-22 Closed boundary over shoals.....	58

## List of tables

Table 2-1 Cargo forecast .....	6
Table 2-2 Calculation of income.....	6
Table 2-3 Total income '99-'00 .....	7
Table 2-4 Income 2010 .....	7
Table 2-5 Expected dredging quantities .....	8
Table 2-6 Outline of costs.....	8
 Table 4-1 Erosion/sedimentation quantities.....	 12
Table 5-1 Sediment transport formulas .....	18
 Table 6-1 Coordinate locations.....	 28
Table 6-2 In/efflux mixed tide.....	28
 Table 7-1 Combinations.....	 33
Table 7-2 Sed/ero quantities 4,5,6.....	34
Table 7-3 Sed/ero quantities 19,22,25.....	36
Table 7-4 Sed/ero quantities 28,31,34.....	38
Table 7-5 Sed/ero quantities 22, 28.....	39
Table 7-6 Sed/ero quantities 4,12,22,30.....	41
Table 7-7 Difference in terms of percentage.....	43
Table 7-8 Sed/ero quantities for manipulated depth .....	44
Table 7-9 Morphological development of current situation .....	45
 Table 8-1 Expected morphological development.....	 48
Table 8-2 Dredging quantities future situation .....	49
Table 8-3 Morphological development concept 1.....	51
Table 8-4 Morphological development concept 2.....	53
Table 8-5 Morphological development concept 3.....	56

## List of symbols

$A_i$	= amplitude	[m]
$c$	= sediment concentration (volume%)	[-]
$c'$	= constant value [= $C^2c/(2g)$ ]	[-]
$c_a$	= (reference) concentration at level $z = a$	[m <sup>3</sup> /m <sup>3</sup> ]
$c_s$	= depth averaged sediment concentration	[m <sup>3</sup> /m <sup>2</sup> ]
$c_{se}$	= equilibrium concentration of suspended sediment	[m <sup>3</sup> /m <sup>3</sup> ]
$c(z)$	= local, time averaged concentration at level $z$ above the bed	[m <sup>3</sup> /m <sup>3</sup> ]
$C$	= Chézy coefficient	[m <sup>1/2</sup> /s]
$C_{2D}$	= two dimensional Chézy coefficient	[m <sup>1/2</sup> /s]
$d$	= depth below reference plane	[m]
$D$	= representative particle diameter (generally $D_{50}$ )	[m]
$D_{50}$	= sediment diameter for which 50 % of the grains are smaller	[m]
$D_{90}$	= sediment diameter for which 90 % of the grains are smaller	[m]
$D_x, D_y$	= dispersion coefficient x,y-direction	[m <sup>2</sup> /s]
$F_{x,y}$	= x and y component of external forces	[kg/ms <sup>2</sup> ]
$K_{x,y}$	= x and y viscosity components	[m]
$h$	= local water depth	[m]
$H$	= total local water depth	[m]
$n$	= Manning coefficient	[s/m <sup>1/3</sup> ]
$N$	= number of frequency components	[-]
$S_{...}$	= $S_{b\xi}, S_{b\eta}, S_{s\xi}, S_{s\eta}$ for TTXA, TTYA, TTXSA and TTYSA	
$S_{bx,sx}$	= sediment transport components x-direction	[m <sup>3</sup> /s/m]
$S_{by,sy}$	= sediment transport components y-direction	[m <sup>3</sup> /s/m]
$T_s$	= adaptation time for vertical sediment concentration profile	[s]
$TT...A$	= TTXA, TTYA for time averaged bed transport in x,y-direction	[m <sup>3</sup> /s]
$TT...A$	= TTXSA, TTYSA for time averaged suspended transport in x,y-direction	[m <sup>3</sup> /s]
$u$	= depth averaged velocity in x-direction	[m/s]
$U$	= magnitude of total velocity ( $U = (u^2+v^2)^{1/2}$ )	[m/s]
$v$	= depth averaged velocity in y-direction	[m/s]
$v(z)$	= local, time averaged velocity at level $z$ above the bed	[m/s]
$w$	= fall velocity of the sediment particles	[m/s]
$w_e$	= effective fall velocity	[m/s]
$z$	= height above the bed	[m]
$z_a$	= bed level	[m]

$\alpha$	= coefficient (2.3 for low to 4.6 for high Reynolds numbers)	[-]
$\alpha_{bs}$	= coefficient, specified by user	[-]
$\alpha_{nn}$	= the stability coefficient	[-]
$\beta$	= a factor describing the difference in the diffusion of a discrete sediment particle from the diffusion of a fluid 'particle'	[-]
$\varepsilon_f$	= fluid diffusion coefficient	[m <sup>2</sup> /s]
$\varepsilon_{por}$	= bed porosity	[-]
$\varepsilon_s(z)$	= diffusion coefficient for sediment	[m <sup>2</sup> /s]
$\eta$	= instantaneous water elevation	[m]
$\eta$	= free surface elevation above reference plane	[m]
$\nu$	= cinematic viscosity coefficient	[m <sup>2</sup> /s]
$\zeta_c$	= bottom roughness height	[m]
$\rho$	= mass density of fluid	[kg/m <sup>3</sup> ]
$\rho_s$	= mass density of sediment	[kg/m <sup>3</sup> ]
$\rho_w$	= mass density water	[kg/m <sup>3</sup> ]
$\tau_c$	= bottom shear stress	[N/m <sup>2</sup> ]
$\tau(z)$	= shear stress at level z above bed	[N/m <sup>2</sup> ]
$\varphi$	= a factor expressing the damping of the fluid turbulence caused by the sediment concentration	[-]
$\varphi_i$	= phase	[degrees]
$\omega_i$	= frequency	[degrees/hour]

## Abbreviations

ADI	= Alternating Direction Implicit
bln	= billion ( $10^9$ )
cum	= cubic metre
CD	= Chart Datum (MSL –3,884 m)
CWPRS	= Central Water and Power Research Station
DCI	= Dredging Corporation of India
DWT	= Dead Weight Tonnage
IPA	= Indian Port Association
KPT	= Kandla Port Trust
mln	= million ( $10^6$ )
MSL	= Mean Sea Level
NEI	= Netherlands Economic Institute
PIANC	= International Navigation Association
ppm	= parts per million
ppt	= parts per tonne
SBM	= Single Buoy Mooring
VLCC	= Very Large Crude Carrier
ULCC	= Ultra Large Crude Carrier
UTM	= Universal Transverse Mercator



# 1 Problem description

## 1.1 Introduction

### Geographical location

The port of Kandla is situated in the Kandla creek, which is a part of the Kandla-Hansthal creek system. This complicated creek system lies at the north eastern end of the Gulf of Kachchh, along the north western coast of India (see figure 1-1). The width at the entrance is about 50 kilometres with a maximum depth of 58 metres. The width and depth gradually reduce to the eastern end of the gulf. The port is situated about 140 km from the Arabian Sea in protected waters, along the western bank of the Kandla Creek. The Kandla Creek runs through tidal flats, Khengarji Bet to the west and Sathsaida Bet to the east, which get submerged during the higher waters of spring tide by about 1 meter.

Kandla port has the following coordinates: latitude:  $23^{\circ} 01' N$   
longitude:  $70^{\circ} 13' E$

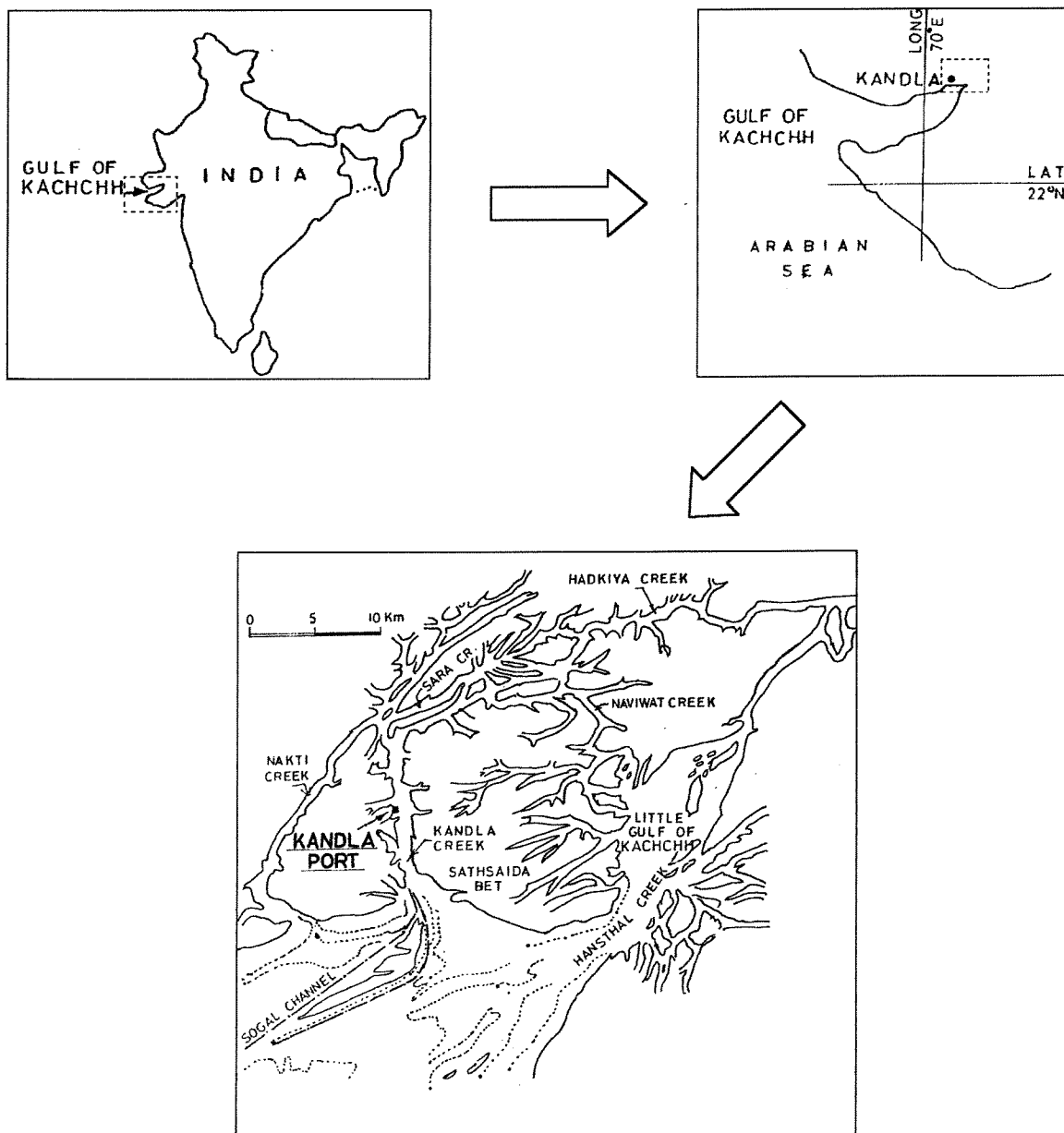


Figure 1-1 Geographical location

### History

Development of Kandla Port started in the 1930's as a port with a jetty located in the creek with 9.14 m as maximum permissible draught. Due to the partition of Karachi Port to Pakistan in 1947, Kandla was selected for development as a major port of India to cater the north western part of India as its hinterland. The jetty was converted to an oil jetty with infrastructure facilities and Kandla was declared a major port on April 8<sup>th</sup>, 1955. Since then the port has grown considerably achieving high ranking amongst the 11 major ports of India. The infrastructural facilities have been housed on reclamation areas along the west bank on Khengarji Bet. Though the natural depths in Kandla Creek are stable, the depths in the approaches are not stable due to the dynamic presence of shoals and bars. About five different channels are used since the first development stages of the port; the present channel used is Sogal Channel, which is maintained at 5.5 m below Chart Datum (CD = MSL -3.884 m).

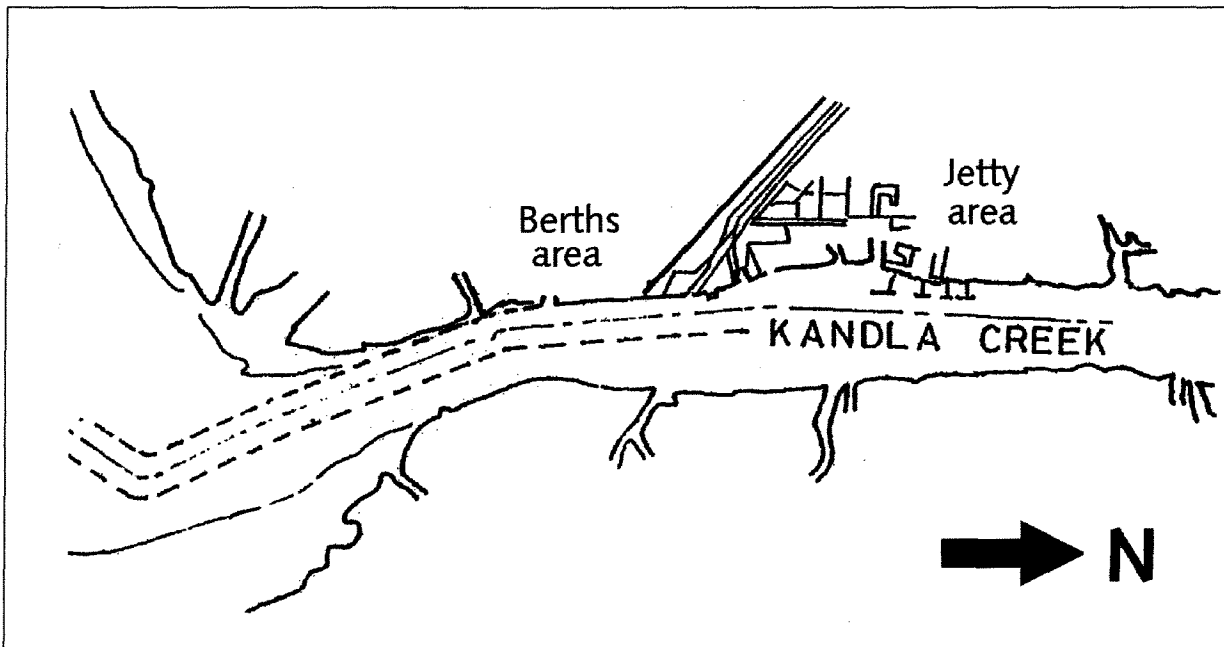


Figure 1-2 Port layout

### 1.2 Goal of study

The Kandla Port Trust is preparing major expansion of the harbour. The objective is to allow post Panamax vessels to enter the port. Sogal Channel will have to be deepened from 5.5 to 8.0 metres below Chart Datum and Kandla Creek will have to be deepened from 10.7 to 14.2 metres below CD. The amount of maintenance dredging is expected to increase dramatically; from 5 mln cum/year currently to about 90 to 111 mln cum/year in the future situation. These figures have been calculated by the Central Water and Power Research Station (CWPRS) and Kandla Port Trust (KPT) [1999]. The costs for maintaining the desired depth in the harbour and its approach channel are much higher than the extra income generated by the increase in annual turnover. It seems economically not feasible to deepen Sogal Channel and Kandla Creek.

The goal of this study is twofold:

- The first goal of this study is to simulate the current situation and the future situation after deepening of Sogal Channel and Kandla Creek and to validate the occurring and determine the expected dredging quantities.
- The second goal is to determine the effect of possible technical solutions (i.e. applying training wall) on the sedimentation of Sogal Channel.

The process-based software package Delft3D will be used to achieve the goals. The results will consist of data calculated with the model. Velocities of flow, directions of flow, concentrations of sediment, rate of siltation and morphological changes will be the outcome of interpreting the data. These quantities will give insight into the effectiveness of the proposed technical solutions.

### 1.3 Structure of report

In chapter 2 a more detailed analysis is made of the port and its expansion plans. Especially the cargo forecast will be highlighted as well as the influence on the dredging activities. Chapter 3 explains the basic process of sediment transport due to currents. In chapter 4 the available measured data that are useful as input for the model will be analysed. The theoretical background of the simulation programme Delft3D is explained in chapter 5. The governing equations as well as the mathematical computational method are described. Chapter 6 handles the set-up of the model. The hydrodynamic part is set up and calibrated, before the morphodynamic part is constructed. A more elaborate calibration of the morphodynamic part of the model is done in chapter 7. A sensitivity analysis is made for a few parameters and the eventual settings will be determined. Chapter 8 consists of the different simulation runs that were made. The current situation and the future situation after deepening are simulated apart from three concepts that imply different training walls. The conclusions of this study are finally presented in chapter 9. A few recommendations that could improve the results are also presented in this chapter.

## 2 Development of the port

### 2.1 Current situation

#### hydrodynamic conditions

A semidiurnal tide prevails in the creek system. The tidal range varies from 3 to 7 m for neap and spring tide, with an average of 5 m. No wave protection is required; even during the southwest monsoon season no severe wave climate occurs in the approach channel to the harbour. The flow in the Kandla creek is generally uniform and quite strong with velocities in the magnitude of 1.0 m/s. The creek is subjected to large-scale sediment movements. Concentrations of sediment flows can be as high as 1000 ppm. Due to the connection of the different creeks the efflux during ebb is about 20% higher than the influx during flood. This efflux is canalised along the Sogal Channel and causes some natural flushing of sediment towards downstream reaches. Rainfall is very scanty in the arid Kandla region and therefore the freshwater discharge is negligible. The salinity of the water is generally around 32 ppt. Considering these aspects the influence of density currents on the sedimentation processes can be considered to be of no significance [CWPRS, 2001].

#### cargo handling

The main features of the port are 10 general cargo berths and 6 liquid bulk jetties. In the helicopter assessment [NEI Transport, 2001] about commodity analysis and cargo forecast the smaller ports in the Gujarat region have been surveyed in detail. Figures involving the port of Kandla seem to be a rough estimate and detailed descriptions are not given. According to this report the port of Kandla handled 40 mln tonnes of cargo in 1999-2000, which includes 16 mln ton of crude oil pumped through two SBMs at Vadinar. These SBMs are located in deeper water about 70 km southwest of Kandla, where draughts of 20 metres are permissible. About 1850 ships called on Kandla, with an average of 21.700 DWT.

#### dredging activities

Maintenance dredging in front of the general cargo berths is marginal. The area in front of the liquid bulk jetties requires more dredging. In the 17 km long approach channel (see figure 2-1) from the Outer Tuna Buoy to the Kandla Creek Outfall only a stretch of 2.3 km between buoy 8 and 10 has to be dredged continuously, albeit quite extensively.

About 400.000 cum/month has to be dredged in total in order to ensure ships with a draught of 10.7 m to be able to call on the port of Kandla, which costs about 300 mln Rupees a year (€ 7.3 mln) [CWPRS, 1999]. These ships are about 28.000 DWT, but occasionally partly laden ships of 45.000 DWT enter the port also.

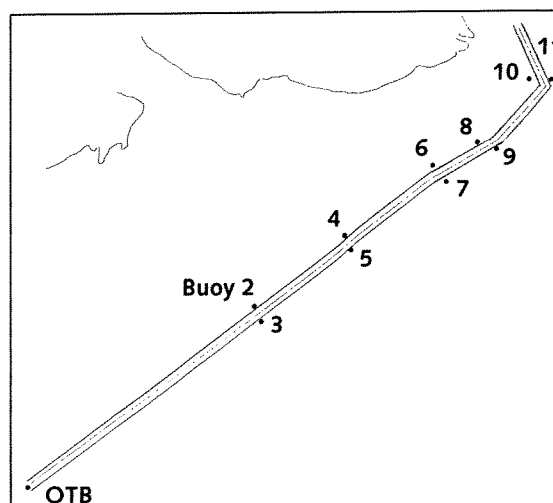


Figure 2-1 Sogal Channel

## 2.2 Future situation

### port expansion

The Kandla Port Trust has an ambitious expansion plan. Berthing capacity will be increased with 30% by constructing a 11<sup>th</sup>, 12<sup>th</sup> and 13<sup>th</sup> general cargo berth. The permissible draught will gradually be increased from 10.7 to 14 m, which will allow vessels of up to 80.000 DWT to call at the port [PIANC, 1997]. In order to keep up with this growth the capacity of cranes, storage and other services will also be increased. The permissible draught at Vadinar will also be enlarged in order to facilitate berthing of VLCC's and ULCC's [Internet, KPT-site and IPA-site].

### cargo forecast

A cargo forecast is given for the year 2010 in the helicopter assessment [NEI Transport]. Bearing in mind a modest expansion of the ports facilities a trade estimate of 65 mln tonnes is made. This number isn't backed by elaborate calculations. The annual growth rate will thus be 5%, whilst the annual growth rate of the smaller ports will be 15% (49 mln tonnes 1999, 195 mln tonnes in 2010).

The above mentioned expansion plan however will enable a bigger growth of the annual turnover, than foreseen by the helicopter assessment [NEI Transport, 1997]. If the berthing capacity is increased with 30%, it is safe to assume the same growth in number of ships. This means that 2400 ships will call at the port in 2010. Furthermore the average vessel size will also increase, because larger ships can call at the port in 2010. Assuming a future average of 40.000 DWT, the annual turnover in 2010 will amount to 96 million tonnes (2400 ships times 40.000 DWT), which means an annual growth rate of 9%.

Table 2-1 Cargo forecast

	Capacity (no. of ships)	Draught (m)	Maximum (DWT)	Average (DWT)	Turnover (mln tonnes)
'99-'00	1850	10.7	28.000	21.700	40
2010	2400	14	80.000	40.000	96

### income

The generated income has been calculated as follows. On the website of the Kandla Port Trust the costs per tonne of handling different types of cargo are given as well as the different costs for services. The distribution of the different cargo types handled in Kandla in 1999-2000 is summed up in the table below [Internet, KPT-website]. The cargo revenues are calculated by multiplying the annual totals of different types by the costs per tonne, whilst the services are calculated for the average ship before multiplying it by the total number of ships.

Table 2-2 Calculation of income

Commodity		(x 1000 ton)	Rs./ton	mln. Rupees
major bulk		2105	30	63
minor bulk		4911	35	172
liquid bulk	crude oil	18020	12	216
	oil products	13384	35	468
general cargo		1297	50	65

Use of port	Rs./GRT	average ship	Rs./ship	1850 ships (mln)
port dues	3,30	21.700 DWT	47850	88,5
berth hire	0,88	=	12760	23,6
mooring service	1,20	14.500 GRT	17400	32,2

The total income is summed up in the table below. The comparison with Rotterdam is made in the European currency Euro. A referential comparison is made with the figures for the port of Rotterdam [Internet, Port of Rotterdam site]. The revenues at Kandla are € 0,69 per tonne; in Rotterdam this is € 1,18 per tonne.

Table 2-3 Total income '99-'00

<b>TOTAL</b>	total tonnes (x 1000)	total income (mln Rupees)	income (rupees/tonne)
Kandla	39.717	1130	28,45

<b>TOTAL (Euro)</b>		(mln Euro)	(euro/tonne)
Kandla	39.717	27,6	<b>0,69</b>
Rotterdam	315.000	372	<b>1,18</b>

The expected income for the year 2010 is calculated in table 1.4. With the assumption that the berthing capacity as well as the draught will be increased, which will be a starting point in this study, the total cargo handled in 2010 will amount to 96 mln tonnes creating revenues of 2730 mln rupees or 66,6 mln euros.

Table 2-4 Income 2010

	mln. ton	Rupees (mln)	Euro (mln)
'99-00'	40	1130	27,6
2010	96	2730	66,6

#### **dredging activities**

Deepening of the harbour will require huge quantities to be dredged. KPT and CWPRS have calculated that in order to enable ships with a draught of 14 m to enter the port, Sogal Channel will have to be dredged to CD -8.0 m with a width of 300 m from the existing depth of CD -5.5 m and width of 180 m. Kandla Creek will have to be deepened to CD -14.2 m with a width of 400 m. The increase in width to 300 metres would allow two way traffic in Sogal Channel. It remains to be seen if this is necessary. The intensity of the largest ships entering or leaving the harbour has to be quite high to justify two way traffic. A tidal window is already instigated for Kandla Port, which leads to planning of traffic. It could be possible to plan the arrival and departure of the largest ships in a way that only one way traffic occurs in the channel. This would reduce the dredging amount considerably. Desk studies using analytical calculation methods have shown that in order to achieve these depths capital dredging of 28 to 35 mln cum is needed in total. Different proposals have been made. The Kandla Port Trust (KPT) proposal preserves the present navigation track, whilst the Central Water and Power Research Station (CWPRS) proposal suggests a more westerly alignment in Kandla Creek and an extra 100 m width in the inside of the bend between buoy no. 8 and 10. This will provide a cushion area for reducing siltation in the critical zone and better manoeuvrability for ships. Maintaining these depths will require dredging too. Staggering amounts of 3.73 to 5.48 mln cum/month in Kandla creek and 3.75 mln cum/month in Sogal channel have been calculated by KPT and CWPRS [1999]. This adds up to maintenance dredging of 90 to 111 mln cum/year, which will cost 6.3 to 7.8 bln Rupees a year (€ 150 to 190 mln). Table 2.1 gives an overview of the different quantities.

Table 2-5 Expected dredging quantities

Proposal	Capital (cum)	Maintenance (cum/month)
<b>Kandla Creek</b>		
KPT	$24 \times 10^6$	$5.48 \times 10^6$
Extended KPT	$30.2 \times 10^6$	$4.7 \times 10^6$
CWPRS	$25.3 \times 10^6$	$3.73 \times 10^6$
<b>Sogal Channel</b>		
KPT	$4.14 \times 10^6$	$3.75 \times 10^6$
CWPRS	$5.31 \times 10^6$	$3.75 \times 10^6$

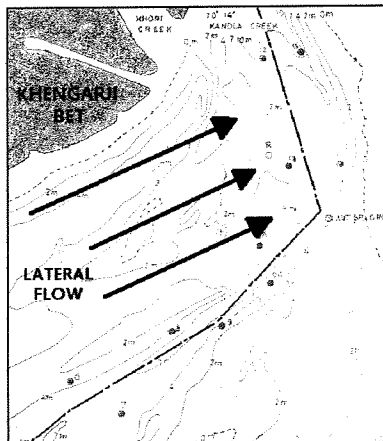


Figure 2-2 Lateral flow

results of which indicated that a reduction of 50% of the maintenance dredging could be met (these tests did not include deepening). During ebb the flow is canalised along the Sogal Channel, which helps in some natural flushing of sediment towards downstream reaches [CWPRS, 2000].

Siltation of the creek area will occur due to lateral flow coming in from the eastern edge of the creek as well as reduction of the velocities of the entire flow (and thus sediment transport capacity) due to increase of the cross section. The main cause for siltation in the critical area of the Sogal Channel is the entry of lateral flow from the shallow region south of Khengarji Bet during flood (figure 2-1). The Kandla Port Trust is contemplating to implement flow training works in order to prevent that lateral flow to develop (see figure 2-2). Different constructions were tested in a physical model, the

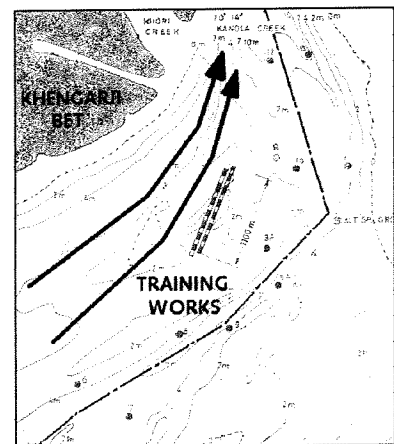


Figure 2-3 Training works

## 2.3 Outline of costs

It can be seen from table 2-6 that the expected annual revenues do not weigh up to the annual costs of the calculated dredging quantities of CWPRS and KPT. The costs for the capital dredging as well as the costs for the expansion are not even taken into account.

Table 2-6 Outline of costs

	CWPRS	KPT
Costs (mln Rupees)	6300	7800
Revenues (mln Rupees)	2730	2730

### 3 Sediment transport

#### 3.1 Introduction

Due to gradients in sediment transport the bathymetry of coastal regions is constantly changing. In general sediment transport occurs due to waves, currents or a combination of the two. The total sediment transport can be calculated by the following formula:

$$S = \int_0^{h+\eta} c(z) \cdot v(z) dz \quad (3.1)$$

in which:

$h$	= local water depth	[m]
$\eta$	= instantaneous water elevation	[m]
$v(z)$	= local, time averaged velocity	[m/s]
$c(z)$	= local, time averaged sediment concentration	[m <sup>3</sup> /m <sup>3</sup> ]

In case of a deep water situation sediment transport primarily occurs due to tidal currents. In case of a shallow water situation (especially the surf zone near the shore) the transport is primarily induced by (breaking) waves. In this study only the effects of tidal currents are taken into account, as the port of Kandla is naturally sheltered from wave attack.

#### 3.2 Current induced transport

In this thesis only current induced sediment transport is taken into account. The tidal fluctuation can be regarded as a large wave, but if the timescale used in computations is small enough the flow conditions can be regarded as constant. This assumption allows the use of sediment transport theories based on uniform stationary flow, which are widely used in river morphology.

Van Rijn [1984] developed a transport relation, which makes a distinction between bed load transport ( $S_b$ ) and suspended transport ( $S_s$ ) (see annex A). Bed load transport takes place in a small layer just above the bed. The sediment jumps or rolls along the bottom. Due to turbulence the disturbed sediment on the bottom can be brought into suspension. The fall velocity of the individual sediment particles however works against this process and an equilibrium concentration will develop. The advection-diffusion equation used in the computations (see section 5.3) uses this equilibrium suspended sediment concentration to calculate the residual sediment transport.

The bed load transport is calculated with a Shields-like relation. The value is dependant on the particle diameter and a bed shear parameter. The bed shear parameter indicates the difference between the actual bed shear stress and the critical bed shear stress at which particles start to move. The flow velocity used for these calculations is the depth-averaged velocity as calculated by the hydrodynamic equations.

The suspended transport is calculated with the aid of a reference concentration, which is dependant on the particle diameter, the bottom roughness height and the bed shear parameter. The value is calculated by multiplying the reference concentration by the depth averaged velocity, the depth and a shape factor, which primarily depends on a depth to bottom roughness ratio. This total equilibrium suspended transport is used to derive the local



equilibrium concentration used in the advection-diffusion equation in the transport module of the mathematical model. The actual sediment concentration is thus obtained and can be used to calculate the actual suspended transport components.

The bed load and suspended load transport components are then used in the bed level continuity equation, which makes use of the assumption of sediment conservation. The morphological development is thus calculated and a new bathymetry is obtained.

Small sized sediment is brought into suspension more easily than larger sized sediment. In this situation the sediment consists of fine sand and silt, which has a small mean diameter. This will cause the suspended sediment transport to be dominant over the bed load transport. In figure 3-1 an indication is given of transport mechanism. In this case the bottom transport will be small in comparison with the suspended transport. In the mathematical model the velocity will be averaged over the depth.

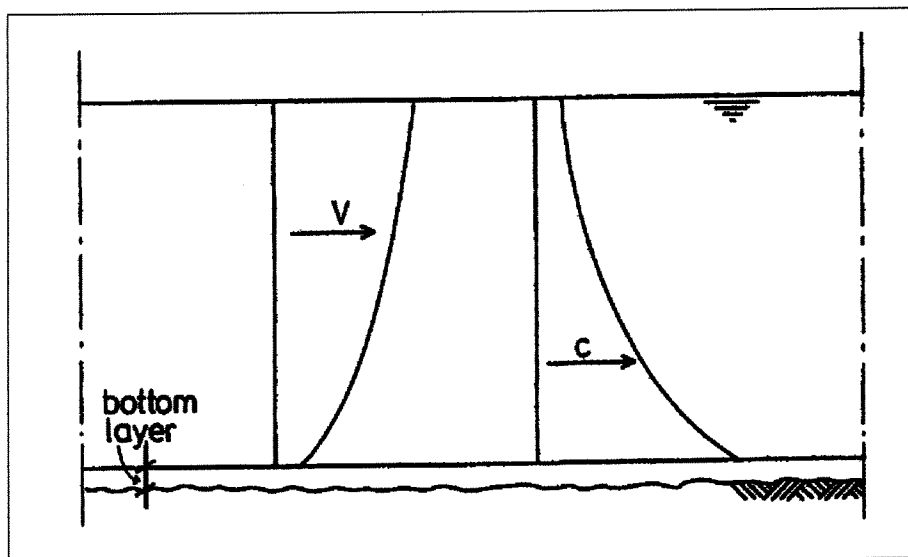


Figure 3-1 Velocity and concentration profile

## 4 Data

### 4.1 Introduction

The Kandla Port Trust deploys a measurement vessel, which surveys the area constantly. It collects data on bathymetry, flow velocity and water levels. These data will be used to set up the model (see chapter 6).

The bathymetry data can also be used to obtain insight in the morphological development of the region. In section 3 a comparison will be made between the bathymetry of 1999 and 2000. The bathymetries consist of data collected during the year (i.e. survey of the Kandla region started in January and ended in December). This prohibits the comparison to be quantitative; the bathymetry already changed during the survey. The comparison thus will be qualitative. Sogal Channel however was surveyed more frequently (i.e. monthly), especially the part which needs dredging (see section 1.2). Therefore a more detailed development can be monitored in this section of the approach channel.

### 4.2 FLOW boundary conditions

Data that can serve as input for the FLOW module consists of three components. Firstly water levels are measured at certain points. Secondly velocity measurements are taken simultaneously. These two quantities will serve as the basis on which the definite input values are obtained (see figure 4-1). Thirdly the influx and efflux are known. A net efflux of 67 mln cum prevails during the mixed tide [CWPRS, 1999, 2002].

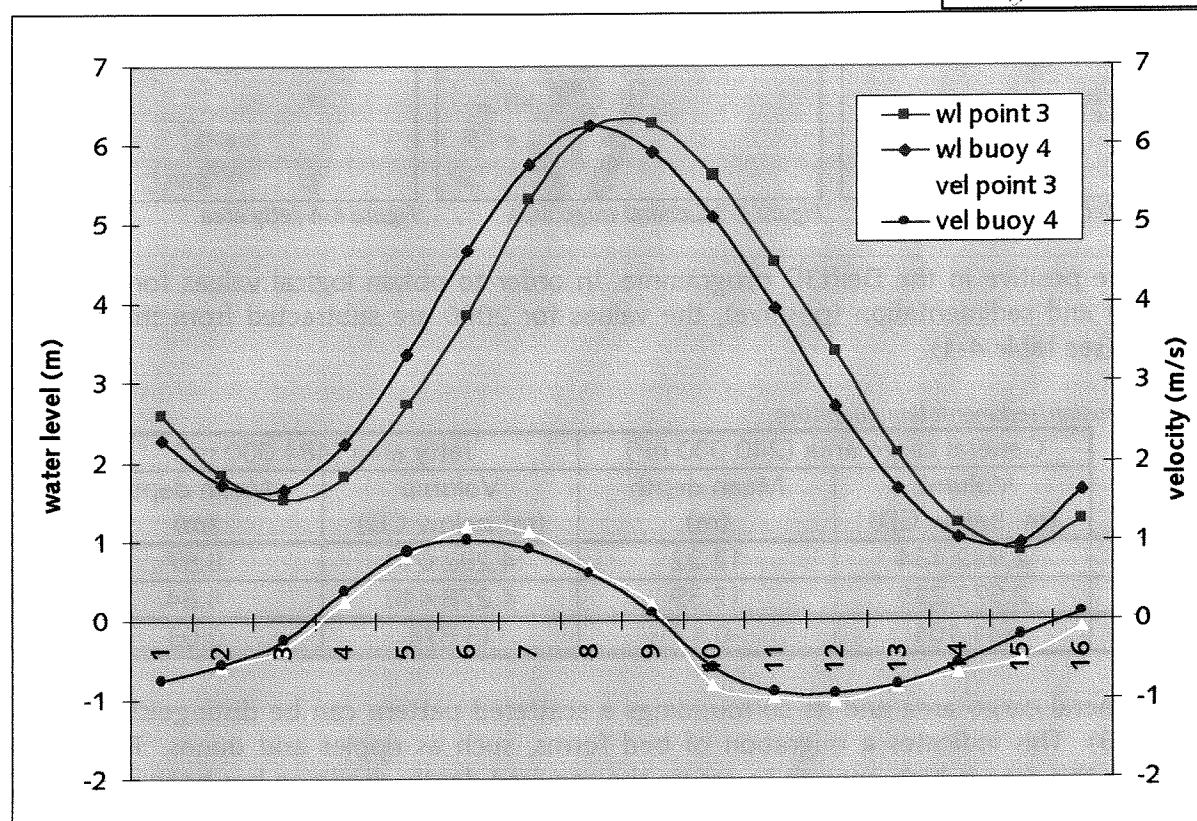
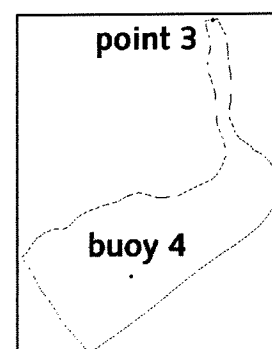


Figure 4-1 Water level and velocity measurements at buoy 4 and point 3

### 4.3 Morphological development

#### total bathymetry

The bathymetries of 1999 and 2000 were obtained by transforming the data to the right format for Delft-QUICKIN (see section 5.3). This program enables the user to subtract the bathymetries in order to construct a sedimentation/erosion pattern. A few specific areas can be distinguished in figure 4-2: general cargo area, jetty area and Sogal Channel (the latter will be described in the next section). General cargo area consists of the area just in front of the quay. The jetties are located more towards the middle of Kandla Creek, where a greater depth is available.

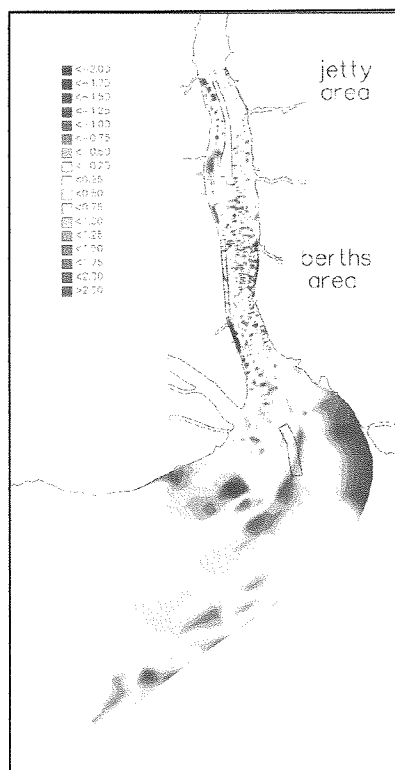


Figure 4-2 Sedimentation/erosion

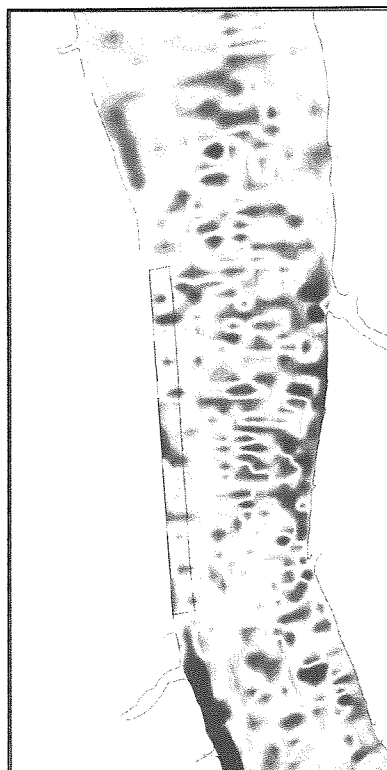


Figure 4-3 General cargo area



Figure 4-4 Jetty area

Depths are positive in the Delft3D programme. In order to obtain logical values for erosion (negative) and sedimentation (positive), the values for 2000 are subtracted from the values for 1999 (see table 4-1).

Table 4-1 Erosion/sedimentation quantities

	General cargo area (240.000 m <sup>2</sup> )		Jetty area (484.000 m <sup>2</sup> )	
	Volume (m <sup>3</sup> below CD)	Mean depth (m)	Volume (m <sup>3</sup> below CD)	Mean depth (m)
1999	2.932.134	12.22	4.292.014	8.87
2000	2.973.235	12.39	4.278.440	8.84
difference	-41.101	-0.17	13.574	0.03

In the general cargo area and its surroundings a scattered pattern can be distinguished (see Figure 4-3). This indicates a migration of bed forms, such as ripples and dunes. The flow velocity in this area is high enough to assure the required depth; dredging has been marginal (see section 2.1).

In the jetty area however almost no erosion or sedimentation has taken place in comparison with the direct surroundings (see Figure 4-4). This indicates that the jetty area has been dredged to ensure the required depth for loading and unloading of ships.

### Sogal Channel

The 2.3 km stretch of Sogal Channel that needs constant maintenance dredging (see section 2.1), is monitored more frequently. Every month a survey is made of the particular area, which is divided into four zones. From figure 4.6 it can be seen that Sogal Channel is already being deepened. The left axis indicates the total cubic metres of volume below CD (Chart Datum), the right axis indicates the average depth.

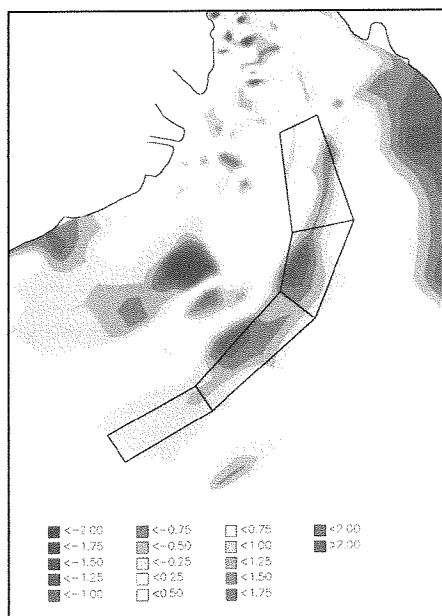


Figure 4-5 Four zones of Sogal Channel

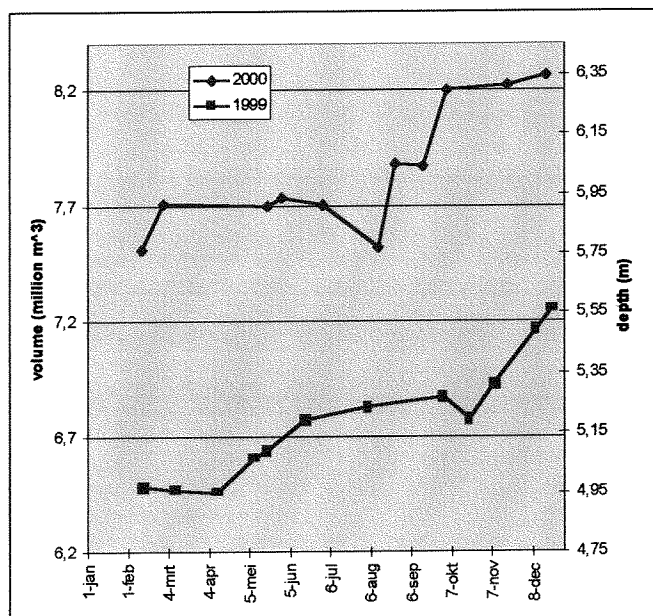


Figure 4-6 Development Sogal Channel

A distinct trend is visible. Sogal Channel has been deepened by means of dredging in order to allow ships of larger draught to call on the port of Kandla. Figure 4-6 shows the development of the two middle parts of Sogal Channel as seen in figure 4-5.

### dredging activities

According to CWPRS [1999] the total amount of maintenance dredging in the entire Kandla Port adds up to 400.000 m<sup>3</sup>/month. In this report it is not clear how this amount is determined. Another document [reply to letter No. KPC/5009-DC] is more specific about the maintenance dredging in Sogal Channel itself. Dredging activities have been suspended in Sogal Channel from 18/11/2001 until 31/12/2001. In this period surveys were carried out to assess the rate of siltation in the four areas visible in figure 4-5. It was found that 8082 m<sup>3</sup>/day was deposited in these combined areas. This leads to a monthly rate of siltation of 246.000 m<sup>3</sup>, which causes a reduction of the average depth of 19 cm/month. If the maintenance dredging in front of the berths is neglected, 400.000 – 246.000 = 154.000 m<sup>3</sup>/month has to be dredged in the jetty area, this is an accretion of 32 cm/month.

## 5 Description Delft3D

### 5.1 Introduction

As mentioned before a mathematical model is used to simulate the problem. In this chapter a description is given of the theoretical background of the model and its calculation methods.

WL I Delft Hydraulics has developed a fully integrated computer software suite for a multi-disciplinary approach and 3D computations for coastal, river and estuarine areas. It is a process-based model that can carry out simulations of flow, sediment transport, waves, water quality, morphological development and ecology. The Delft3D suite is composed of several different modules, grouped around a mutual interface, which are capable to interact with one and other. In this case a morphological development will be modelled. This has consequences for the required modules. The general module for this type of simulation is the Delft3D-MOR module, which has been designed to simulate the morphodynamic behaviour of rivers, estuaries and coasts, due to the complex interaction between waves, currents, sediment transport and bathymetry, on a time scale of days to years. All of these processes are dealt with in separate modules (Delft3D-WAVE\FLOW\TRAN\BOTT). These modules can be arranged by the user in a process tree. This process tree sets up the hierarchical structure that forms the overall morphodynamic system. Time intervals for the different elementary processes are defined as well as when and how often a process has to be executed. The overall structure of Delft3D is given below.

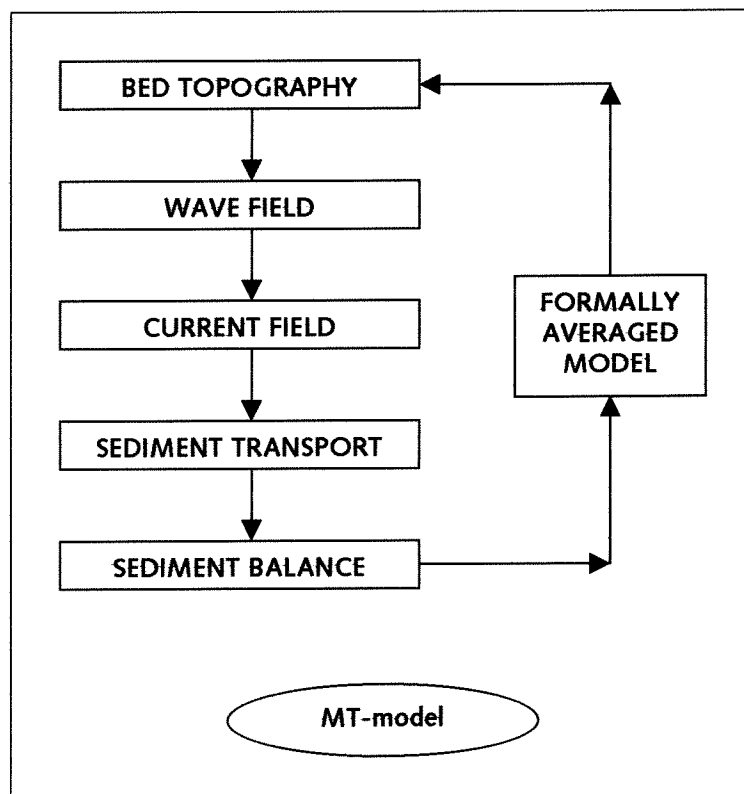


Figure 5-1 Medium term morphological model

## 5.2 Delft3D-FLOW

### physical background

In the Delft3D-FLOW module, also known as TRISULA, the non-linear shallow water equations are solved. If the fluid is vertically homogeneous, as is the case here, the two dimensional (i.e. depth averaged) approach is used. The equations are derived from the three dimensional Navier Stokes equations for incompressible free surface flow. Because of the shallow water assumption the vertical momentum equation is reduced to the hydrostatic pressure relation.

The following physical phenomena are taken into account:

- The effect of the earth's rotation (Coriolis force).
- Turbulence induced mass and momentum fluxes.
- Tidal forcing at open boundaries.
- Space varying shear stress at the bottom.
- Drying and flooding of tidal flats.
- Effect of secondary flow on depth averaged momentum equations.

### hydrodynamic equations

The depth averaged shallow water equations consist of two basic equations: a continuity equation (conservation of mass) and a momentum equation (conservation of momentum; in two horizontal directions). The effect of turbulence is integrated via a dispersion term.

The momentum equation in x-direction (depth and density averaged) reads:

$$\frac{\partial u}{\partial t} + u \frac{\partial u}{\partial x} + v \frac{\partial u}{\partial y} + g \frac{\partial \eta}{\partial x} - f v + \frac{g u |U|}{C^2(d+\eta)} - \frac{F_x}{\rho_w(d+\eta)} - K_x \left( \frac{\partial^2 u}{\partial x^2} + \frac{\partial^2 u}{\partial y^2} \right) = 0 \quad (5.1)$$

(1)   (2)   (3)   (4)   (5)   (6)   (7)   (8)

The momentum equation in y-direction (depth and density averaged) reads:

$$\frac{\partial v}{\partial t} + u \frac{\partial v}{\partial x} + v \frac{\partial v}{\partial y} + g \frac{\partial \eta}{\partial y} + f u + \frac{g v |U|}{C^2(d+\eta)} - \frac{F_y}{\rho_w(d+\eta)} - K_y \left( \frac{\partial^2 v}{\partial x^2} + \frac{\partial^2 v}{\partial y^2} \right) = 0 \quad (5.2)$$

(1)   (2)   (3)   (4)   (5)   (6)   (7)   (8)

The following terms can be recognised:

- (1) = acceleration
- (2),(3) = advection
- (4) = pressure gradient
- (5) = Coriolis force
- (6) = bottom friction
- (7) = external forces (boundary conditions)
- (8) = dispersion

The continuity equation (depth and density averaged) reads:

$$\frac{\partial \eta}{\partial t} + \frac{\partial (d+\eta)u}{\partial x} + \frac{\partial (d+\eta)v}{\partial y} = 0 \quad (5.3)$$

in which:

$u$	= depth averaged velocity in x-direction	[m/s]
$v$	= depth averaged velocity in y-direction	[m/s]
$U$	= magnitude of total velocity ( $U = (u^2 + v^2)^{1/2}$ )	[m/s]
$\eta$	= free surface elevation above reference plane	[m]
$d$	= depth below reference plane	[m]
$C$	= Chézy coefficient	[m <sup>1/2</sup> /s]
$\rho_w$	= density water	[kg/m <sup>3</sup> ]
$F_{x,y}$	= x and y component of external forces	[kg/ms <sup>2</sup> ]
$K_{x,y}$	= x and y viscosity components	[m]

### numerical background

To solve the partial differential equations the modelled area is divided into a finite number of orthogonal grid cells (the grid is constructed in a separate program called Delft-RGFGRID, see chapter 4). In the horizontal plane TRISULA uses a staggered grid principle (see Figure 4.1). Water levels and velocity components with the same index are not defined in the same place: water level point (pressure points) are defined in the centre of a (continuity) cell, whilst the velocity components are perpendicular to the cell faces where they are situated.

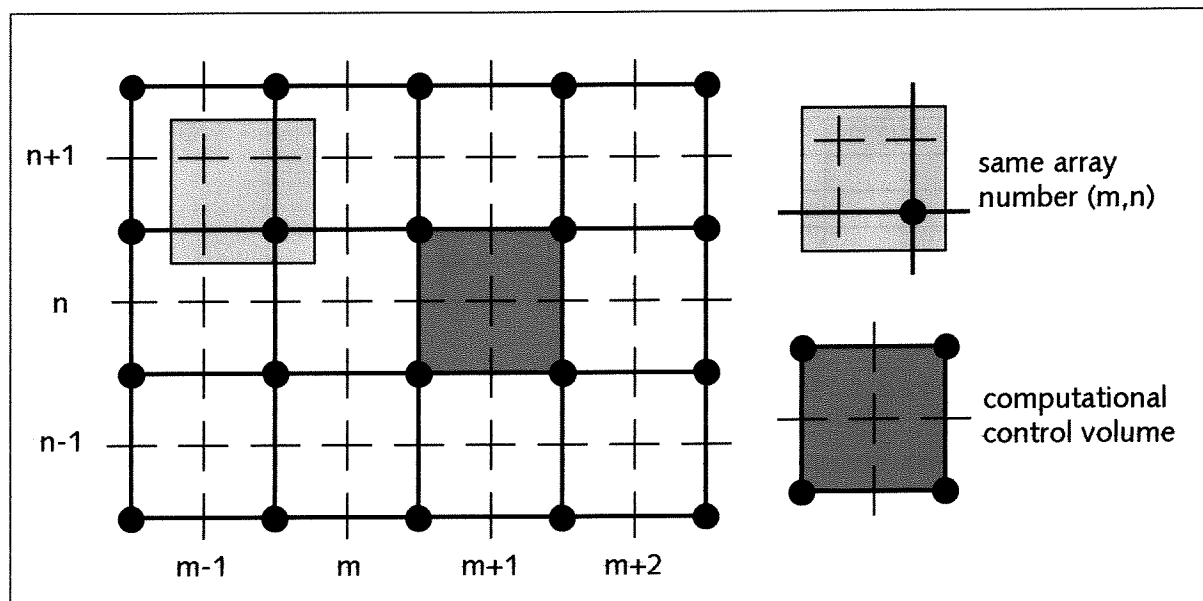


Figure 5-2 Staggered grid

#### Legend:

full lines	= the numerical grid
+	= water level point
—	= horizontal velocity component x-, $\xi$ -, u- or m-direction
	= horizontal velocity component y-, $\eta$ -, v- or n-direction
●	= depth point

The standard time integration method is the "Alternating Direction Implicit (ADI)" method, Stelling (1984). The ADI-method splits one time step into two stages. Each stage consists of half a time step. In the first stage the V-momentum equation, Eq. (4.2), is solved followed by the U-momentum equation, Eq. (4.1), which is implicitly coupled with the continuity equation, Eq. (4.3), by the free surface gradient. In the second stage this is reversed: first the U- and then the V-momentum equation, which is coupled to the continuity equation. Also in the stage in which the barotropic pressure term (i.e. water level gradient) is integrated implicitly, the advection and viscosity terms are integrated explicitly, and vice versa. This

method proves to be unconditionally stable. The accuracy of the results is influenced by the Courant number, which depends on the local cell size, the depth and the time step. In practical situations the Courant number should not exceed a value of 10 (see section 6.4).

More details on the FLOW module can be found in the User Manual Delft3D-FLOW (version 3.06, 2001).

### 5.3 Delft3D-TRAN

#### physical background

The TRAN module determines the sediment transport for a 2D horizontal area at a set of times. In order to do so it uses the FLOW data on a communication file and a prescribed sediment transport relation. A number of transport formulas are available; each of which are derived for different conditions. In Delft3D-TRAN two transport modes can be used. TRSTOT calculates the total transport whereas TRSSUS makes a clear distinction between the bed load and the suspended sediment.

Table 5-1 Sediment transport formulas

Formula	TRSTOT	TRSSUS
Engelund-Hansen (1967)	YES	NO
Meyer-Peter-Muller (1948)	YES	NO
Swanby (Ackers-White, 1973)	YES	NO
General formula	YES	NO
Bijker (1971)	YES	YES
Van Rijn (1984)	YES	YES
Ribberink-Van Rijn (1994)	YES	YES

#### transport equations

The transport of bed load is derived directly from the prescribed transport formula. The transport of suspended sediment however is determined with an advection-diffusion equation. To determine the depth averaged suspended sediment concentrations, the advection-diffusion equation is derived from a 3D advection-diffusion equation by assuming algebraic approximations for the vertical diffusion coefficients. The computed concentration is the depth-averaged concentration ( $c_s$ ) defined by:

$$c_s = \int_0^1 c(\zeta) d\zeta \quad (5.5)$$

The advection-diffusion equation to be solved for  $c_s$  reads:

$$\frac{\partial h c_s}{\partial t} + \frac{\partial h u c_s}{\partial x} + \frac{\partial h v c_s}{\partial y} + \frac{\partial}{\partial x} \left( D_x h \frac{\partial c_s}{\partial x} \right) + \frac{\partial}{\partial y} \left( D_y h \frac{\partial c_s}{\partial y} \right) = \frac{h(c_{se} - c_s)}{T_s} \quad (5.6)$$

in which:

$c_s$	= depth averaged sediment concentration	[m <sup>3</sup> /m <sup>2</sup> ]
$c_{se}$	= equilibrium concentration of suspended sediment	[m <sup>3</sup> /m <sup>3</sup> ]
$h$	= depth	[m]
$u, v$	= velocity components x,y-direction	[m/s]
$D_x, D_y$	= dispersion coefficient x,y-direction	[m <sup>2</sup> /s]
$T_s$	= adaptation time for vertical sediment concentration profile	[s]



The equilibrium suspended sediment transport, which is computed by an algebraic sediment transport formula specified by the user, will be used to derive the local equilibrium concentration ( $c_{se}$ ) by the expression:

$$c_{se} = \frac{S_{se}}{\alpha_s u_s h} \quad (5.7)$$

The bottom and suspended sediment transports are determined by averaging the computed transports over a time interval in both directions ( $\xi, \eta$ ); thus creating four components. An initial adaptation time [ $t_a, t_a + T_i$ ] can be excluded from the averaging interval to compensate for the inaccurate computations in the first few time steps. The averaging interval thus becomes: [ $t_a + T_i, t_b$ ], in which  $t_a$  is the simulation start time and  $t_b$  is the simulation stop time. The averaging formula reads:

$$TT...A = \frac{1}{(t_b - t_a - T_i)} \int_{t_a + T_i}^{t_b} S_{...} dt \quad (5.8)$$

where:

TT...A = TTXA, TTYA for time averaged bed transport in x,y-direction

TT...A = TTXSA, TTYSA for time averaged suspended transport in x,y-direction

S... =  $S_{b\xi}, S_{b\eta}, S_{s\xi}, S_{s\eta}$  for TTXA, TTYA, TTXSA and TTYSA

Since none of the algebraic sediment transport formulas (see Table 5-1) contains the effects of bed level gradients, a correction can be included via a physical slope effect term ( $\alpha_w$ ). The magnitude of the sediment transport ( $S'$ ) thus becomes:

$$S = \alpha_w S' \quad (5.9)$$

The bed level correction term ( $\alpha_w$ ) is a function of the bed level gradient in the sediment transport direction ( $s$ ), and reads:

$$\alpha_s = 1 + \alpha_{bs} \frac{\partial z_b}{\partial s} \quad (5.10)$$

$\alpha_{bs}$  = coefficient, specified by user [-]

More details on the TRAN module can be found in the User Manual Delft3D-MOR (version 3.00, June 2001).

## 5.4 Delft3D-BOTT

### physical background

In the bottom module the bed level variations are based on the gradients in the sediment transport fields as calculated in the transport module. The module will execute one morphological time step. This time step can be imposed on the input file of the steering module MORSYS or it can be automatically calculated in the TRAN module. The choice depends on stability and accuracy conditions.

### morphodynamic equation

The BOTT module is a sediment conservation model that solves the bed level continuity equation:

$$(1 - \varepsilon_{por}) \frac{\partial z_a}{\partial t} + \frac{\partial S_{bx}}{\partial x} + \frac{\partial S_{sx}}{\partial x} + \frac{\partial S_{by}}{\partial y} + \frac{\partial S_{sy}}{\partial y} = 0 \quad (5.11)$$

in which:

$\varepsilon_{por}$	= bed porosity	[-]
$z_a$	= bed level	[m]
$S_{bx, sx}, S_{by, sy}$	= sediment transport components	[m <sup>3</sup> /s/m]

The sediment transport components are computed by expression (5.8).

### numerical background

The numerical scheme used to solve the continuity equation is the FTCS scheme. To guarantee stability this scheme has been extended to a LAX-type scheme. This extension can be approximated by introducing a slope depended correction to the computed transport rates in the TRAN module. Although the correction has to be applied because of stability demands in the BOTT module, it is calculated in the TRAN module so that it can be included in the averaged transports written to the Transport data group on the communication file. Similarly to the physical slope effect correction term, the stability correction term reads:

$$\alpha_n = 1 + \alpha_{nn} \frac{\partial z_a}{\partial s} \quad (5.12)$$

A number of options are available to compute the stability coefficient ( $\alpha_{nn}$ ), which are derived for a substantially simplified set of equations.

In view of accuracy a restriction is imposed on the time step with regard to the Courant number. Because of the explicit LAX-type scheme, the Courant number should not exceed the value of one, but should not be chosen too small either as low Courant numbers generally induce numerical diffusion.

The sediment concentrations are calculated in the water level points on the staggered grid (see Figure 4-1), while the bed level changes are calculated in the depth points of the same grid. The bed level update is calculated via the four surrounding (corrected) sediment transport components.

More details on the BOTT module can be found in the User Manual Delft3D-MOR (version 3.00, June 2001).

## 5.5 Delft3D-MOR

Delft3D-MOR contains the overall steering module for the entire morphodynamic simulation, which allows the user to link model input and output for the model components. This module 'manages' the system via a process tree. Dynamic coupling is also imbedded in the module, which allows feedback between the processes. This is necessary as the processes influence one and other. The individual elementary processes with different time intervals are called upon in a preset sequence specified by the user. Stop criteria for the different processes are also declared here.

In morphodynamic simulations a sequence of modules has to be run repetitively. In general the FLOW and WAVE modules are run first in order to obtain the hydrodynamic quantities. Then the TRAN module uses these quantities to calculate the sediment transport components. Subsequently the BOTT module calculates the bed level changes due to gradients in the sediment transport components.

As the FLOW module is by far the most demanding in computational time, the TRAN and BOTT modules can apply a so-called continuity correction. This method essentially approximates a new flow field based on the original flow results and the updated bed level. The assumption is made that the velocity patterns are not significantly influenced by small bed level changes. By using the discharge and the water level components from the FLOW data group on the communication file and the updated bathymetry, the TRAN module approximates a new velocity field according to continuity.

$$Q(T1) = Q(T2)$$

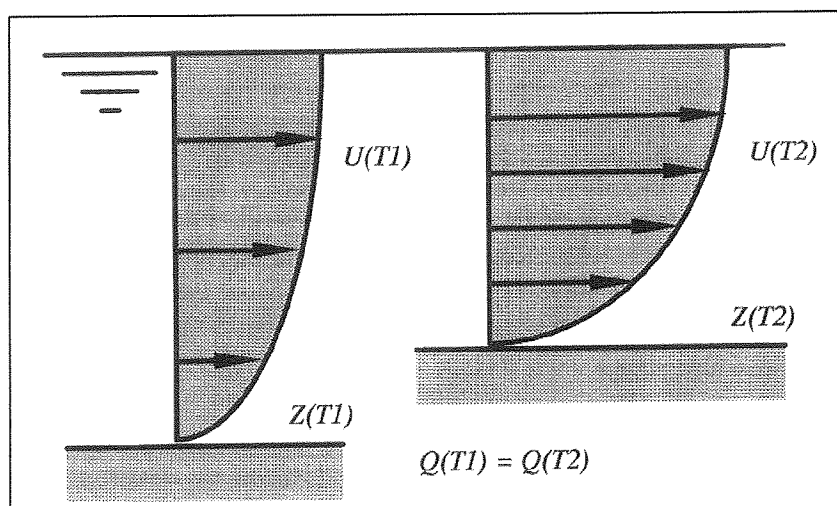


Figure 5-3 Continuity correction

## 6 Model set-up

### 6.1 Introduction

As mentioned in chapter one the Kandla-Hansthal creek system is very complicated. It consists of a large number of creeks and inlets of which about a dozen are subject to large water and sediment movement. Constructing a mathematical model of this complex system would take much longer to complete than this study would permit. In this perspective limitations and assumptions will have to be made in order to simplify the problem.

The bathymetric survey does not cover the entire gulf of Kutch. The area that is surveyed starts at the deeper parts of the approach channel (Outer Tuna Buoy) and go up all the way into Kandla Creek to where the creek splits into Sara Creek and Phang Creek. This limits the model area (see section 2).

The region is well protected against wave attack. Even during the monsoon period the wave climate doesn't contribute much to the sediment transport processes [CWPRS, 2000]. The effect of waves is thus neglected in this particular case and the WAVE module becomes superfluous.

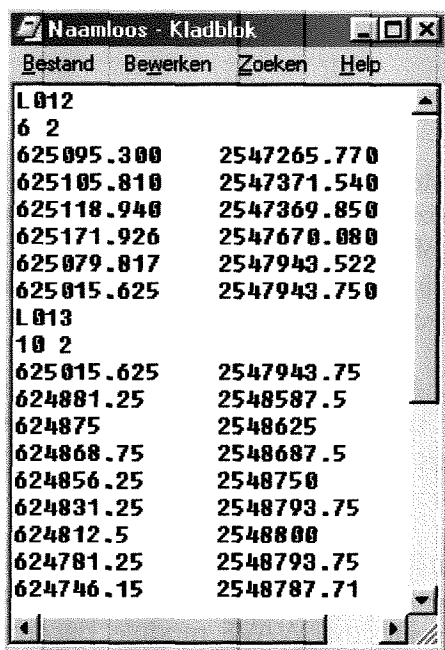
In this chapter the process of constructing the model will be explained. The different modules require different data as input. Some of the data was ready for use, but most of the data had to be manipulated into formats that can be read by Delft3D. All of the input files for the model are in ASCII format. This enables the user to view the different files in any arbitrary ASCII-editor (for instance Notepad or Wordpad). The majority of the input however can be done with an input processor, which has a Windows interface.

### 6.2 Delft-RGFGRID

As described in chapter 3 the hydrodynamic calculations are made on a prefixed difference grid. The program Delft-RGFGRID is used to create orthogonal, curvilinear model grids for the Delft3D-FLOW water motion program. Known land boundaries act as the basic input on which a grid can be formed. The user can sketch a coarse grid with splines that can be transformed by the program to a more detailed grid. Special features can be used to manipulate the grid, so that it meets a few requirements. Gridlines can be snapped to land boundaries, ensuring an exact imitation of the geographical reality. In order to avoid inaccuracies the grid should be orthogonal (i.e. as orthogonal as possible). A tool within the program enables the user to automatically orthogonalise the grid. Finally the grid should be smooth. This means that the dimensions of adjacent grid cells may not vary too much.

More details can be found in the User Manual Delft-RGFGRID (version 3.10, September 1999).

The first step of making a grid is inserting a land boundary. In this case the land boundary was only available in an AutoCAD drawing and was drawn as a set of polygons. An additional tool (polyxyz) was used to transform the polygons to xyz-coordinates and write them to text files. These text files were combined to create one text file to serve as input for RGFGRID (see figure 6-1).



L012	
6	2
625095.300	2547265.770
625105.810	2547371.540
625118.940	2547369.850
625171.926	2547670.080
625079.017	2547943.522
625015.625	2547943.750
L013	
10	2
625015.625	2547943.75
624881.25	2548587.5
624875	2548625
624868.75	2548687.5
624856.25	2548750
624831.25	2548793.75
624812.5	2548800
624781.25	2548793.75
624746.15	2548787.71

Figure 6-1 ASCII-type lbd-file

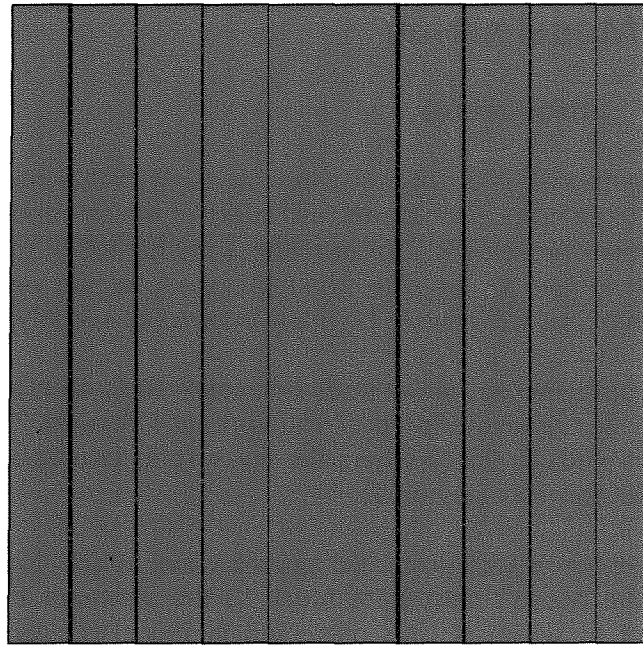


Figure 6-2 Landboundary

Now the model area is clearly visible in figure 6-2. The second step is to draw splines. Spline points are inserted at different locations and the programme neatly curves a line through the points. Perpendicularly to these splines a second set of spline completes the process and thus creates square-like areas. These can then be transformed by the programme into a grid. The grid can be manipulated as described above creating a smooth curvilinear, orthogonal grid. This process is visualised in figures 6-3, 6-4 and 6-5.

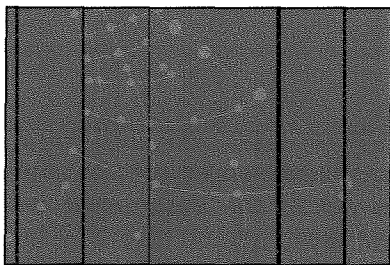


Figure 6-3 Splines drawn by user

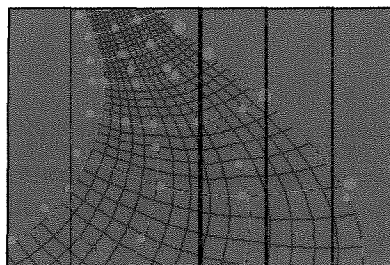


Figure 6-4 Splines into grid

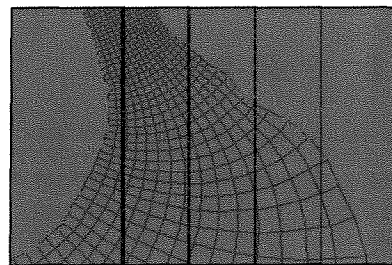


Figure 6-5 Manipulated grid

The flow velocities in Kandla Creek, in general, are quite uniform and well distributed across the width and there is no distinct separation of flow during flood and ebb. The creek extends up to a distance of 13 km north of the creek outfall. A northern boundary at LAT 23° 02' 36" N would create a large enough area. Furthermore velocity measurements were taken at that location. These measurements can act as input for the boundary condition in the FLOW module (see section 5.4). The cross section at the Outer Tuna Buoy in NW-SE direction, perpendicular to the flow direction, will make up the second boundary. A practical limitation is that depth measurements, which are required in Delft-QUICKIN (see section 4.3), aren't available further southwest of this location. The last boundary will lie over the natural shoals in the area. These shoals (Kala Dara Shoal and Mid Shoal) cause the flow to be directed in the direction of the proposed boundary.

The grid consists of 181 lines in m-direction and 16 lines in n-direction, creating  $180 \times 15 = 2700$  grid cells. The maximum grid cell dimensions are 730 and 650 metres, while the minimum dimensions are 34 and 38 metres in m- and n-direction.

### 6.3 Delft-QUICKIN

The bathymetry of the modelled area is created by the program Delft-QUICKIN on the grid that is created in Delft-RGFGRID. A set of scattered x,y co-ordinates and z values, raw data called 'samples', will be interpolated to obtain the depth points (see Figure 3-1).

The raw data that were used for this study came in PDS1000 format, which is a format used by the measurement equipment in Kandla. This format is not recognisable by QUICKIN and had to be transformed into ASCII format (similar to Figure 6-1). The data were so extensive and detailed, that an averaging programme was used to compress the data. This was permissible since the resolution of the grid was smaller (minimum distance 34 metres) than the resolution of the averaged data (distance 25 metres).

The grid created in RGFGRID is loaded into QUICKIN. Subsequently the raw (averaged) data (called samples) are loaded onto the grid (see figure 6-6). In order to obtain values in the depth points the samples have to be averaged or interpolated. The first method used is grid cell averaging, in which the surrounding samples are averaged to one single value. The remaining depth points on the edge of the grid were manipulated manually. To complete the process internal diffusion was applied creating depths in all the points (figure 6-7). In figure 6-8 a part of the model area is presented in a three dimensional view.

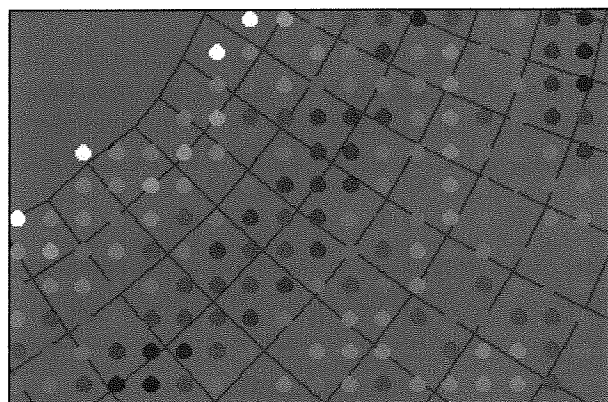


Figure 6-6 Samples

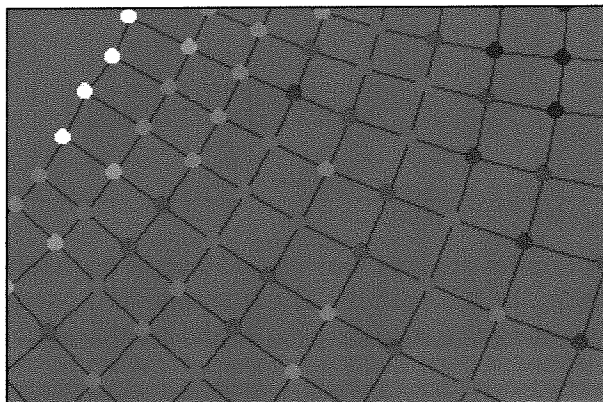


Figure 6-7 Depth points

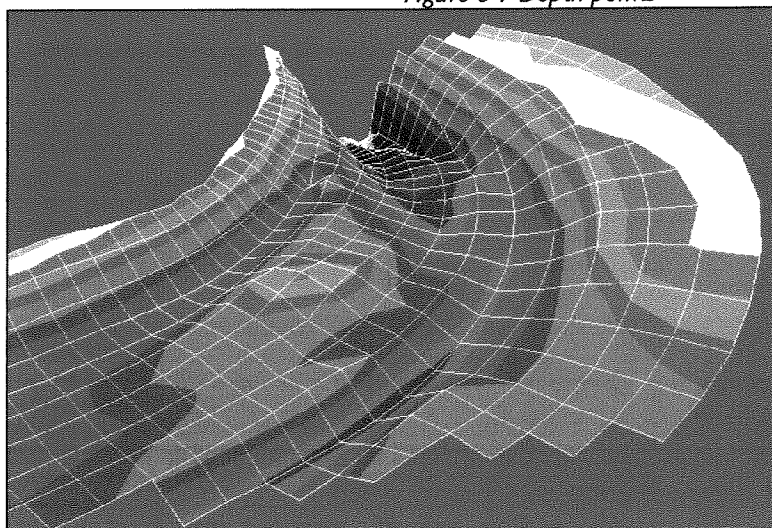


Figure 6-8 3D view of (part of) bathymetry

Details can be found in the User Manual Delft-QUICKIN (version 3.10, September 1999).

## 6.4 Delft3D-FLOW

First a few assumptions are made to simplify the problem. Considering the fact that Kandla area is an arid zone, rainfall is very scanty. In comparison with the huge volume of salt seawater entering the Kandla-Hansthal creek system every tidal cycle, the fresh water discharge is negligible. Because of the absence of fresh water and the large water movement, the salt seawater is well mixed. Different measurements have indicated that the salinity is about 32 ppt. The distribution of temperature over the vertical is uniform as well, due to the turbulent exchange of temperature flux between different layers. The above described assumptions certify the negligence of density flows. This has consequences for the mode in which the FLOW module is run. A 2D approach will be sufficient to cope with the problem.

### boundary conditions

The boundary conditions consist of a harmonic water level elevation type at Outer Tuna Buoy and a harmonic current type at the northern boundary. For the OTB-boundary a representative mixed tide was used with a period of 25 hours (CWPRS, 2001). The numbers

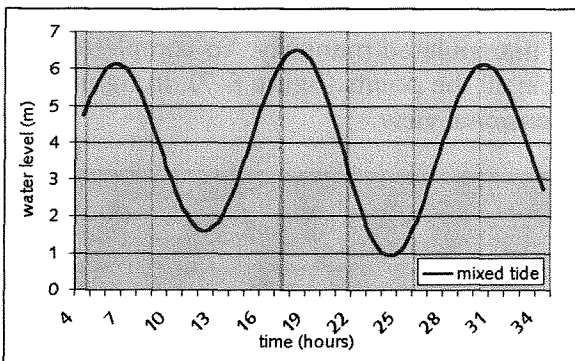


Figure 6-9 Mixed tide

are given in metres above Chart Datum, which is 3.884 m above MSL (see figure 6-9). The initial water level is set to MSL+6.5 metres, which is approximately the high water level.

Measurements showed that the phase lag between high water at OTB and high water at the northern boundary is about 25 minutes. The amplitude of the tide at the northern boundary is increased by about 7% (see annex D).

A Fourier analysis was carried out to transform the data into a set of harmonics to serve as input for the module. The harmonic boundary signal in FLOW ( $F(t)$ ) is constructed by superimposing the following individual components:

$$F(t) = \sum_{i=1}^N A_i \cdot \cos(\omega_i \cdot t - \phi_i) \quad (6.1)$$

where:

N	= number of frequency components	[-]
$A_i$	= amplitude	[m]
$\omega_i$	= frequency	[degrees/hour]
$\phi_i$	= phase	[degrees]

At the northern boundary of the modelled area a harmonic current condition has been imposed. Measurements taken at point 3 (E 70° 13' 24", N 23° 02' 36", CWPRS, 2002), were used. Again a Fourier analysis was applied to obtain suitable input for the FLOW module (Eq. 5.1). A good approximation was found when five harmonics were superimposed. The phase lag between the maximum flow velocity and the first high water at the northern boundary is about 2 hours and 15 minutes (see figure 6-10).



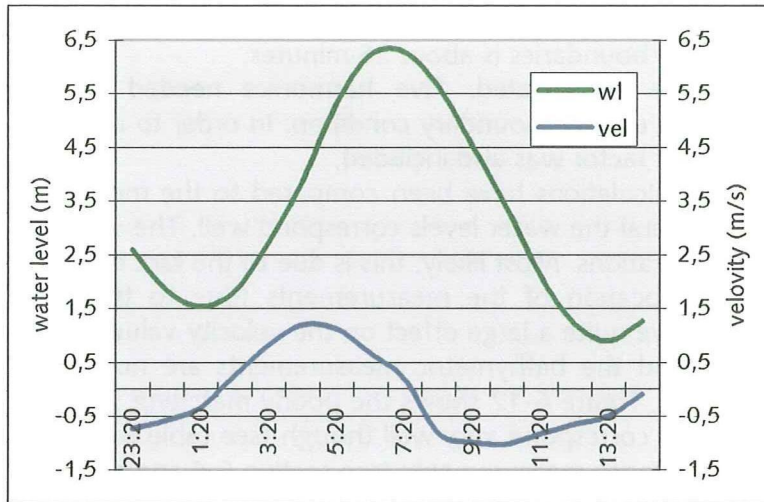


Figure 6-10 Measurements northern boundary

The exact values of both boundary conditions were determined in the calibration process, which will be described later on in this section. For full details on the input reference is made to annex E.

### physical parameters

As mentioned above measurements have shown a well-distributed salinity of 32 ppt. The temperature of the water is set to 25° Celsius. The density of the water is a function of these two factors; its value is 1021 kg/m<sup>3</sup>. Other parameters, such as roughness coefficients, will be described in chapter 7, because they are determined in the calibration process.

### time step

The time step used in Delft3D-FLOW is based on accuracy arguments. The accuracy is mostly dependent on the Courant number, which is defined by:

$$Cr = \frac{\Delta t \sqrt{gh}}{\{\Delta x, \Delta y\}} \quad (6.2)$$

{Δx, Δy} = characteristic value of the grid spacing

This characteristic value can be calculated in the QUICKIN program for the entire grid. The Courant number generally should not exceed 10. As  $g$ ,  $h$ ,  $\Delta x$  and  $\Delta y$  are constants (per grid cell),  $\Delta t$  has to be altered until the condition is met. This resulted in a hydrodynamic time step of 12 seconds.

### calibration FLOW boundaries

In the FLOW module the water level boundary and the current velocity boundary have to be adjusted until the measured data are represented by the calculations. As the water motion is the basis on which all other quantities are calculated the calibration is carried out before the TRAN and BOTT module were set up. At a few points in the model area simultaneous measurements are taken of water level and flow velocity. As mentioned earlier in this chapter a Fourier analysis is made to obtain the different components of the harmonic oscillating boundary conditions. The optimum values have been determined by trial and error.

The imposed condition on the south boundary of the model area is a harmonic oscillating water level. The Fourier analysis resulted in two superimposed harmonics, the basic frequency being the semidiurnal one. One higher harmonic frequency completes the boundary



condition. The tide propagates into Kandla Creek causing the amplitude to increase by about 7%. The phase lag between south and north boundaries is about 25 minutes.

The velocity boundary condition is more complicated. Five harmonics needed to be superimposed in order to obtain an accurate enough boundary condition. In order to account for the difference in in- and efflux a constant factor was also included.

At a few locations in the model area the calculations have been compared to the measured data (see table 6-1 and figure 6-11). In general the water levels correspond well. The velocity values however differ quite a bit on some locations. Most likely, this is due to the fact that the calculations are not done at the precise location of the measurements (due to the grid spacing). A small difference in depth can have quite a large effect on the velocity values. Also the fact that the current measurements and the bathymetric measurements are not done simultaneously contributes to the inaccuracy. Figure 6-12 shows the poorly matching velocity profile at buoy 6. The total influx and efflux correspond very well though (see table 6-2) and this is valued as more important than the velocity measurements (see section 6.4 and annex F for details).

Table 6-1 Coordinate locations

	UTM coordinates	
buoy 6	623247 E	2534469 N
buoy 12	626960 E	2540128 N
	grid cell M	grid cell N
buoy 6	21	6
buoy 12	48	10
cross section	67	2-16

Table 6-2 In/efflux mixed tide

	measured (m <sup>3</sup> )	calculated (m <sup>3</sup> )
influx	352 x 10 <sup>6</sup>	352.7 x 10 <sup>6</sup>
efflux	419 x 10 <sup>6</sup>	420.0 x 10 <sup>6</sup>
difference	67 x 10 <sup>6</sup>	67.3 x 10 <sup>6</sup>

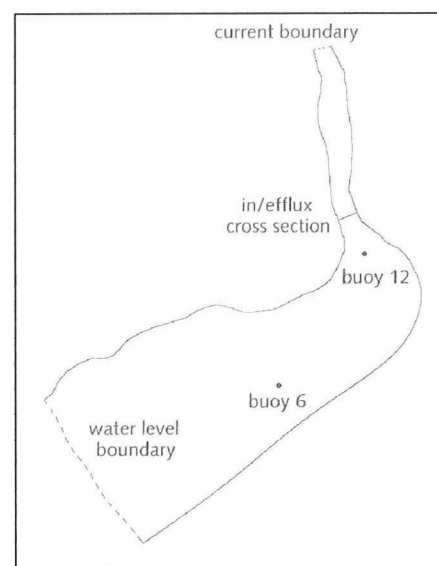


Figure 6-11 Locations in model area

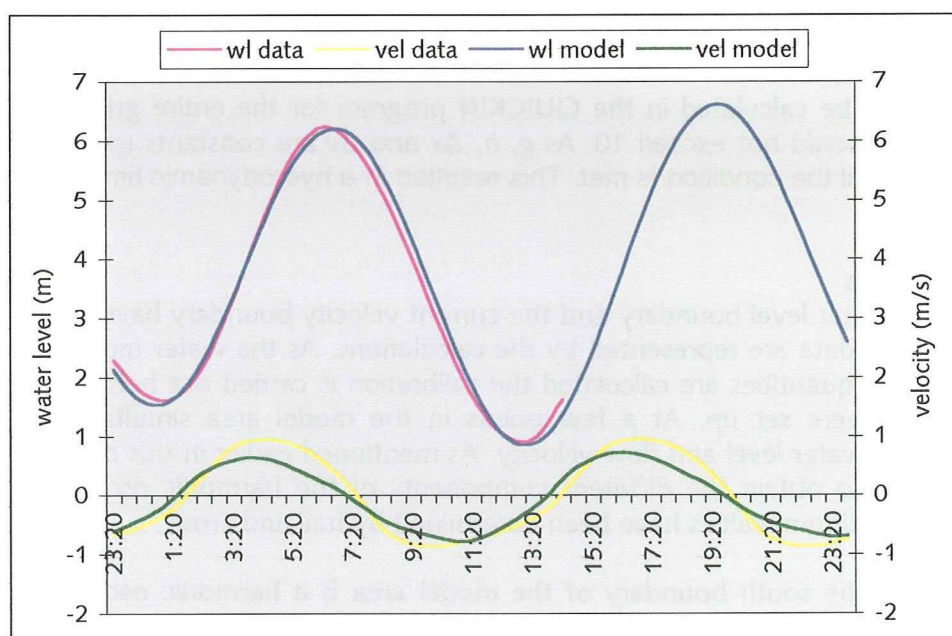


Figure 6-12 Buoy 6 compared

## 6.5 Delft3D-TRAN/BOTT

The TRAN module calculates the sediment transport. As mentioned in chapter 5 a few different formulas are available. Because of the absence of waves the most commonly used formula is that of Van Rijn [1984]. He proposes a distinction between bed load and suspended load. For details on this formula reference is made to annex A.

### sediment properties

As would be expected the sediment properties are of great importance to the transport volumes. In addition to a few common parameters, which have to be set for all transport equations, four distinct values have to be entered for the Van Rijn formula. The majority of the input doesn't need further explanation and is summed up in annex E. One particular aspect however will be handled here, be it brief.

The settling velocity of suspended material (fall velocity) depends on the mean sediment diameter, its relative density and the cinematic viscosity of the water. In case of a solitary sand particle smaller than about 100  $\mu\text{m}$  in "clear" water, its value can be calculated by the following formula (Velden, September 2000):

$$w = \frac{1}{18} \frac{(\rho_s - \rho)gD^2}{\rho\nu} \quad (6.2)$$

where:

w	= particle fall velocity	[m/s]
$\rho_s$	= mass density of sediment	[kg/m <sup>3</sup> ]
$\rho$	= mass density of fluid	[kg/m <sup>3</sup> ]
D	= representative particle diameter (generally $D_{50}$ )	[m]
$\nu$	= cinematic viscosity coefficient	[m <sup>2</sup> /s]

In case of high sediment concentrations the fall velocity is reduced considerably. This phenomenon is called 'hindered settling' (Richardson & Zaki [1954]). The effect is represented by:

$$w_e = (1 - c)^\alpha w \quad (6.3)$$

in which:

$w_e$	= effective fall velocity	[m/s]
w	= particle fall velocity in clear water	[m/s]
c	= sediment concentration (volume%)	[-]
$\alpha$	= coefficient (2.3 for low to 4.6 for high Reynolds numbers)	[-]

Normal values for sediment concentrations in coastal engineering are about 1 volume%.

The values for the fall velocity,  $D_{50}$ ,  $D_{90}$  and the bottom roughness height, will be described in chapter 7, as they were determined in the calibration process.

### numerical parameters

As described in section 5.3 a few numerical parameters have to be entered. Some parameters have to be entered to ascertain the level of influence of certain effects, while other parameters are needed for numerical stability and accuracy.

The parameter in Eq. 5.10 is set to 1 (both for bed load and suspended load), which signifies a maximum influence of the bed slope effect on the transport magnitude. Also factors for the influence of a bed level gradient on the transport direction can be specified.

The dispersion coefficient in Eq. 5.6 must be specified by the user. In this model set-up an algebraic relation was used, in which  $A_{dif}$  and  $B_{dif}$  serve as input for the following formula:

$$D = A_{dif} \cdot 0.16 \cdot U^* \cdot H + B_{dif} \quad (6.4)$$

An important parameter in the BOTT module is the stabilisation factor in the bottom update computation ( $\alpha_{nn}$  in Eq. 5.12). In this case a spatially varying stability correction is used, which is applied to the time averaged transport rates. Furthermore a prescribed time step of twenty-four hours is used in the bottom update computation.

#### time step

The transport time step is expressed in TSCALE, which is the time step of the FLOW module. In case of a suspended sediment calculation the time step must be an even integer. The time step is set to ten times TSCALE, which means a period of two minutes.

#### dredge scenarios

The BOTT module enables the user to implement different dredging scenarios. A minimum depth is required in some areas (see section 1.2 and 1.3); Sogal Channel, the area in front of the general cargo berths and the area in front of the jetties. The reference dredging bed level has to be specified in a separate file, which is created in the QUICKIN program. If the computed depth exceeds the required depth, dredging occurs in that specific grid cell.

Two scenarios were used in this study. The first handles the current situation. Ships with a draught of 10.7 m need to be able to enter the port at high water and reside in the port at low water during (un)loading. Sogal Channel has a minimum depth of 5.5 m and both other areas a minimum depth of 10.7 m below CD (keel clearance of one metre). This scenario is used in the calibration process (see chapter 7). The second scenario handles the future situation after expansion of the port. Vessels with a draught of 14 m are now able to call on the port of Kandla. The minimum depths are set to 8 and 14.2 m below CD. This scenario has been used in the simulation runs

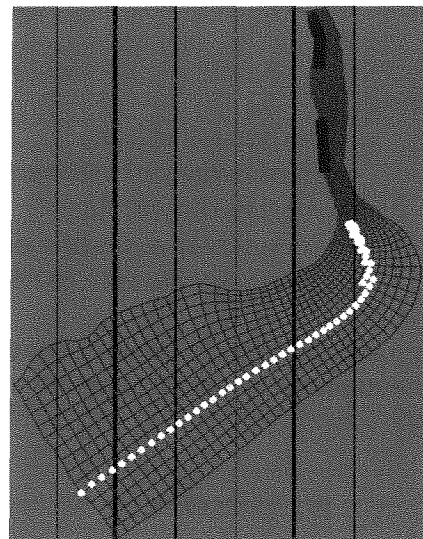


Figure 6-13 Dredging scenario 2

## 6.6 Delft3D-MOR

In Delft3D-MOR the different modules are dynamically coupled via a process tree, in which the user can specify which module has to run for how long and when it has to stop.

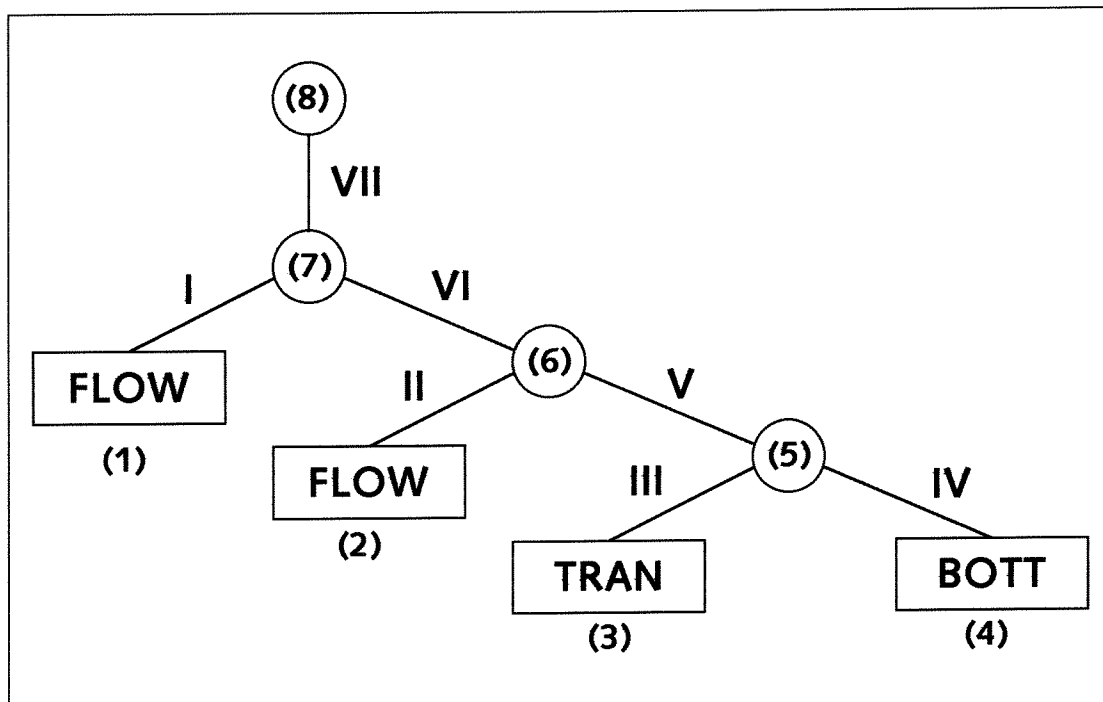


Figure 6-14 Process tree Delft3D-MOR

in which:

(1)...(8) = nodes  
I...VII = branches

Nodes 1 through 4 are called 'end nodes' and contain the different modules. The branches connect parent nodes with child nodes. The branches represent the controllers of the child nodes. The controllers indicate which node has to operate for how long and when it has to stop. The process starts from the 'root node' (node 8). The hierarchical order in which the simulation is built is as follows:

- Branch VII: The simulation starts with this controller. It "tells" branch I to start the FLOW module. It is executed only once.
- Branch I: The initial FLOW run has an adaptation time which is substantially longer than the adaptation time described in section 5.3, because the model area is in rest. An initial time period of 10 hours is excluded from the computation; the FLOW module thus is run for 35 hours (a mixed tide of a 25 hour period is used).
- Branch VI: The total number of times, in which the combination of FLOW and TRAN-BOTT modules is run, is specified in this branch, i.e. the number of weeks that the user wants to simulate (see branch IV).
- Branch II: This branch is similar to branch I with the exception of the adaptation time. Here the adaptation time is just one hour (see section 5.3). The total time this node is run thus becomes 26 hours.

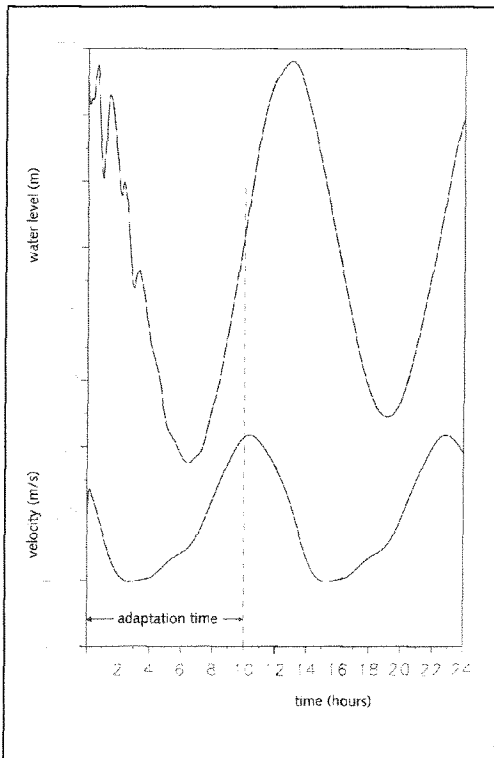


Figure 6-15 Adaptation time

**Branch V:** The continuity correction (see section 5.3) is handled here. In this case the TRAN and BOTT module are executed seven times before the FLOW module is run again.

**Branch III:** The TRAN module is run for 25 hours in order to calculate the average sediment transport over one mixed tidal period.

**Branch IV:** This branch is used to update the bathymetry. The averaged transports of the TRAN module are kept constant for a period of time specified by the user. A time step of 24 hours (one day) is used, which is more convenient than the 25 hours of the other modules. This means that the continuity correction is executed for one week.

A simulation would look like this: first the FLOW module is run for 35 hours. Then the FLOW module is run again, this time for 26 hours. The outcome of these calculations is used in the TRAN module, which is run for 25 hours. The average transports are used to update the bed level in the BOTT module. Via the continuity correction the TRAN module is run again, then the BOTT module again, etc. After this process is repeated for seven times (one week has been simulated by now), the FLOW module is run again to calculate the new hydrodynamic situation due to a new bathymetry. Then the TRAN and BOTT modules come into play once again, etc, etc. The user must specify the number of weeks that have to be simulated in the MOR module.

## 7 Calibration

### 7.1 Introduction

As mentioned in chapter 6 a few parameters for the input will be varied in the calibration process. A comparison will be made with measured data to obtain the optimum values (see chapter 4). In the TRAN and BOTT module a few parameters will be varied. Two different values for the sediment diameter will be used with their matching fall velocities. The Chézy coefficient will be set to a uniform value (which will be varied; three values) or will be calculated via the Manning coefficient (which in its turn will be varied; also three values). A last parameter that has to be specified in the Van Rijn formula is the bottom roughness height (again three values). These different parameters will lead to 36 possible combinations.

### 7.2 Parameters

#### bottom roughness height

The formula of Van Rijn requires a bottom roughness height (see annex A) as input. In this case three values were used: 0.01, 0.03 and 0.05 m. The symbol for this parameter is:  $\xi_c$ .

#### Chézy coefficient

The simplest formulation is the spatially constant Chézy coefficient. A more sophisticated formulation is Manning's formulation. It reads:

$$C_{2D} = \frac{\sqrt[6]{H}}{n} \quad (7.1)$$

in which:

$C_{2D}$	= two dimensional Chézy coefficient	[m <sup>1/2</sup> /s]
H	= total local water depth	[m]
n	= Manning coefficient	[s/m <sup>1/3</sup> ]

This formulation causes deeper parts of the model area to be less rough. Water will flow more easily through the deep channels than over shallow parts.

#### sediment size and fall velocity

The Van Rijn formula requires a  $D_{50}$  and a  $D_{90}$  value. Two types of sediment were used; a  $D_{50}/D_{90}$  of 80/100  $\mu\text{m}$  and a  $D_{50}/D_{90}$  of 60/75  $\mu\text{m}$ . Via Eq. 6.2 and Eq. 6.3 the matching fall velocities are calculated; they are 0,0053 m/s and 0,003 m/s.

Table 7-1 Combinations

D <sub>50</sub> /D <sub>90</sub> 80/100 $\mu\text{m}$ fall velocity 0,0053 m/s						D <sub>50</sub> /D <sub>90</sub> 60/75 $\mu\text{m}$ fall velocity 0,003 m/s					
Nr.	Chézy	$\xi_c$	Nr.	Manning	$\xi_c$	Nr.	Chézy	$\xi_c$	Nr.	Manning	$\xi_c$
1	60	0,01	10	0,02	0,01	19	60	0,01	28	0,02	0,01
2		0,03	11		0,03	20		0,03	29		0,03
3		0,05	12		0,05	21		0,05	30		0,05
4	70	0,01	13	0,025	0,01	22	70	0,01	31	0,025	0,01
5		0,03	14		0,03	23		0,03	32		0,03
6		0,05	15		0,05	24		0,05	33		0,05
7	80	0,01	16	0,03	0,01	25	80	0,01	34	0,03	0,01
8		0,03	17		0,03	26		0,03	35		0,03
9		0,05	18		0,05	27		0,05	36		0,05

### 7.3 Results

#### bottom roughness height

Figure 7-1 shows the rate of siltation for combination numbers 4, 5 and 6 in the channel area. The only parameter varied in these calibration runs is the bottom roughness height, which can be interpreted as the bed load layer thickness. The figures in table 7-2 were obtained by the programme KUBINT, which calculates the total volume below a reference level in an area defined by the user (see figure 7-1). Negative values indicate erosion, positive values sedimentation.

Table 7-2 Sed/ero quantities 4,5,6

Area	Run no.	$\xi_c$ (m)	m <sup>3</sup> /month	cm/month
Channel	4	0,01	6502	2
	5	0,03	4833	1
	6	0,05	3965	1
Berths	4	0,01	-35639	-15
	5	0,03	-22757	-9
	6	0,05	-17685	-7
Jetty	4	0,01	63528	13
	5	0,03	39536	8
	6	0,05	30115	6

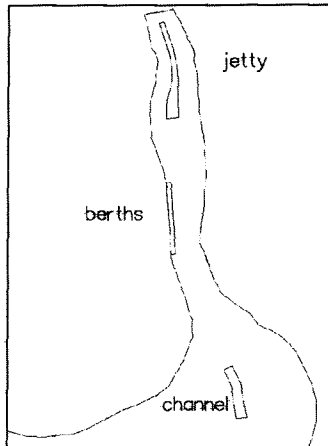


Figure 7-1 Areas of comparison

It can be seen that as the bottom roughness height increases, the values of sedimentation and erosion decrease. This holds for all simulations (see annex G). Theoretically according to the Van Rijn formula the sediment transports decrease with increasing bottom roughness. Thus the results are trustworthy. From figure 7-2 and 7-3 it can be seen that the suspended sediment transport is dominant. The residual suspended transport is about a factor 500 larger than the residual bed load transport.

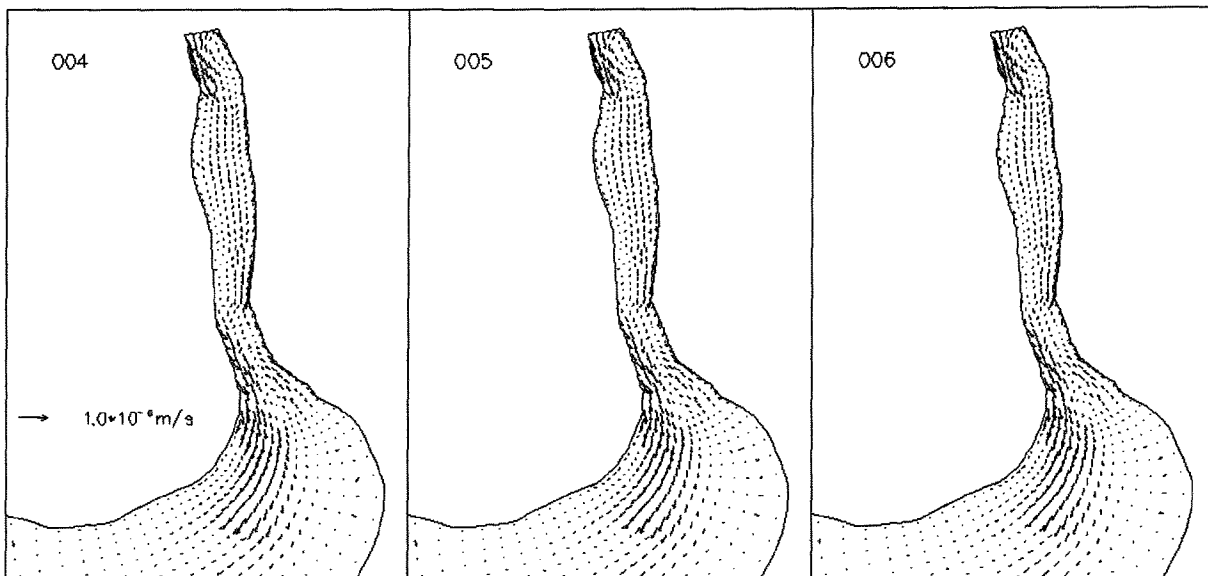


Figure 7-2 Residual bed load transport, combinations 4, 5 and 6

The bed load transport doesn't differ much in the regarded simulation runs. This is actually the case in all calibration runs.

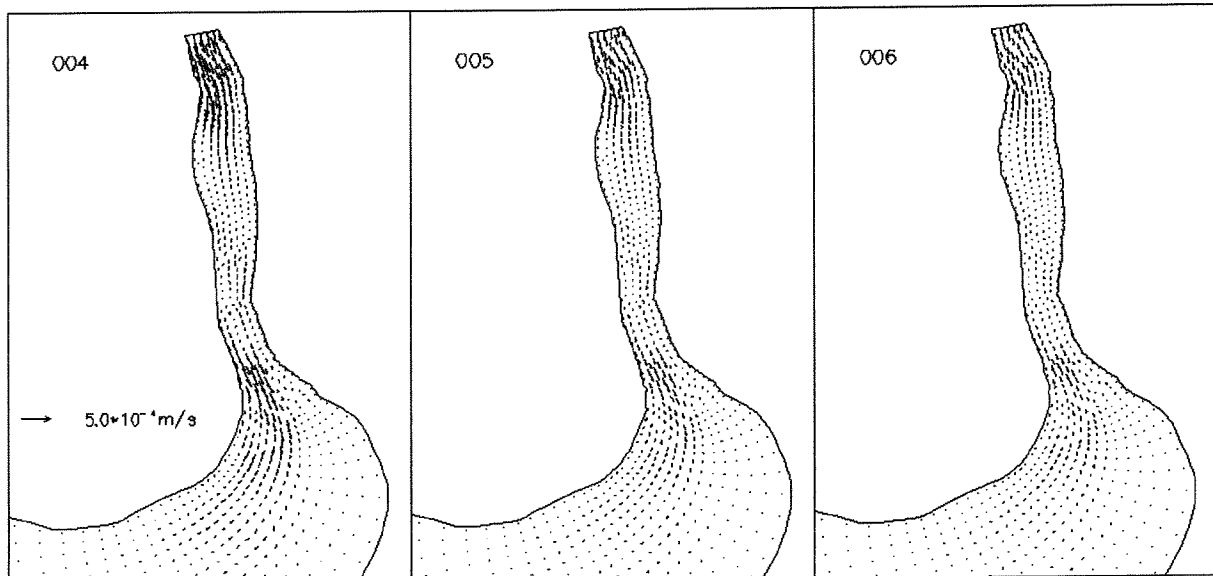


Figure 7-3 Residual suspended transport, combinations 4, 5 and 6

As the suspended transport is much larger than the bed load transport, the latter is neglected. The magnitude of the suspended sediment transport decreases from run number 4 to 6. In this sequence only the bottom roughness is enlarged. The residual transport is largest in the parts of the model area where the width of the creek is smallest. The flow velocities in these parts are highest and the net efflux of the tidal flow causes the sediment transport to be directed southward.

The sedimentation/erosion patterns can be recognised in figure 7-4. It is clear that a lot of sediment is deposited in the area just south of the jetties, where the creek suddenly widens. The maximum width here is more than 1300 metres, while the width at the northern boundary is less than 800 metres. The flow velocity decreases and loses part of its transport capacity, causing sediment to settle. This area is coloured red. The residual sediment that prevails at the creek outfall settles immediately as the flow velocity decreases rapidly. It is not transported further into Sogal Channel. The distinct sedimentation and erosion spots west of the bend in Sogal Channel are a result of a shoal in that area. As a net efflux prevails, the shoal migrates in the flow direction. This can be recognised as the north eastern part is subject to erosion and further downstream the south western part is subject to sedimentation.

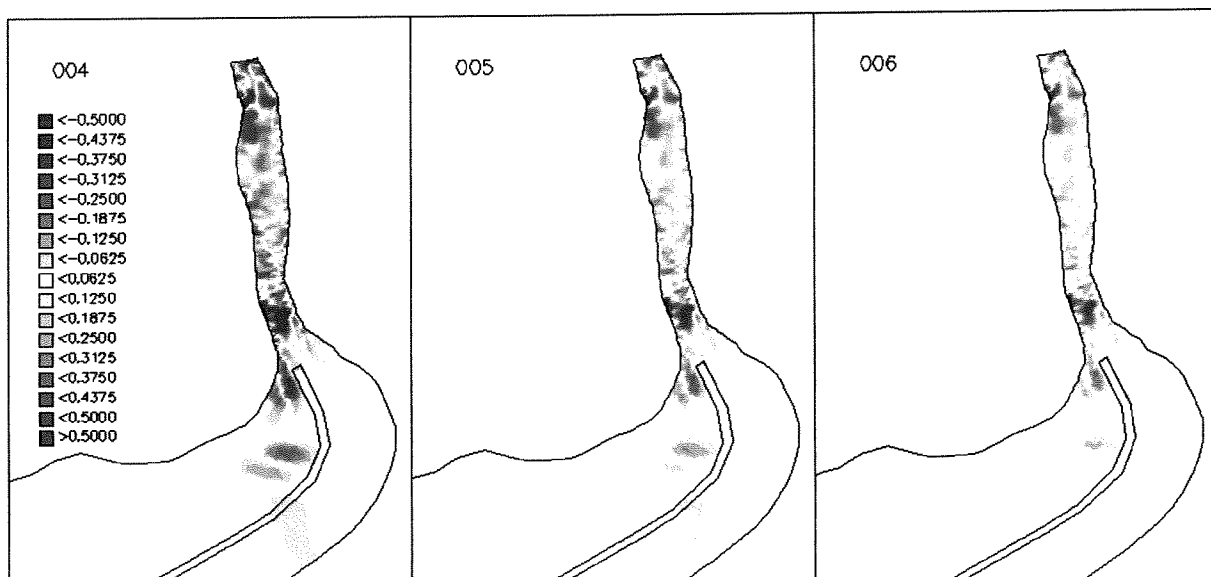


Figure 7-4 Sedimentation/erosion pattern, combinations 4, 5 and 6



In figure 7-5 the weekly sedimentation and erosion quantities are calculated for the channel area in order to assess the development in time. The rate of siltation decreases rapidly. A more elaborate description of this phenomenon is made later on in this section.

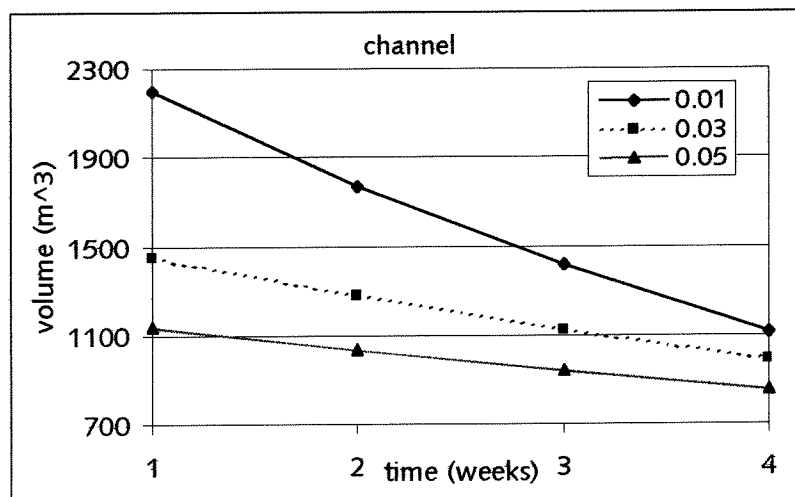


Figure 7-5 Weekly sedimentation in channel area, combinations 4, 5 and 6

### Chézy coefficient

The Chézy coefficient (C) has been given by three constant values and has been calculated via the Manning formulation with three values for the Manning coefficient. Firstly table 7-3 shows the quantities of sedimentation or erosion for the situation with uniform (but varying) Chézy coefficient (i.e. combination 19, 22 and 25).

Table 7-3 Sed/ero quantities 19,22,25

Area	Run no.	C (m <sup>1/2</sup> /s)	m <sup>3</sup> /month	cm/month
Channel	19	60	26982	7
	22	70	27861	8
	25	80	29217	8
Berths	19	60	-70877	-30
	22	70	-54783	-23
	25	80	-41684	-17
Jetty	19	60	108741	22
	22	70	114075	24
	25	80	117851	24

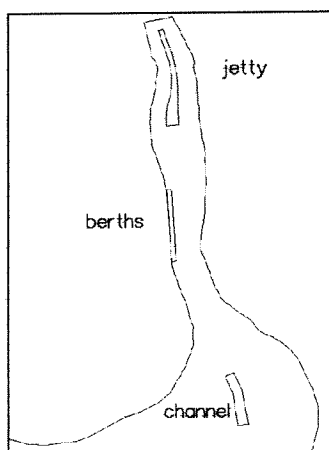


Figure 7-6 Areas of comparison

As the uniform Chézy value increases there is slightly more sedimentation and a lot less erosion. In theory if the Chézy value increases the critical shear stress and critical velocity decrease. The sediment is picked up more easily and higher concentrations are the effect. During high and low water slack more sediment is thus deposited. Figure 7-7 shows the sediment concentration during maximum ebb flow.

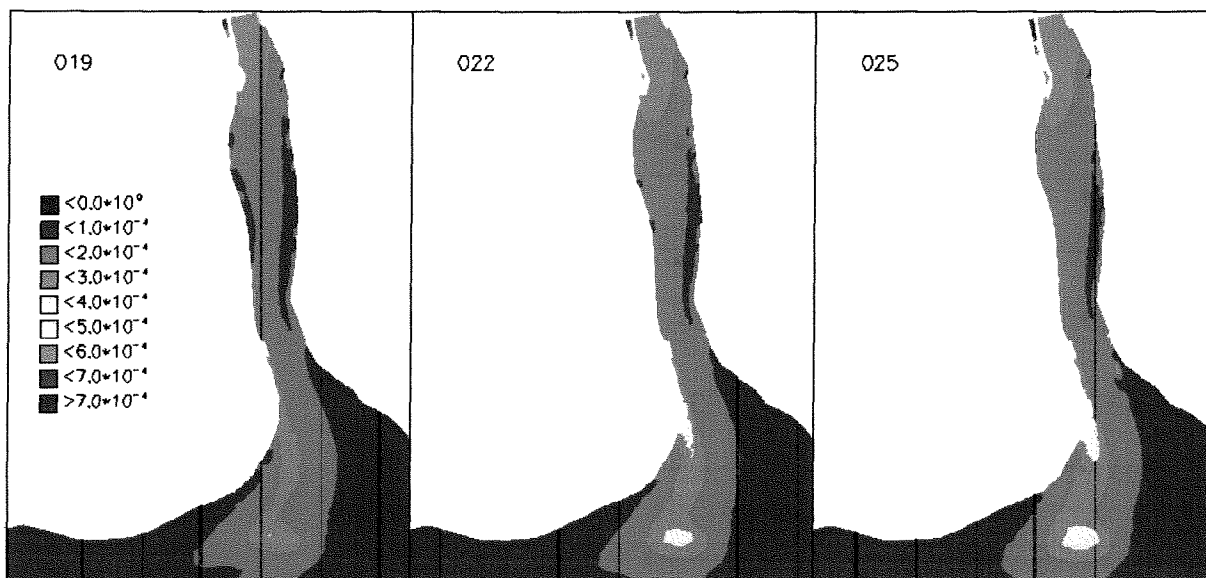


Figure 7-7 Sediment concentrations, combinations 19, 22 and 25

As the quantities in the jetty area and the channel area differ marginally, the focus is put on the berths area. Figure 7-8 shows the residual suspended transport for this area. Although a net efflux prevails in Kandla Creek, the residual transport is directed into the creek. This can be explained by the fact that the velocities outside the creek are not high enough to pick up large amounts of sediment. During flood water with a low sediment concentration flows into the creek. As the flow has passed the narrowest part of the creek inlet, sediment is gradually brought into suspension (the arrows become larger in northern direction). This sediment then settles in the wider area just north of the berths area. When the flow turns around again water with low concentration is forced through the berths area. As it accelerates it starts to pick up sediment (this is just visible in the bottom part of the pictures in figure 7-8). This process causes the berths area to erode.

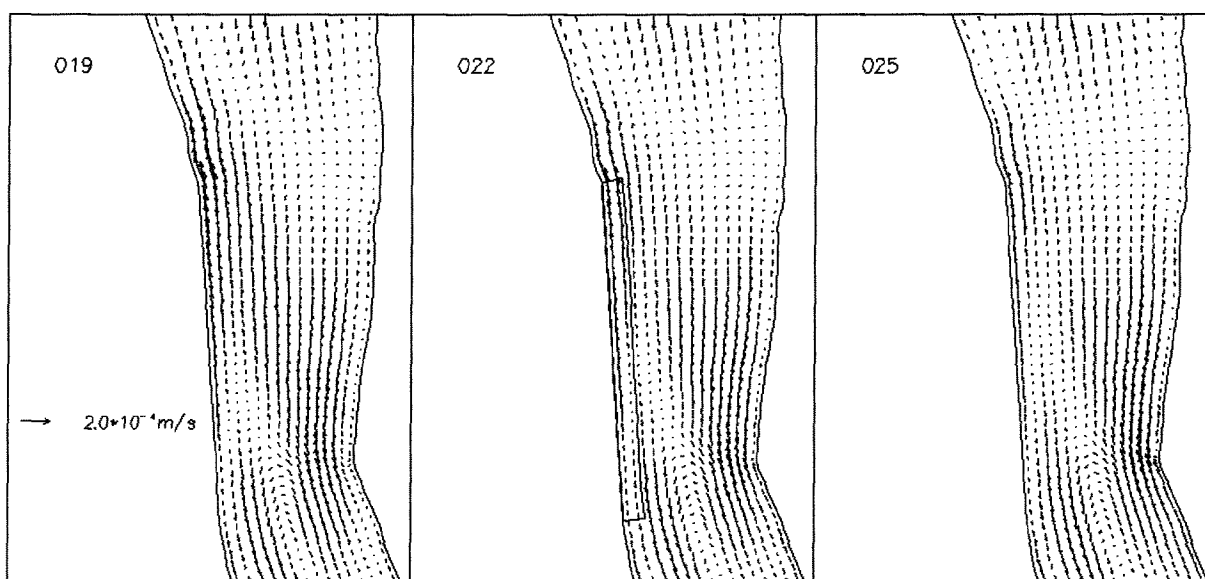


Figure 7-8 Residual suspended transport, combinations 19, 22 and 25

The rate of erosion decreases with time in the berth area (see figure 7-9).

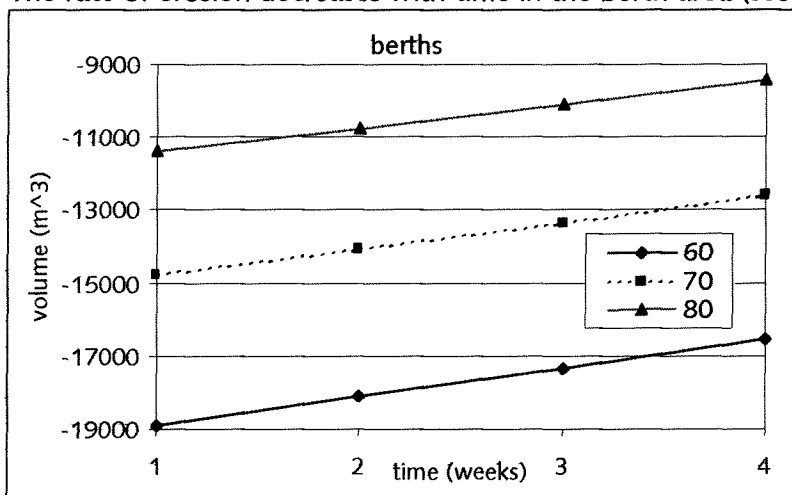


Figure 7-9 Weekly erosion in berths area, combinations 19, 22 and 25

Secondly table 7-4 shows the results for the calibration runs in which the Manning coefficient (n) is varied. The numbers of the combinations are: 28, 31 and 34.

Table 7-4 Sed/ero quantities 28,31,34

Area	Run no.	N (s/m <sup>1/3</sup> )	m <sup>3</sup> /month	cm/month
Channel	28	0,02	19145	5
	31	0,025	17785	5
	34	0,03	19743	5
Berths	28	0,02	-68712	-29
	31	0,025	-96165	-40
	34	0,03	-121044	-50
Jetty	28	0,02	101813	21
	31	0,025	90964	19
	34	0,03	80440	17

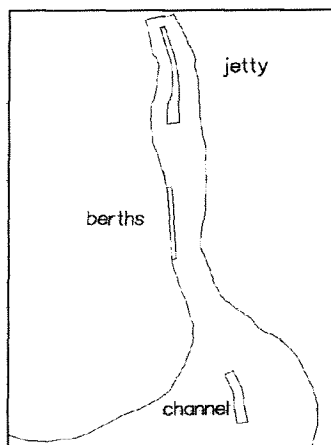


Figure 7-10 Areas of comparison

With increasing Manning coefficient the Chézy coefficient decreases and the shear stress increases. As a result sediment is moved less easily. In fact the opposite happens of what is described above (increasing uniform Chézy value). The Manning formula introduces a depth dependant Chézy coefficient (see Eq. 7.1). The Chézy coefficient increases with increasing depth. Therefore deep areas are smoother than shallow areas. This means that water will flow more easily through deeper parts and less easily over the shallow parts of the model area. Figure 7-11 shows the residual suspended transport. The same phenomenon can be observed as in figure 7-8, only on a larger scale, which follows from table 7-4.

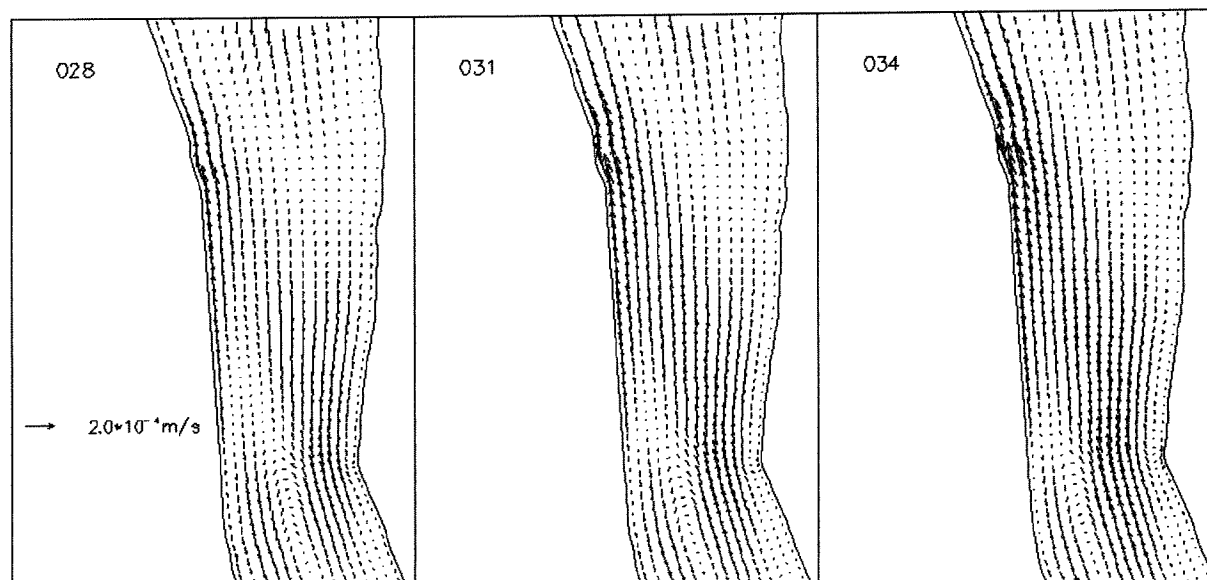


Figure 7-11 Residual suspended transport, combinations 28, 31 and 34

Once more it is shown that the rate of erosion declines (figure 7-12).

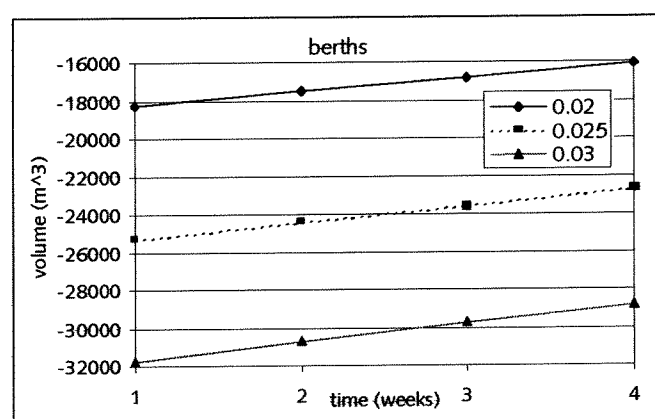


Figure 7-12 Weekly erosion in berths area, combinations 28, 31 and 34

Comparing table 7-3 and 7-4, it can be seen that applying a Manning coefficient to calculate the Chézy coefficient causes less sedimentation in the channel and jetty area and more erosion in the berths area than in case of a uniform value for the Chézy coefficient. The effect is twofold. On the one hand, if more water flows through deeper parts, the velocities will be higher and sediment will be picked up more quickly. On the other hand, if less water flows over the shallow areas, the overall sediment concentrations will be smaller, thus sedimentation will be less. A comparison is made between calibration run 22 (Chézy value 70) and 28 (Manning coefficient 0,02); see table 7-5.

Table 7-5 Sed/ero quantities 22, 28

Area	Run no.	n	m <sup>3</sup> /month	cm/month
Channel	22	C = 70	27861	8
	28	n = 0,02	19145	5
Berths	22	C = 70	-54783	-23
	28	n = 0,02	-68712	-29
Jetty	22	C = 70	114075	24
	28	n = 0,02	101813	21

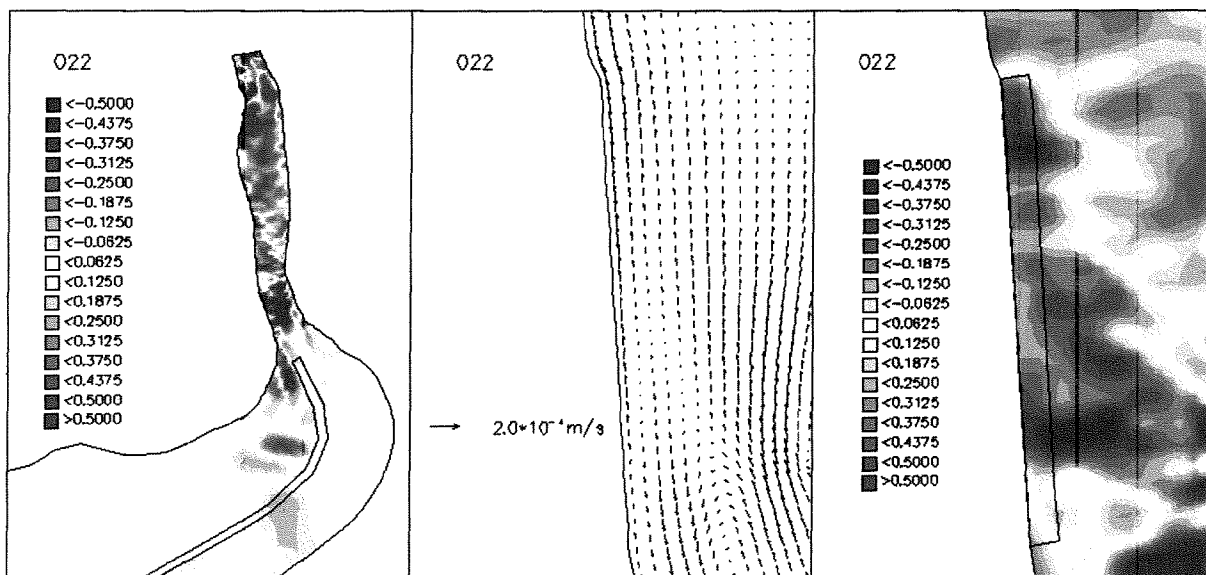


Figure 7-13 Sedimentation/erosion pattern and residual suspended transport, no. 22

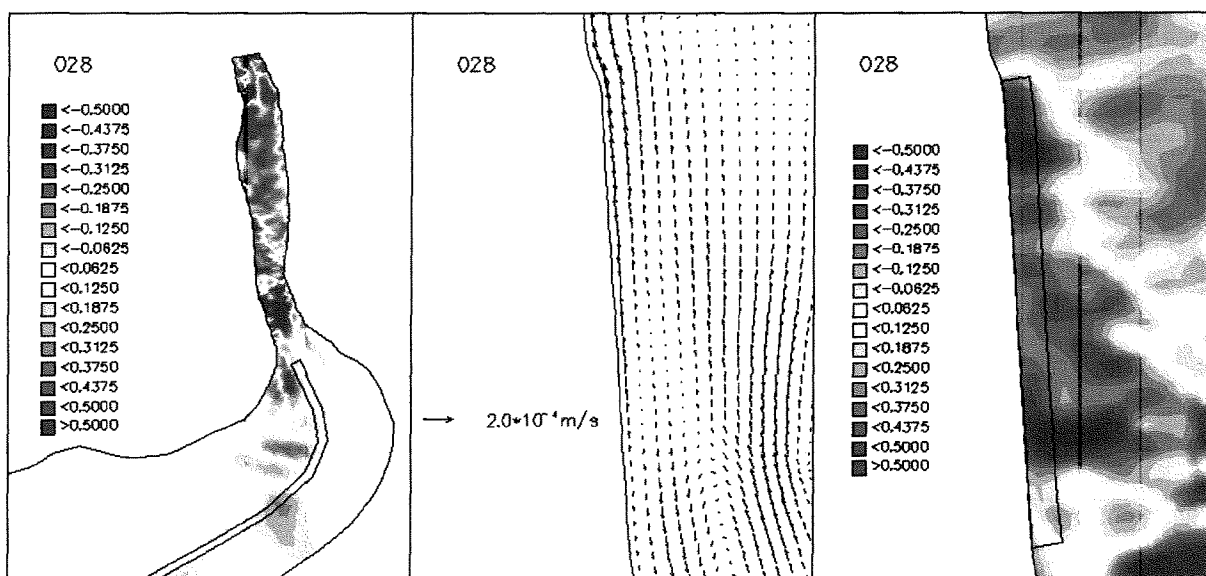


Figure 7-14 Sedimentation/erosion pattern and residual suspended transport, no. 28

Although the differences are small a few notes are made. In the first picture of figures 7-13 and 7-14 it can be seen that there is less sedimentation in the part of Sogal Channel that lies directly in front of the creek outfall. The water flows more easily through this deep part when a Manning coefficient is applied (run no. 28) and this causes more natural "flushing". Also the morphological activity around the shoal to the west of the bend in Sogal Channel is less severe in case no. 28. The flow over these shallow parts experiences more resistance and thus "avoids" the shoal.

From the second and third pictures in figures 7-13 and 7-14 it can be noticed that there is more erosion in the berths area in case of the Manning formulation. The depth causes this area to be less rough than in case of the uniform Chézy value.

### sediment size and fall velocity

Two sediment sizes have been used in the calibration process ( $D_{50}$  of 60  $\mu\text{m}$  and 80  $\mu\text{m}$ ). Two comparisons will be made: one with a bottom roughness of 0,01 m and a uniform Chézy value of 70  $\text{m}^{1/2}/\text{s}$  (combination numbers 4 and 22) and one with a bottom roughness of 0,05 m and a Manning coefficient of 0,02  $\text{s}/\text{m}^{1/3}$  (combination numbers 12 and 30). A comparison with constant bottom roughness but varying Chézy value has proved to be useless as the same phenomenon occurs with different sediment sizes.

Table 7-6 Sed/ero quantities 4,12,22,30

Area	Run no.	$\xi_c$ (m)	$D_{50}$ ( $\mu\text{m}$ )	$\text{m}^3/\text{month}$	$\text{cm}/\text{month}$
Channel	4	0,01	80	6502	2
	22		60	27861	8
	12	0,05	80	1307	0
	30		60	8328	2
Berths	4	0,01	80	-35639	-15
	22		60	-54783	-23
	12	0,05	80	-22911	-10
	30		60	-24416	-10
Jetty	4	0,01	80	63528	13
	22		60	114075	24
	12	0,05	80	26478	5
	30		60	37815	8

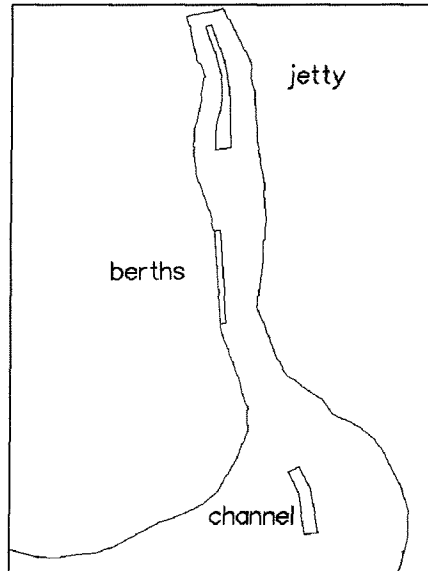


Figure 7-15 Areas of comparison

It is obvious that a smaller sediment size causes increasing sedimentation and increasing erosion in the considered areas (table 7-6). Smaller sediment is brought into motion more easily during maximum flow velocities causing more erosion. This also causes higher concentrations. During slack periods the sediment settles and sedimentation is larger than in the case of the larger sediment particles.

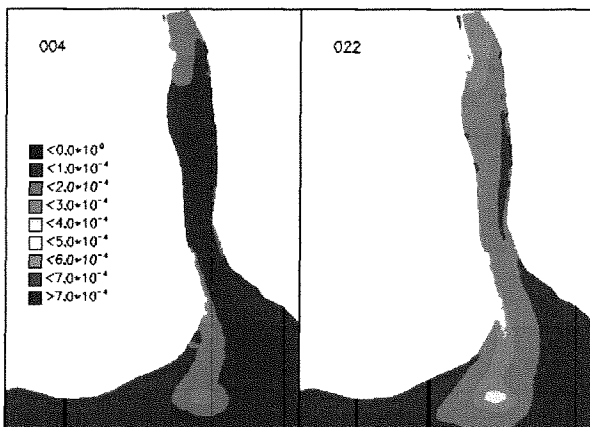


Figure 7-16 Sediment concentration 4 and 22

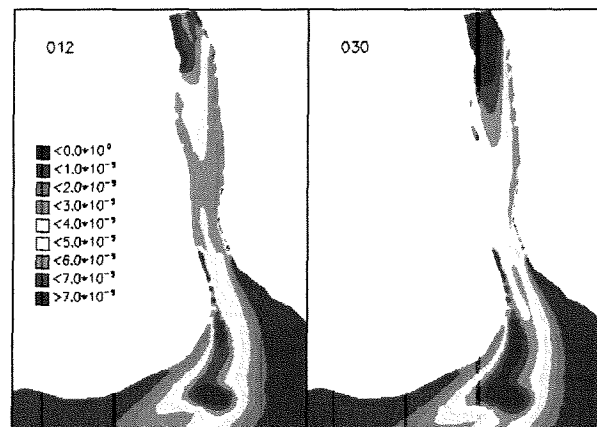


Figure 7-17 Sediment concentration 12 and 30

Figures 7-16 and 7-17 show that the calibration runs with a small sediment size (22 and 30) cause higher concentrations than the calibration runs with a larger sediment size (4 and 12). The difference between run number 4 and 22 is more distinct than the difference between run 12 and 30. The scale in figure 7-17 is ten times smaller than the scale in figure 7-16. This is done, because the concentrations in run 12 and 30 are so small that a distinction is not noticeable if the larger scale is used. The difference in concentration is due to the different

Chézy coefficient. In run 4 and 22 a uniform value is used, which causes the entire model area to be equally rough. Run numbers 12 and 30 use a Manning coefficient, thus causing the flow to "avoid" the shallow areas. In run 4 and 22 sediment is easily picked up from the shallow areas, while in run 12 and 30 the amount of sediment that is picked up in the shallow parts is significantly less.

The difference in sedimentation and erosion is larger in case of a bottom roughness of 0,01 m (figure 7-18) than in case of a bottom roughness of 0,05 m (figure 7-19). This is in compliance with the fact that a larger bottom roughness has the same effect as a larger sediment size (see description of bottom roughness above).

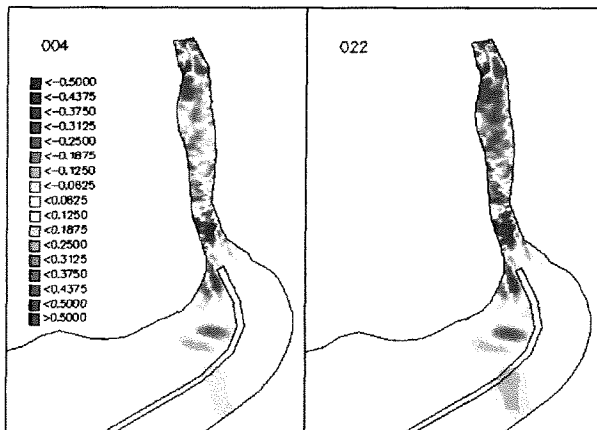


Figure 7-18 Different patterns 0.01 m, 4 and 22

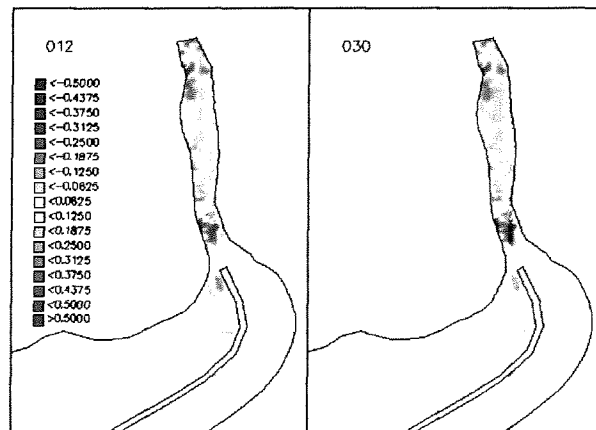


Figure 7-19 Different patterns 0.05 m, 12 and 30

### rate of siltation

As can be seen from figures 7-5, 7-9 and 7-12 the rate of siltation declines in time. The concept of an equilibrium state can help to explain this phenomenon. It occurs, as the deviation from an equilibrium state is larger at the beginning of a simulation than at the end of one. The redistribution of sediment equalizes this deviation. Figure 7-20 clearly shows the development of the rate of siltation for run number 26. In order to illustrate this effect more explicitly, the simulation time was set to one year. Figure 7-21 shows the development of the average depths in the different areas. Both the channel area and the berths area converge to an equilibrium. The development of the jetty area fluctuates. First there is sedimentation, but this changes to erosion later on. The value of erosion also declines in time, which could indicate that an equilibrium is reached via a fluctuation around the equilibrium value.

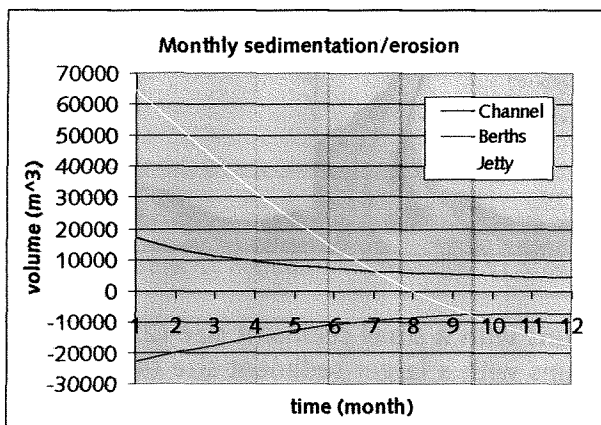


Figure 7-20 Monthly development, combination 26

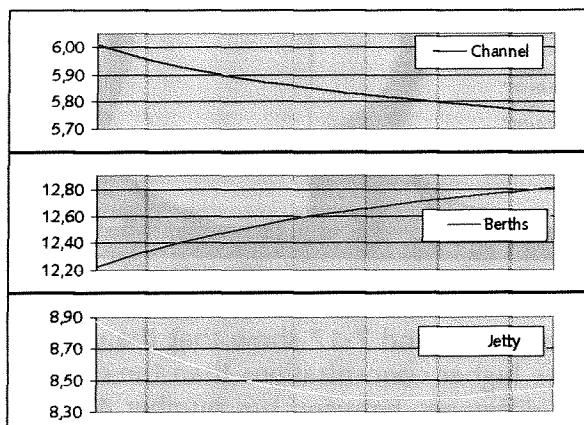


Figure 7-21 development average depth

The effect of the decline in time causes all calculated sedimentation and erosion quantities to be too small. The areas that are subject to sedimentation are dredged to the required depth and the sedimentation is likely to be constant. Table 7-7 shows the average difference in terms of percentage of all 36 calibration runs between the calculated rate of siltation and a constant rate of siltation. The results are separated for the different areas and the different values for bottom roughness. The sediment size and the Chézy value don't have a large influence on the percentages. The constant rate is obtained by calculating the sedimentation in the first 24 hours and multiplying that amount by 28 (= four weeks).

Table 7-7 Difference in terms of percentage

	0,01 m	0,03 m	0,05 m
Sogal Channel	+ 46%	+ 24%	+ 17%
Berths area	+ 3%	+ 2%	+ 2%
Jetty area	+ 19%	+ 8%	+ 5%

The effect is not of great influence on the rate of erosion in the first month of simulation in the berths area. If the simulation time is set longer however (a year for instance, see figure 7-20), the decline is clearly visible. The decline in the other two areas manifests itself in the first month already. The effect is largest for a small bottom roughness. Both areas are subject to sedimentation and as the sediment accumulates the flow velocities increase (due to the decline in cross section over the area) and the sediment transport capacity increases.

### dredging activities

In 1999 the most shallow part of Sogal Channel was about 5,1 metres, the average depth in the berths area was 12,2 metres and the average depth in the jetty area was 8,9 metres. As the bathymetry of 1999 was the initial bathymetry used in the simulations the depths in the channel and the jetty area weren't sufficient (5,5 and 10,7 metres below Chart Datum are minimum depths). A dredging scenario is included to assess the quantities of material that would settle if the required depths are set in the initial bathymetry. The decline of the rate of siltation in time suggests that if the depths are further from an "equilibrium" depth, the initial rate of siltation will be higher than calculated in the combinations described above. The influence of this effect has been assessed by manipulating the depth-file in Delft-QUICKIN so that the required depths are met and calculating the morphological development. The different depths in the jetty area are shown in figure 7-22 and 7-23. A comparison is made with run number 26.

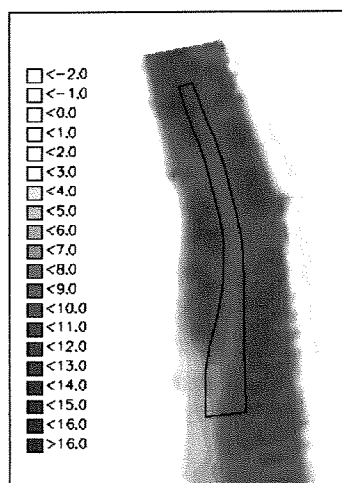


Figure 7-22 Initial depth jetty

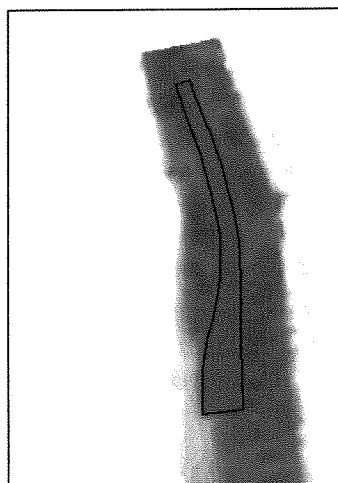


Figure 7-23 Manipulated depth



Table 7-8 Sed/ero quantities for manipulated depth

Run number	Sogal Channel	Berths area	Jetty area
26	16037	-21529	60633
26-manipulated depth	18943	-23028	111667
	+ 18%	+ 7%	+ 84%

The effect is the largest in the jetty area. The deviation of the required depth from the initial depth is the largest in this area. In Sogal Channel the initial depth is manipulated less severely.

## 7.4 Overall findings

In general the calibration runs with varied parameters result in explicable differences in outcome. The areas of interest show logical sedimentation and erosion patterns. With regard to the measured data and known dredging quantities however deviations still exist.

The jetty area is subject to sedimentation. In order to keep that area at the required depth all the accreted material should be dredged. The before mentioned amount of 154.000 m<sup>3</sup> or 32 centimetre accretion per month is represented by a few of the calibration runs. If the effect of the declining rate of siltation is taken into account as well as the effect of the manipulated depths the total amount of deposited material is between 40.000 and 258.000 m<sup>3</sup>.

The average depth in the berths area has increased during 1999. The measured data show that 41.100 m<sup>3</sup> has been removed, either by the marginal dredging (see section 2.1) or by erosion. The calculations of the model show that the berths area is subject to erosion. The amounts are between 16.500 and 133.400 m<sup>3</sup> per month.

Like the jetty area Sogal Channel is subject to sedimentation. According to CWPRS [1999] the amount of material dredged from the channel is 246.000 m<sup>3</sup> per month in order to prevent sedimentation of 19 centimetres a month. The simulations however do not show such vast sedimentation. The calculations show amounts between 1800 and 50.300 m<sup>3</sup> a month.

The right parameters for the simulations that will be run have to be chosen. As the parameters represent physical concepts they will have some sort of coherence. It would be logical to assume that a small sediment size accompanies a small bottom roughness and a high Chézy coefficient (or low Manning coefficient). The opposite goes for larger sediment sizes.

Firstly the assumed negligence of waves may account for the rather low sedimentation in Sogal Channel. In the shallower parts of the model area waves could contribute a lot to the sediment transport processes, even if the wave climate isn't that severe. The sediment concentration would be higher and during the flood period more sediment would be transported into Kandla Creek. At slack periods the sedimentation would be larger (and erosion in the berths area smaller). It seems a reasonable explanation for the absence of morphological activity in the area around Sogal Channel. The flow velocities are not high enough to cause sedimentation or erosion.

Secondly the area that is considered in the calculations is smaller than the area as mentioned by CWPRS. The part of Sogal Channel that is located directly at the outfall of Kandla Creek however is subject to quite large sedimentation. The decline in average depth thus is a better quantity for comparison than the absolute numbers of cubic meters. In Sogal Channel the rate of decline of the average depth is about 20 cm a month according to CWPRS [1999]. The calibration runs show a rate of 1 to 8 cm. The effects of the decline of the rate of siltation as well as the effect of the dredged depths are not taken into account yet.

The simulation run that represents the measured data the closest is number 25. A few factors contribute to this. The combination of a small sediment size, a small bottom roughness height and a high uniform Chézy coefficient, causes the material to be transported more easily. This can also be seen from the residual transport pattern in annex H. The simulation runs of chapter 8 will all be done with the parameters of combination 25, which are:

$$\begin{aligned} D_{50}/D_{90} &= 60/75 \text{ } \mu\text{m} \\ w_{\text{fall}} &= 0.003 \text{ m/s} \\ \text{Chézy} &= 80 \text{ m}^{1/2}/\text{s} \\ \xi_c &= 0.01 \text{ m} \end{aligned}$$

In order to verify the current dredging amounts a simulation is made with the manipulated depth as mentioned in section 7.3. The average depth in Sogal Channel is set to 5.5 m below CD and the depth in the berths and jetty area is set to 10.7 m below CD. The results are summed up in table 7-8, the effect of the declining rate of siltation is already taken into account.

Table 7-9 Morphological development of current situation

area \ develop-ment	amounts (m <sup>3</sup> /month)	average accretion (cm/month)
Sogal Channel	43260	12
Berths	-45156	-19
Jetty	247884	51

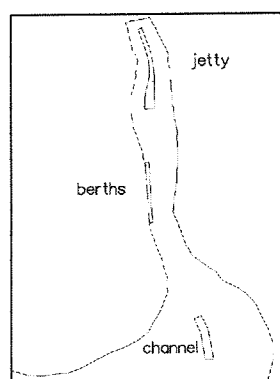


Figure 7-24 Location areas

The amount of sedimentation in Sogal Channel does not reach the 246.000 m<sup>3</sup> mentioned by CWPRS [1999]. However as stated above the accretion in centimetres is a more useful quantity for comparison. According to CWPRS the accretion is 19 centimetres a month, while the calculated accretion is 12 cm a month. These values are of the same order of magnitude. The negligence of wave influence could account for the fact that the amount is still too low. Measurements have shown that the berths area has been deepened by 17 cm in a year, probably by marginal dredging (see section 4.3). The model has calculated erosion at a rate of 19 cm a month. This is a lot more than the measured data, although the rate of erosion declines in time (see figure 7-5).

The jetty area is subject to large sedimentation. The amount is more than 60% higher than the 154.000 m<sup>3</sup> or 32 cm accretion per month mentioned by CWPRS. This can be explained by the fact that the manipulated depth used for this simulation is larger than the measured depth. Table 4-1 shows that the depth in 1999 was about 9 metres below CD. The required depth of 10.7 metres wasn't available then. A simulation with the measured data is also run, which leads to more realistic sedimentation in this area. The accretion amounted to 138.768 m<sup>3</sup> or 29 cm per month. The difference with the 154.000 m<sup>3</sup> or 32 cm is very small, which justifies the choice of the used parameters.

As a whole the calibration process has not shown the validation of the occurring dredging quantities as pursued by the goal of this study. Especially the shallow area around Sogal Channel isn't subject to the morphological activity as measured during 1999 and 2000, which is shown in figure 4-2. As described earlier in this section, the negligence of wave influence could be the cause of this discrepancy. The parameter settings that are chosen to simulate the

future situation in the next chapter represent the measured data the closest. As mentioned before it isn't clear how the dredging amounts given by CWPRS are measured. In general dredging quantities given by the Dredging Corporation of India (DCI), which is the government owned dredging company, are too high. Experts have encountered this phenomenon in most Indian ports. It is clear that the overall accuracy of the outcome of the simulations has to be handled with care. There are too many uncertainties to be able to make a comparison on which quantitative conclusions can be made.

For the entire details on all the combinations reference is made to annex G, H and I.

## 8 Simulation runs

### 8.1 Introduction

The goal of this study is to assess the effects of applying different training walls in order to reduce the amounts of maintenance dredging in the future situation of port expansion. Firstly however the future situation is simulated without training walls in order to verify the amounts of maintenance dredging as calculated by CWPRS [1999] and KPT. Secondly three concepts with different training walls are simulated. The concept of a training wall is implemented via so-called "thin dams". They are infinitely thin objects defined at the velocity points of the staggered grid (see figure 5-2) and prohibit flow between the two adjacent computational grid cells.

### 8.2 Future situation

The depth in the different areas has been manipulated in the QUICKIN programme. The minimum depth in Sogal Channel is set to 8 metres below CD. This depth allows ships with a draught of 14 metres to enter the port at high water. For ships to be able to reside in the port at low water during loading and unloading the depth in the berths area and the jetty area will have to be in excess of 14,2 metres below CD. The manipulated bathymetry can be observed in figure 8-1. A simulation is made with the new bathymetry to assess the expected rate of siltation.

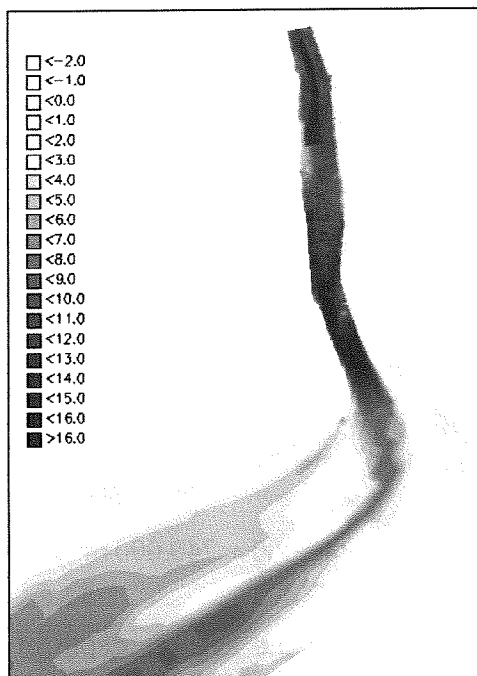


Figure 8-1 Required depth future situation

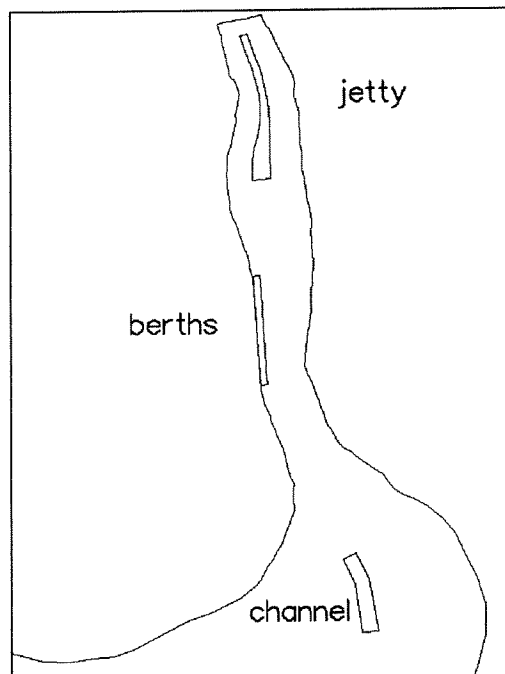


Figure 8-2 Areas of comparison

In comparison with the enormous dredging amounts calculated by the CWPRS and KPT the amounts calculated by the model are very small (see table 8-1).

The proposals of CWPRS and KPT however consist of deepening the areas in front of the general cargo berths and the jetties up to 400 metres wide. In the simulation these areas are only about 120 metres wide. The large ships can only enter (and leave) the port at high water, when the depths in Sogal Channel are sufficient (tidal window). At that time the depths in Kandla Creek are more than sufficient. These ships are now free to manoeuvre and

berth at any desired quay. At low water only the area directly in front of the quay needs to be deep enough. A width of 120 metres is already on the safe side as a vessel with a draught of 14 metres generally has a width of about 40 metres. The difference in width between the CWPRS or KPT proposal and the simulation is a factor 3,3. If this factor is applied to the dredging quantities Kandla Creek would require maintenance dredging of about 1,12 to 1,64 mln cum/month (instead of 3.73 to 5.48 mln cum/month (see table 2-5)). The sedimentation in Sogal Channel is expected to rise to 3.75 mln cum per month. These amounts are unrealistically high. The total amount of maintenance dredging would multiply by a factor 20 while the depths in the different areas increase by a factor 1.3 to 1.45.

The model calculations show other figures, which are summed up in table 8-1.

Table 8-1 Expected morphological development

area \ develop-ment	run no. 25 initial depth		run no. 25 deepened situation	
	amounts (m <sup>3</sup> )	average depth (cm)	amounts (m <sup>3</sup> )	average depth (cm)
Sogal Channel	36932	10	58604	16
Berths	-43568	-18	-14672	-6
Jetty	138768	29	380296	79

The calculated sedimentation in Sogal Channel increases by a factor 1.6. This goes for the small section directly in front of the creek outfall. In the current situation only a stretch of 2.3 km has to be dredged between buoy 8 and buoy 10 (see section 2.1). In the future situation a much larger portion of Sogal Channel will have to be dredged. The natural depth of 8 metres below CD is not met between buoy 4 and buoy 12, which is a stretch of 8.2 km. It is not necessarily so that the sedimentation in the small section of Sogal Channel can be extrapolated to the rest of the channel. The increase by a factor 1.6 is also not necessarily applicable to the entire stretch of 8.2 km, because the depth is not increased by the same magnitude everywhere in the channel. This factor is probably on the high side. In order to assess an estimation of the expected maintenance dredging amounts in the future deepened situation however the extrapolation with a factor 1.6 is used. The total amount of maintenance dredging can thus be calculated as follows:

sedimentation rate according to CWPRS [1999]: 19 cm per month in Sogal Channel (246.000 m<sup>3</sup> in 2.3 km).

calculated rate by model: 16 cm in small part directly in front of outfall.

expected amount Sogal Channel (8.2 km):  $\frac{16}{19} \times \frac{8.2}{2.3} \times 246.000 \approx 740.000 \text{ m}^3 \text{ a month.}$

The erosion in the berths area has diminished. It is possible that the average depth of 14.2 metres is closer to a sort of "equilibrium" state, than the current 10.7 metres. This is only an explanation for the model results. The measured data and the report of CWPRS don't show these amounts of erosion. The erosion can be explained by the fact that the sediment concentrations in the area around Sogal Channel are too low (due to the negligence of waves) and that the flow entering Kandla Creek during flood thus contains to little sediment. The flow velocity increases and picks up sediment from the berths area, which erodes. A similar process takes place at ebb. The sediment that the ebb flow contains settles in the area south of the jetties. The flow then contracts through the narrow berths area and the sediment transport capacity grows, again causing erosion. In reality the flow entering Kandla Creek

contains much more sediment and may not pick up much more sediment while flowing passed the berths area. At slack water period the sediment settles, also in the berths area. During ebb this material could be transported out of Kandla Creek again. The depth in the considered area could thus be in an equilibrium state. This would explain the marginal maintenance dredging in front of the general cargo berths. Figure 8-3 shows the residual suspended transport in the berth area. The same pattern can be seen as in all calibration runs. The magnitude however does differ in those simulations.

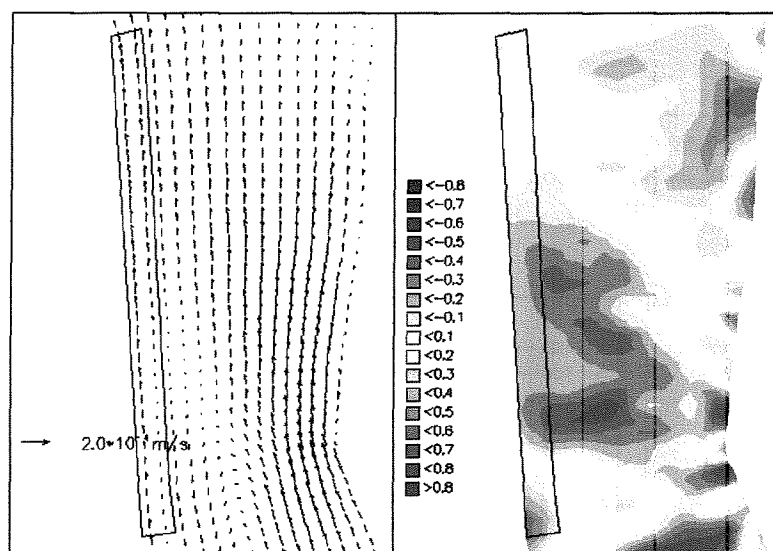


Figure 8-3 Residual transport and sed/ero pattern future situation

The calculations show that the sedimentation in the jetty area increases by a factor 2.75. In order to ensure the depth to be the required 14.2 metres below CD, the maintenance dredging would amount to about 380.000 m<sup>3</sup>.

The total amount of dredging for maintaining the required depths in the different areas of the port on an annual basis would be  $(740.000 + 380.000) \times 12 \approx 13.5$  mln cum. This is 2.8 times the amount that is currently dredged every year. A large difference exists with the forecast of CWPRS [1999].

Table 8-2 Dredging quantities future situation

	Maintenance dredging (m <sup>3</sup> )	
	Monthly	Annual
Sogal Channel	740.000	8.900.000
Jetty area	380.000	4.600.000
<b>Total</b>	<b>1.120.000</b>	<b>13.500.000</b>
<b>Costs (mln Rp.)</b>	<b>70.3</b>	<b>845</b>

The extra costs that have to be made in order to dredge the calculated quantities amount to 540 million Rupees. The extra income generated by the expansion amounts to 1600 million Rupees (see table 2-4). The outcome of the model simulation shows that the expansion of the port is economically viable. The costs for the construction of extra berths and jetties and the purchase of cranes etcetera are not yet taken into account. These costs however are once-only, whilst table 8-2 shows the annual figures.

### 8.3 Concept 1

This concept consists of a training wall in the outer bend of Sogal Channel between buoy 8 and 12 aligned in the main flow direction. The northern part of the wall however is curved more to the west and thus deflects the current somewhat. The flow is concentrated in Sogal Channel, which should increase in strength and transport capacity. This could decrease sedimentation or even cause erosion. The layout of the training wall can be seen in figure 8-4.

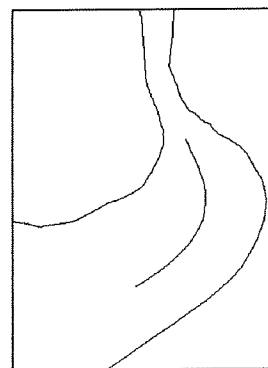


Figure 8-4 Training wall concept 1

The results of the calculations however do not show the pursued effect. The flow velocities are compared with the situation without a training wall in a few observation points in Sogal Channel (see figure 8-5). The calculated amounts of sedimentation and erosion are summed up in table 8-3.

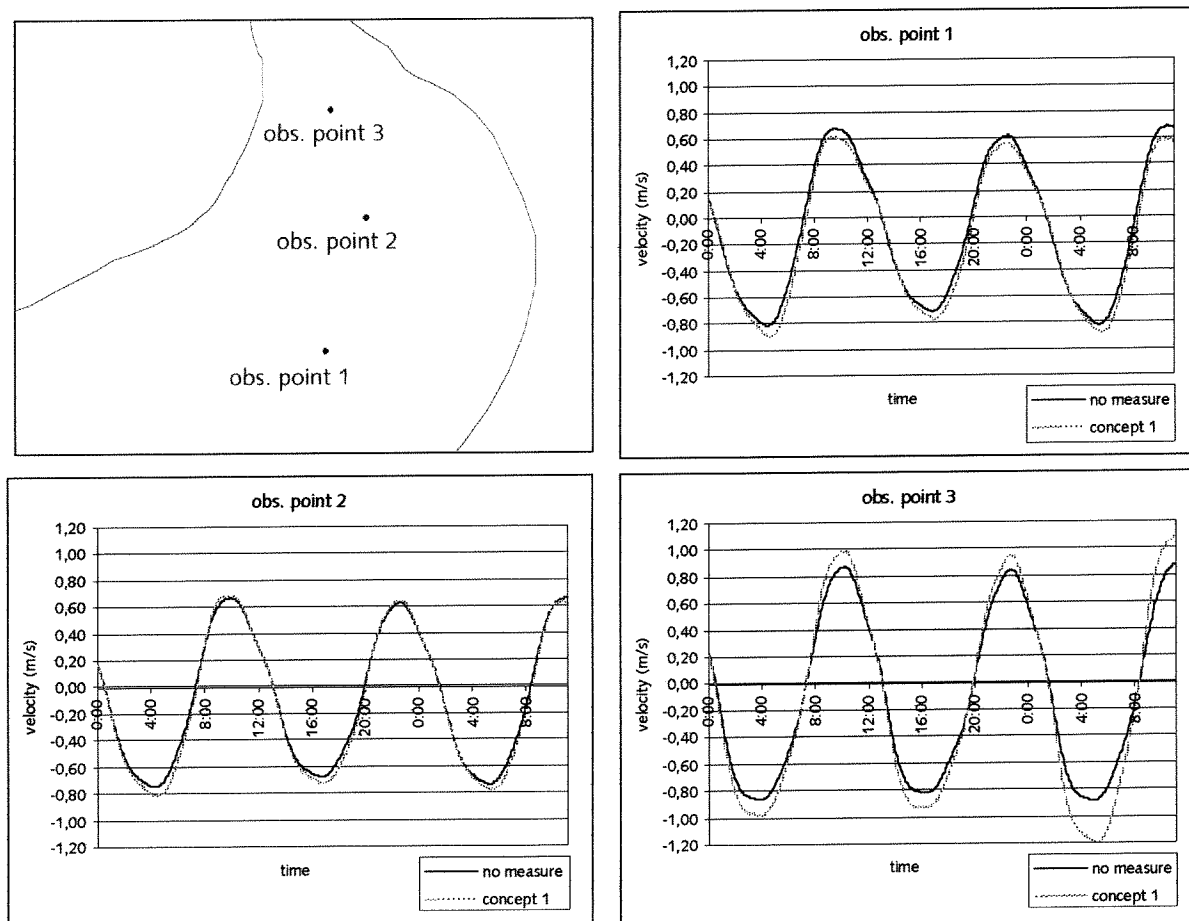


Figure 8-5 Comparison flow velocity concept 1

Figure 8-5 indicates that the velocities increase due to the deflected flow, especially in point 3. In this part of the channel however the depth is already sufficient. The erosion that takes place here (see also figure J-5) is thus not beneficial for the port.

Table 8-3 Morphological development concept 1

area \ develop-ment	no measure		concept 1	
	amounts (m <sup>3</sup> )	average depth (cm)	amounts (m <sup>3</sup> )	average depth (cm)
Sogal Channel	58604	16	118104	32
Berths	-14672	-6	-7236	-3
Jetty	380296	79	381136	79

The training wall does not affect the sedimentation in jetty area. The difference is negligible. The berths area is subject to slightly less erosion. The part of the approach channel the measure is taken for however is subject to twice as much sedimentation as in the situation without a training wall. The effect is counterproductive. This can be seen in the sedimentation/erosion pattern in figure 8-7 and in figure J-5 in annex J. The rest of Sogal Channel also doesn't experience any beneficial effect.

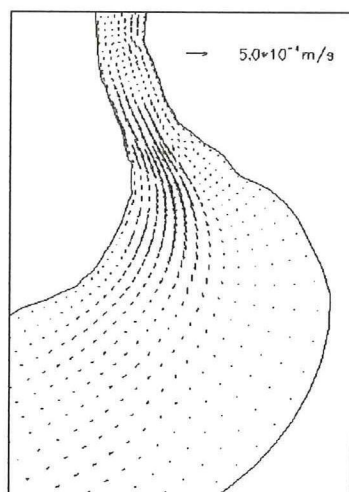


Figure 8-6 Residual suspended transport initial situation

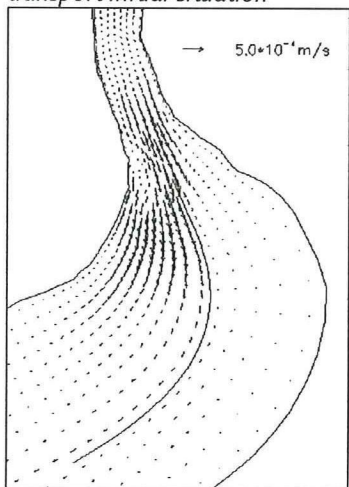


Figure 8-8 Residual suspended transport concept 1

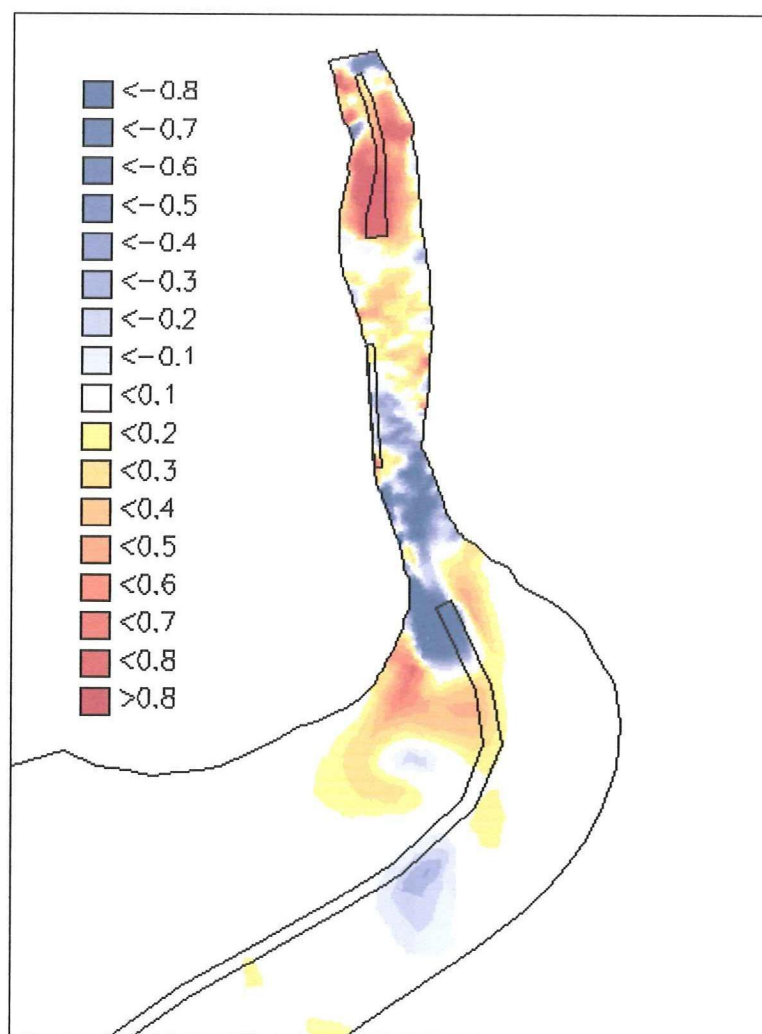


Figure 8-7 Sedimentation/erosion pattern concept 1

From figures 8-6 and 8-8 it is clear that the residual transport that is directed out of the creek in the initial situation is cancelled out by the deflected flow. The training wall has the largest effect on the flood flow. This flow is concentrated and the sediment transport capacity is increased thus creating erosion. The objective of creating erosion in the troublesome bend



however isn't met. The flow velocity is not increased enough in this part (see point 1 and point 2 in figure 8-5). The sediment that leaves Kandla Creek with the ebb flow is deposited in this area.

## 8.4 Concept 2

The main objective of this proposal is to reduce the lateral flow entering Sogal Channel from the shallow parts north of buoy 4 to buoy 8. The same concept is applied as described in section 2.1. The training wall consists of a few smaller sections, which are positioned in a row but are not connected (see figure 8-9).

This layout of a staggered training wall does contribute to the deepening of Sogal Channel. The effect is twofold. Firstly the lateral flow (see figure 2-1) is stopped and less material is transported into Kandla Creek. Secondly the ebb flow coming from the creek is directed more towards the outer bend of Sogal Channel. This causes the velocity and the transport capacity to increase (see figure 8-11) and erosion to occur. The sediment concentrations are also higher as can be seen from figure 8-10. This figure shows the concentration at the time of maximum ebb flow. The higher concentrations are directed more to the outer bend of Sogal Channel (picture 2 of figure 8-10). The concentration is highest just at the point where the influence of the training wall stops. This has a less favourable effect in the more south westerly part of the channel (part 2 in figure 8-12). Here the ebb flow returns to its "normal" velocity and the sediment settles. In order to assess these effects Sogal Channel is divided into two parts.

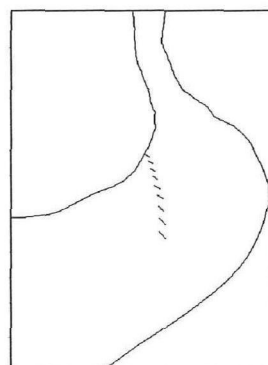


Figure 8-9 Training wall concept 2

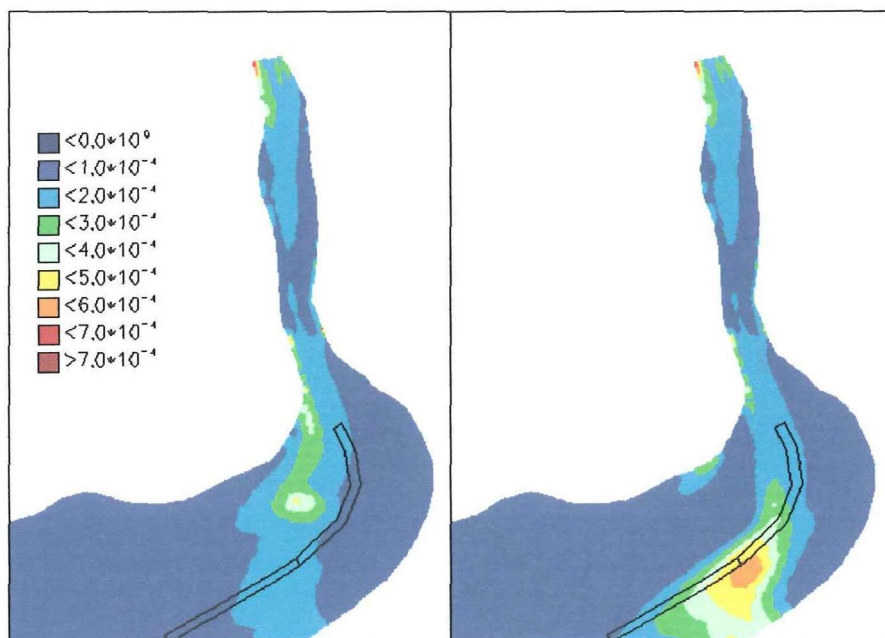


Figure 8-10 Sediment concentration initial and concept 2

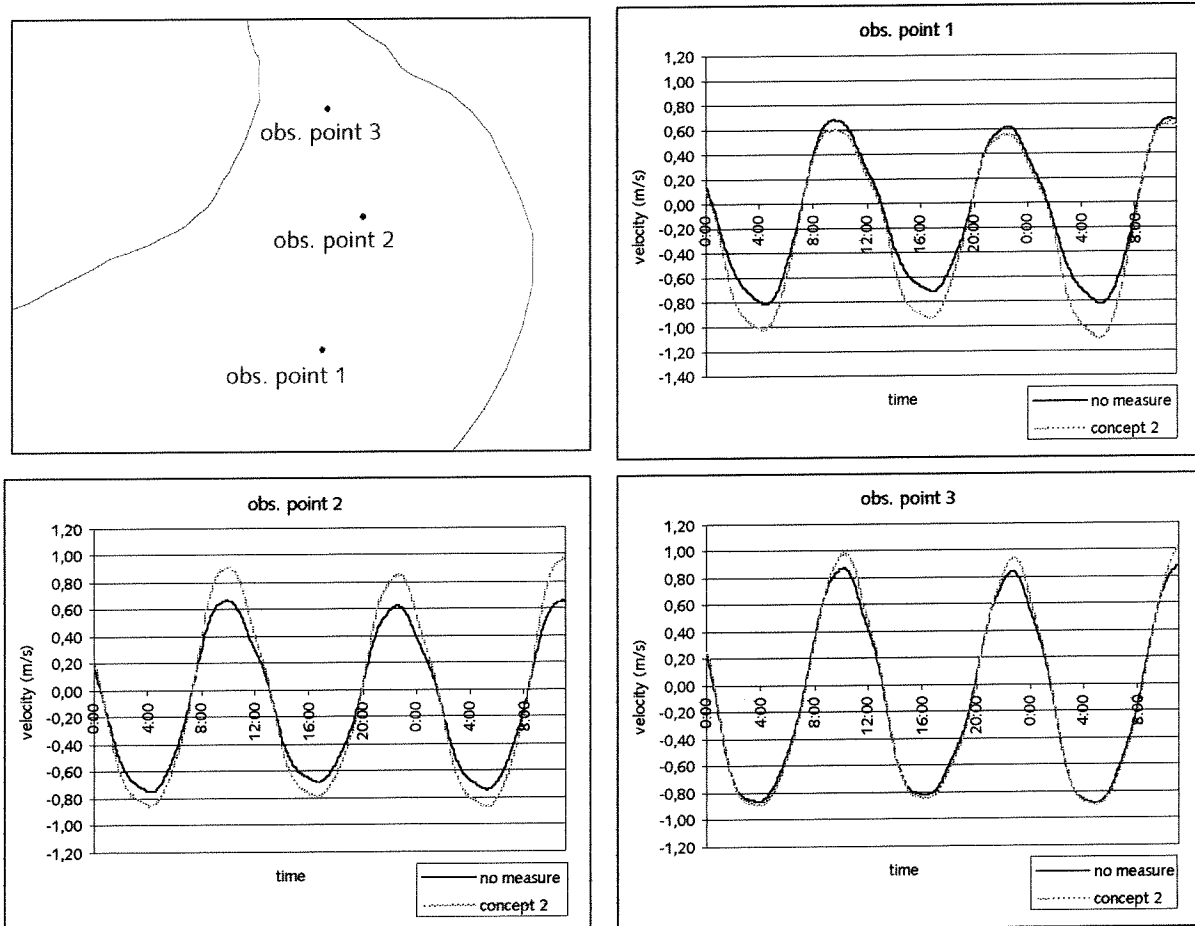


Figure 8-11 Comparison flow velocity concept 2

In point 1 the ebb flow increases, whilst in point 3 the flood flow increases, but just slightly. The increase of ebb flow in point 1 causes quite some erosion in the bend of Sogal Channel. The increase of flood flow also causes erosion. The sediment that is picked up here is transported all the way into Kandla Creek and is deposited near the jetty area.

Table 8-4 Morphological development concept 2

area \ develop-ment	no measure		concept 2	
	amounts (m <sup>3</sup> )	average depth (cm)	amounts (m <sup>3</sup> )	average depth (cm)
Sogal Channel bend	34272	4	-427904	-43
Sogal Channel 2	31920	3	355964	44
Berths	-14672	-6	-39220	-16
Jetty	380296	79	388024	80

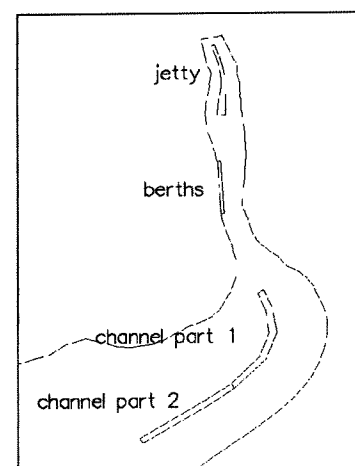


Figure 8-12 Areas of comparison

It can be seen that the erosion in the bend is quite extensive, though the rate declines with time. The other part of the channel however is subject to sedimentation at the same rate. It would be possible to assume that the majority of material picked up in the bend is deposited

in this part of the channel. Therefore the problem is only shifted. The objective of instigating erosion in the bend however is met.

In the berths area the erosion has increased. This can be caused by the lateral flood flow being hindered in entering Kandla Creek. The ebb flow subsequently transports material out of the berths area. The morphological development of the jetty area is hardly affected by the staggered training wall.

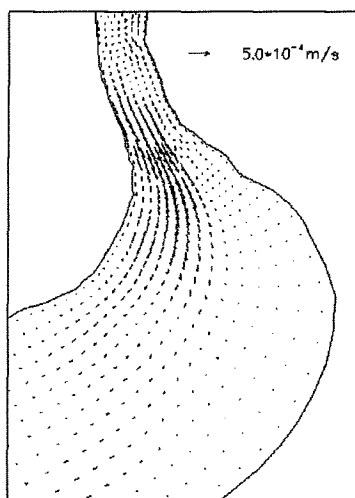


Figure 8-13 Residual suspended transport initial situation

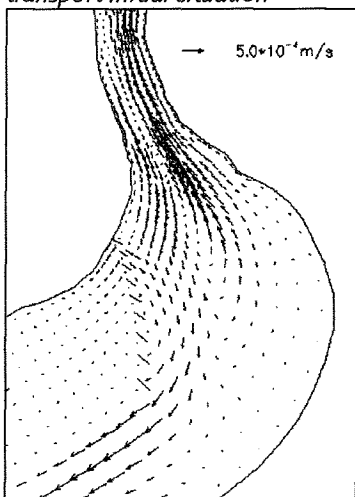


Figure 8-15 Residual suspended transport concept 2

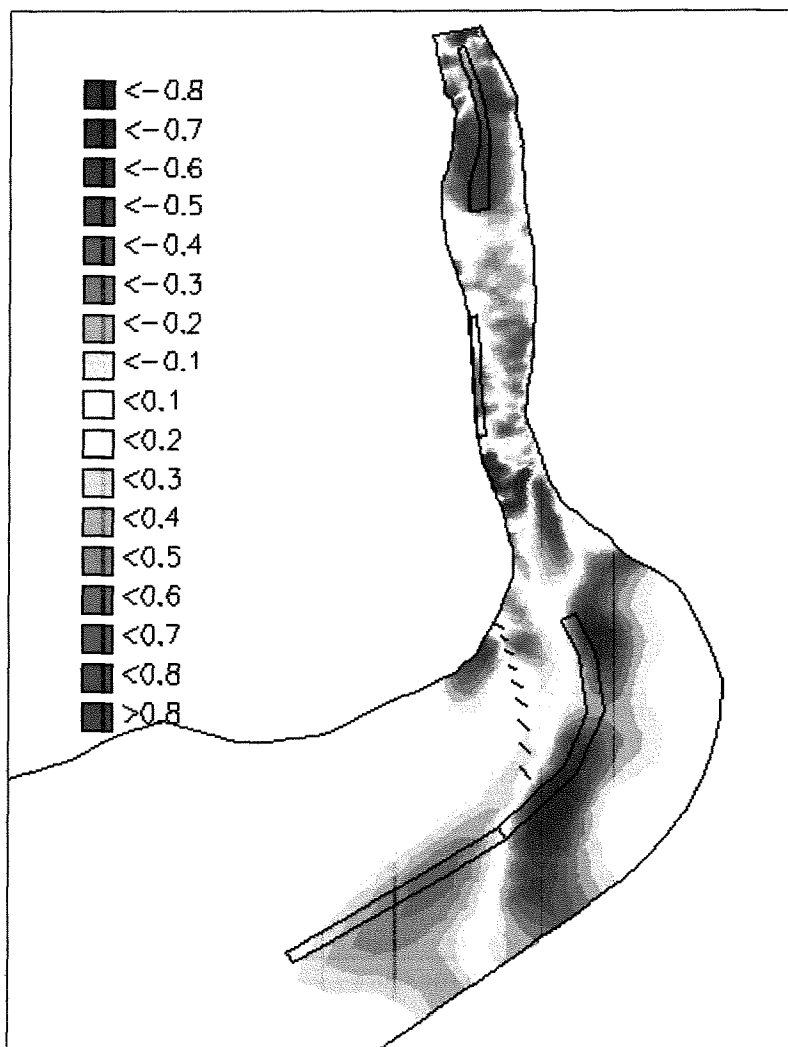


Figure 8-14 Sedimentation/erosion pattern concept 2

From figure 8-15 it can be seen that the residual transport is directed away from the bend (channel part1 in figure 8-12). In the northern part the transport is directed into Kandla Creek, while in the south western part the transport is directed further in south westerly direction. This causes the bend to erode, but the adjacent part of the model area to silt up (the arrows are directed away from the bend). This is also clearly visible from the sedimentation/erosion pattern in figure 8-14.

## 8.5 Concept 3

This concept consists of a few dams positioned perpendicular to the main flow direction (like in rivers). These dams simply concentrate the flow towards the middle of the model area (see figure 8-16). This way flow velocity is increased and sedimentation is reduced.

A similar process takes place as in the former concept. The training walls concentrate the ebb flow in Sogal Channel and cause erosion. This only holds for the bend in the channel. The calculated sedimentation and erosion quantities are presented in table 8-5.

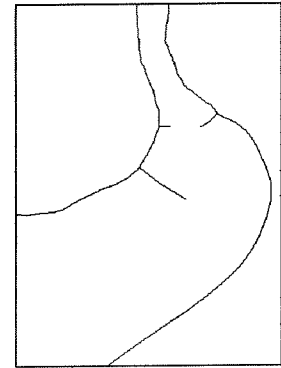


Figure 8-16 Training wall concept 3

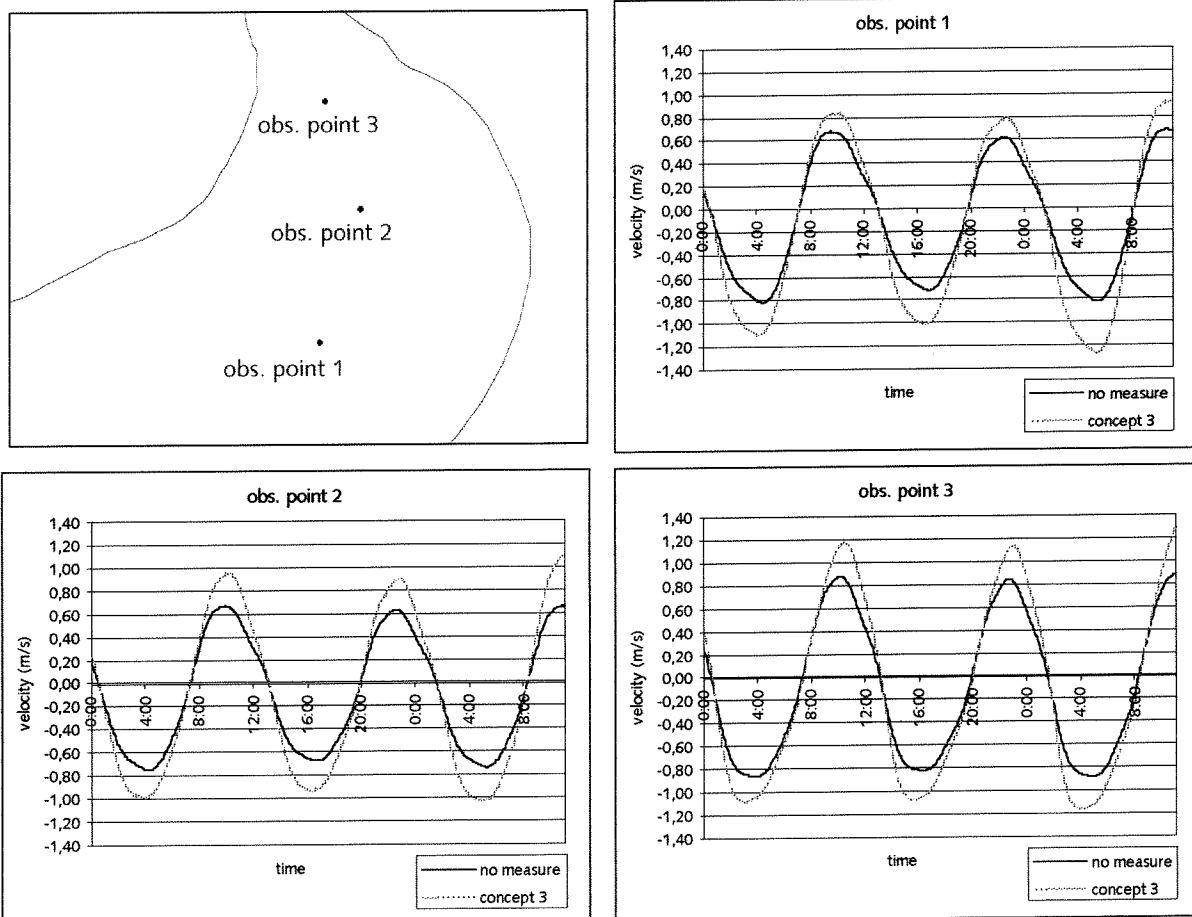


Figure 8-17 Comparison flow velocity concept 3

In all observation points the flow velocity increases, both the ebb flow and the flood flow and does so quite severely. This has a few effects as can be seen from table 8-5.

Table 8-5 Morphological development concept 3

area \ develop-ment	no measure		concept 3	
	amounts (m <sup>3</sup> )	average depth (cm)	amounts (m <sup>3</sup> )	average depth (cm)
Sogal Channel bend	34272	4	-880779	-89
Sogal Channel 2	31920	3	782796	98
Berths	-14672	-6	-10456	-4
Jetty	380296	79	401940	83

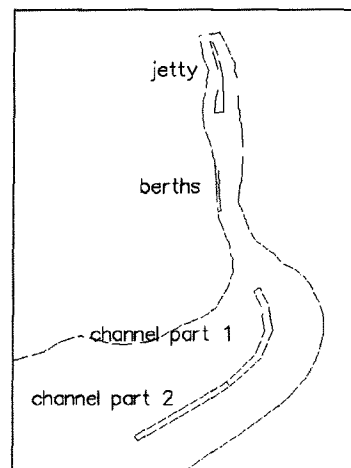


Figure 8-18 Areas of comparison

The two parts of Sogal Channel are subject to the same morphological development as can be observed in concept 2, only at a larger scale. The bend is subject to erosion, but now the problem area lies further to the southwest. The required depth of 8 metres below CD is rapidly diminished in part 2 of the channel (see figure 8-18).

The depth in the berths area isn't affected that much. An explanation could be that the higher sediment concentrations that enter Kandla Creek with the flood flow do not settle in the berths area due to the fact that the flow intensity is increased. The sediment is just transported past the berths area.

The sedimentation in the jetty area has become slightly larger. A part of the extra sediment that is transported into the creek could be the reason for this accretion. The effect is only marginal in comparison with the sedimentation in the situation without a training wall.

The flood flow entering Kandla Creek is contracted quite severely (see figure 8-21) especially in the entrance itself. When the flow has passed the training walls it returns to a more stable flow. The extra sediment that is picked up is gradually deposited in the creek. The ebb flow is also increased as can be seen from figure 8-17. The sediment isn't deposited until the effect of the training walls is cancelled out and the flow returns to its undisturbed situation. The flow then loses its transport capacity very rapidly and Sogal Channel silts up. As mentioned before the problem is shifted to the south west of the bend of Sogal Channel. Maintenance dredging will now have to be done in that part of the approach channel.



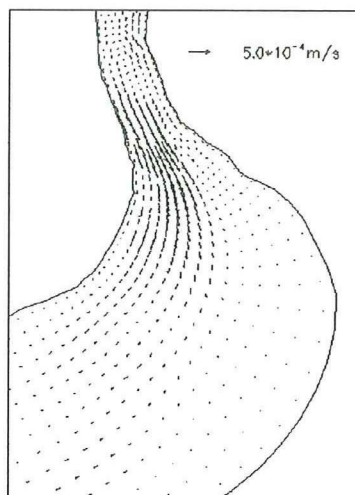


Figure 8-19 Residual suspended transport initial situation

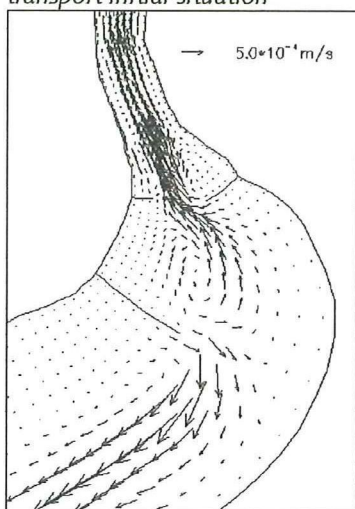


Figure 8-21 Residual suspended transport concept 3

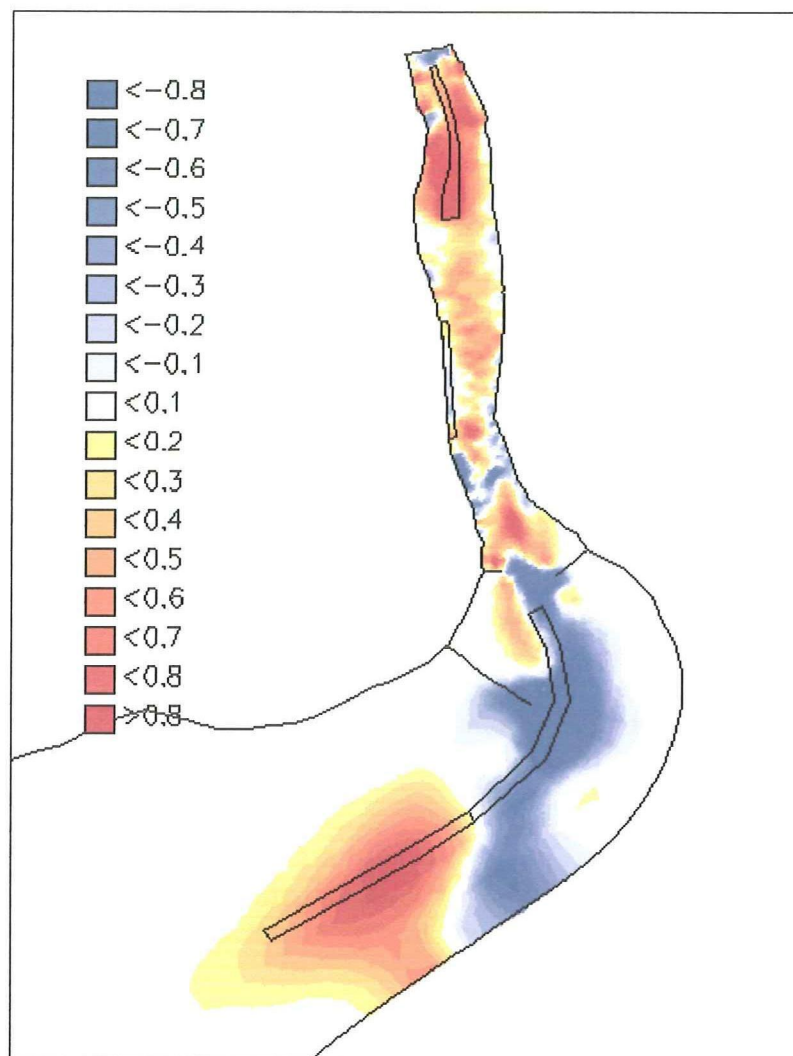


Figure 8-20 Sedimentation/erosion pattern concept 3

## 8.6 Overall findings

The simulation of the future situation has shown that the dredging quantities will increase by about a factor 3, although this is an estimate, especially because of the rough estimation of the sedimentation in Sogal Channel. The enormous quantities calculated by CWPRS and KPT however are not even remotely approximated. An increase of maintenance dredging by a factor 3 is more probable than an increase by a factor 20 and therefore a more realistic magnitude of increase has been obtained.

The proposed training walls have different effects on the morphological development in the model area. Concept 1, a training wall in the outer bend of Sogal Channel, doesn't deflect the flow enough to cause erosion. The flow already has the direction of the training wall. A beneficial effect would be that the bend will become stable in the long run and won't slowly propagate to the east any more. At this moment the channel has to be both deepened and stabilised by the dredging efforts.

Concept 2 and concept 3 have a qualitatively similar effect on the morphological activity. Both training wall layouts deflect the ebb flow towards the outside of the bend, which causes the flow velocities to increase and erosion to occur. The magnitude of the morphological development is quite different though. Concept 2 allows water to flow "through" the wall,

where as concept 3 consists of impermeable walls. A consequence is that the erosion in the bend of Sogal Channel is twice as large in case of the impermeable wall than in case of a staggered wall. In both situations the benefit of the erosion in the bend of the channel is cancelled out by sedimentation in the more south westerly part of Sogal Channel.

As mentioned in section 7-4 the results have to be looked at with great care. A few fairly rough assumptions have been made in the course of the mathematical modelling. The negligence of waves is probably the cause of the low morphological activity in the shallow parts of the model area and the small sedimentation of Sogal Channel. The closed boundary over the shoals prohibits flow perpendicular to this boundary, while in reality water could well flow across this boundary (especially the ebb flow). This boundary however had to be imposed because of the absence of bathymetry data south of the shoals. Because of these shortcomings the quantitative outcome of the simulations may deviate quite severely from reality. Insight into the morphological development of the region however is obtained. It is obvious that the dredging quantities will increase if the different areas are deepened. Training walls that block the flow (partially or entirely) have a huge impact on the morphodynamics in the vicinity of these walls. The rate of this development is so large that in the long run, say 10 years, the whole region can be affected. The proposed measures seem to be too radical. This can be expected, because with the tidal variation of more than 5 metres huge amounts of influx and efflux are diverted completely and disturb the flow considerably.

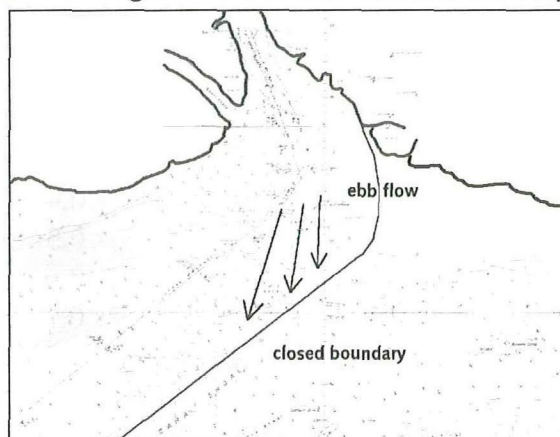


Figure 8-22 Closed boundary over shoals

## 9 Conclusions and recommendations

### Conclusions

- The expansion of the port will result in an increase of maintenance dredging. The amounts calculated by the Central Water and Power Research Station and Kandla Port Trust seem to be exceptionally large. An increase of 1800 to 2200 percent, from 5 to between 90 and 111 million cubic metres annually, is estimated. This study however has shown an increase of about a factor 3.
- The model shows little morphological activity in the shallow parts around Sogal Channel. This is probably due to the negligence of waves. The flow velocities in this area are not high enough to cause significant sediment transport.
- The simulated concepts show different sedimentation and erosion patterns. The Jetty area however isn't affected much by the various proposed training walls. This seems logical, as the area is located far away from the creek outfall.
- Concept 1, the training wall in the outer bend of Sogal Channel, has a counterproductive effect on the depth in the bend. Erosion only takes place in the part where the depth is large enough already. The sediment that is picked up there is probably deposited in the bend where the flow resumes its undisturbed velocity.
- Concept 2 and 3 both prevent flow north of Sogal Channel to enter Kandla Creek. The flow is concentrated in the bend, both ebb and flood, and this causes erosion. The eroded material however is deposited in other parts of the model area. Sediment that is picked up by the flood flow ends up in Kandla Creek and sediment that is picked up by the ebb flow ends up further downstream of the bend in Sogal Channel.
- The impact of the training walls, as proposed by concept 2 and 3, on the morphodynamics of the area is very large. The present hydrodynamic situation is changed so severely that the development of the approach channel in the long term is uncertain and almost impossible to predict.
- The results of this study show that the enlargement of the maximum permissible draught is best obtained and maintained by dredging. The increase in the annual amount of maintenance dredging is economically justifiable and the impact of the training walls is uncertain in the long run.

### Recommendations

- The influence of waves on the sediment transport should be investigated. The Delft3D software package has the possibility to do so. The model as constructed for this study could be extended with the WAVE module. Data will have to be available to implement this feature.
- The closed boundary over the natural shoals (Kala Dara shoal and Mid shoal) parallel to Sogal Channel is a practical limitation as data on bathymetry is not available south of this boundary. It is not clear however if all the flow is directed parallel to this boundary or that



a substantial portion of the flow moves through the boundary. Data on the flow direction in this area should be obtained in order to determine if the closed boundary is valid.

- All the simulations have been done with a course grid. The simulations of the different concepts should probably be done with a more refined grid. The width Sogal Channel is covered by only two grid cells. A finer grid could improve the results.
- More insight into the calculation methods of CWPRS and KPT should be obtained with regard to the expected dredging quantities for the deepened situation. The amounts calculated by the model differ very much from the huge capital and maintenance dredging amounts of CWPRS and KPT.

## References

- CWPRS; Preliminary appraisal of hydraulic aspects for the proposed dredging in the Kandla Creek and its approaches. Technical report no. 3667, Pune, December 1999.
- CWPRS; Hydraulic model studies for evolving training works in the approaches to Kandla Creek. Technical report no. 3718, Pune, August 2000.
- CWPRS; 1-D Mathematical model studies to assess the effect of deepening and widening of Sogal Channel and Kandla Creek. Technical report no. 3822, Pune, October 2001.
- CWPRS; Interim report on 2-D mathematical model studies for hydrodynamics in the approaches to Kandla Creek. Technical report no. 3858, Pune, February 2002.
- Hydraulic engineer; Reply to Chairman's letter No. KPC/5009-DC, 30/01/2002.
- NEI Transport; Helicopter assessment, Commodity analysis & Forecast of cargo in the Gujarat ports. Rotterdam, April 2001.
- Internet: India Port Association homepage, [www.indiaport.com](http://www.indiaport.com)
- Internet: Kandla Port Trust homepage, [www.kandlaport.com](http://www.kandlaport.com)
- Internet: Port of Rotterdam homepage, annual report '99-'00, [www.portofrotterdam.nl](http://www.portofrotterdam.nl)
- PIANC, IAPH; Approach channels, a guide for design. Final report of the joint PIANC-IAPH working group II-30 in cooperation with IMPA and IALA. Supplement to bulletin no. 95, June 1997.
- Veen, Ir. J van; Ebb and flood channel systems in the Netherlands tidal waters. Journal of the Royal Dutch Geographical Society, vol. 67, 1950, pages 303-325.
- Velden, Ir. E.T.J.M. van der; Lecture notes Coastal Engineering, CTwa5309, TUDelft, September 2000.
- Richardson, Y.F. and W.N. Zaki; Sedimentation and fluidisation, Part I: Trans. insts. chem. engrs, volume 32, pp 35-53. 1954
- Rijn, L.C. van; Sediment transport: Part I: Bed load transport, Part II: Suspended load transport, Part III: Bed forms and alluvial roughness, Journal of Hydraulic Engineering, volume 110, No. 10, 11, 12. 1984
- Stelling, G.S.; On the construction of computational methods for shallow water problems. Rijkswaterstaat communications, No. 35, The Hague, Rijkswaterstaat, 1984

## Annexes

Annex A	Van Rijn transport formula
Annex B	Model area and computational grid
Annex C	Initial depth
Annex D	Water level and flow velocity measurements
Annex E	Input parameters
Annex F	Calibration FLOW
Annex G	Sedimentation/erosion quantities of calibration runs
Annex H	Sedimentation/erosion patterns of calibration runs
Annex I	Residual sediment transport of calibration runs
Annex J	Results of simulation runs

## Annex A

Van Rijn transport formula

The Van Rijn (1984) sediment transport relation is the most accurate and commonly used formulation for situations without waves. A distinction is made between bed load transport and suspended transport:

$$S = S_b + S_s \quad (\text{A.1})$$

where:

$$S_b = \begin{cases} 0.0053 (\Delta g d_{50}^3)^{0.5} D_*^{-0.3} T^{2.1} & \text{for } T < 3.0 \\ 0.1 (\Delta g d_{50}^3)^{0.5} D_*^{-0.3} T^{1.5} & \text{for } T \geq 3.0 \end{cases} \quad (\text{A.2})$$

Firstly this bed load transport expression will be explained. In Eq. (A.2)  $T$  is a dimensionless bed shear parameter, written as:

$$T = \frac{\mu_c \tau_{bc} - \tau_{bcr}}{\tau_{bcr}} \quad (\text{A.3})$$

It is normalised with the critical bed shear stress according to Shields ( $\tau_{bcr}$ ), the term  $\mu_c \tau_{bc}$  is the effective shear stress. The formulas of the shear stresses are:

$$\tau_{bc} = 0.125 \rho_w f_{cb} q^2 \quad (\text{A.4})$$

$$f_{cb} = \frac{0.24}{\left( \log_{10} \left( 12 \frac{h}{\xi_c} \right) \right)^2} \quad (\text{A.5})$$

$$\mu_c = \left( \frac{18 \log_{10} \left( 12 \frac{h}{\xi_c} \right)}{C'} \right)^2 \quad (\text{A.6})$$

where  $C'$  is the grain related Chézy coefficient:

$$C' = 18 \log_{10} \left( 12 \frac{h}{3d_{90}} \right) \quad (\text{A.7})$$

The critical shear stress is written according to Shields:

$$\tau_{bcr} = \rho_w \Delta g d_{50} \theta_{cr} \quad (\text{A.8})$$

in which  $\theta_{cr}$  is the Shields parameter which is a function of the dimensionless particle diameter  $D_*$ :

$$D_* = d_{50} \left( \frac{\Delta g}{\nu^2} \right)^{\frac{1}{3}} \quad (\text{A.9})$$

Secondly the suspended transport component will be explained. The suspended transport formulation reads:

$$S_s = f_{cs} q h C_a \quad (\text{A.10})$$

In which  $C_a$  is the reference concentration,  $q$  the depth averaged velocity,  $h$  the water depth and  $f_{cs}$  a shape factor for which only an approximate solution exists:

$$f_{cs} = \begin{cases} f_0(z_c) & \text{if } z_c \geq -1.2 \cdot 10^{-4} \\ f_1(z_c) & \text{if } z_c < 10^{-4} \end{cases} \quad (\text{A.11})$$

$$f_0(z_c) = \frac{(\xi_c/h)^{z_c} - (\xi_c/h)^{1.2}}{(1 - \xi_c/h)^{z_c} (1.2 - z_c)} \quad (\text{A.12})$$

$$f_1(z_c) = \left( \frac{\xi_c/h}{1 - \xi_c/h} \right)^{1.2} \log(\xi_c/h) \quad (\text{A.13})$$

where  $\xi_c$  is the reference level or roughness height (it can be interpreted as the bed-load layer thickness) and  $z_c$  the suspension number:

$$z_c = \min \left( 20, \frac{w_s}{\beta \kappa u_*} + \phi \right) \quad (\text{A.14})$$

$$u_* = q \sqrt{\frac{f_{cb}}{8}} \quad (\text{A.15})$$

$$\beta = \min \left( 1.5, 1.0 + 2 \left( \frac{w_s}{u_*} \right)^2 \right) \quad (\text{A.16})$$

$$\phi = 2.5 \left( \frac{w_s}{u_*} \right)^{0.8} \left( \frac{C_a}{0.65} \right)^{0.4} \quad (\text{A.17})$$

The reference concentration is written as:

$$C_a = 0.015 \alpha_1 \frac{d_{50}}{\xi_c} \frac{T^{1.5}}{D_*^{0.3}} \quad (\text{A.18})$$

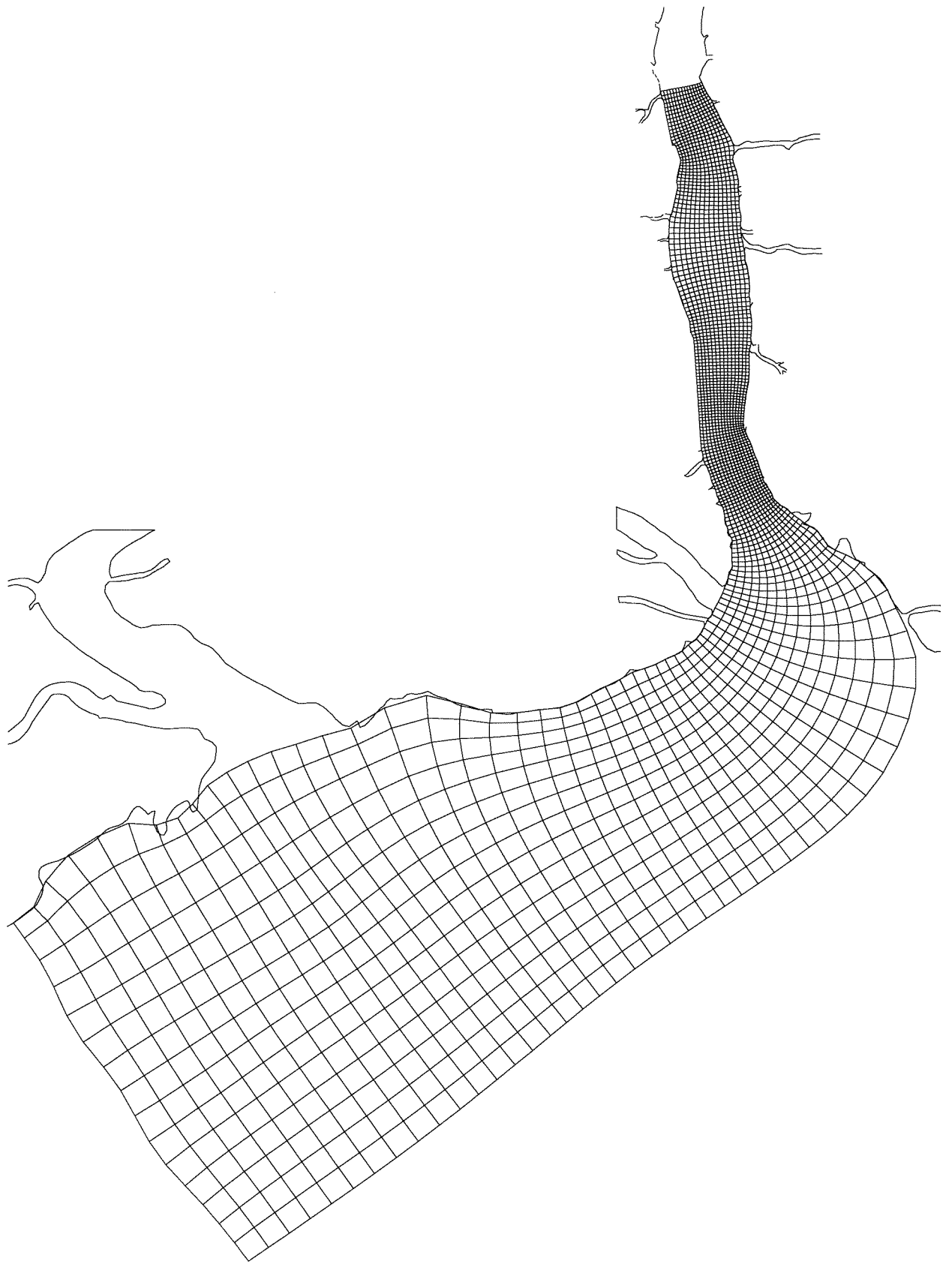
The following formula specific parameters have to be specified in the input files of the TRAN module:

$w_s$  = sediment settling velocity [m/s]  
 $\alpha_1$  = coefficient [-]  
 $\xi_c$  = roughness height [m]  
 $d_{90}$  =  $D_{90}$  particle diameter [m]

## Annex B

### Model area and computational grid



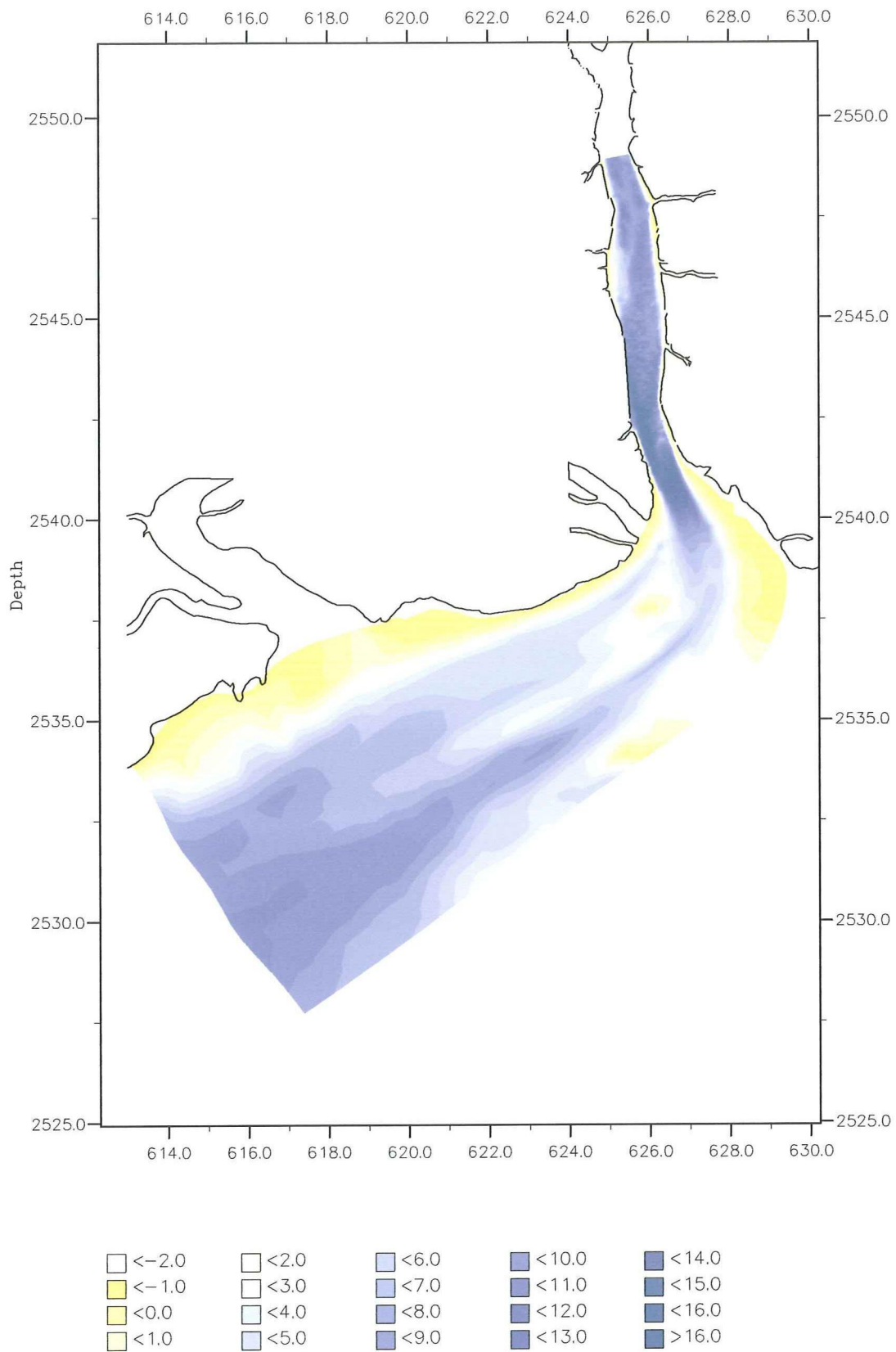


Model area and computational grid

FIGURE B-1

## Annex C

Initial depth



Initial depth

FIGURE C-1

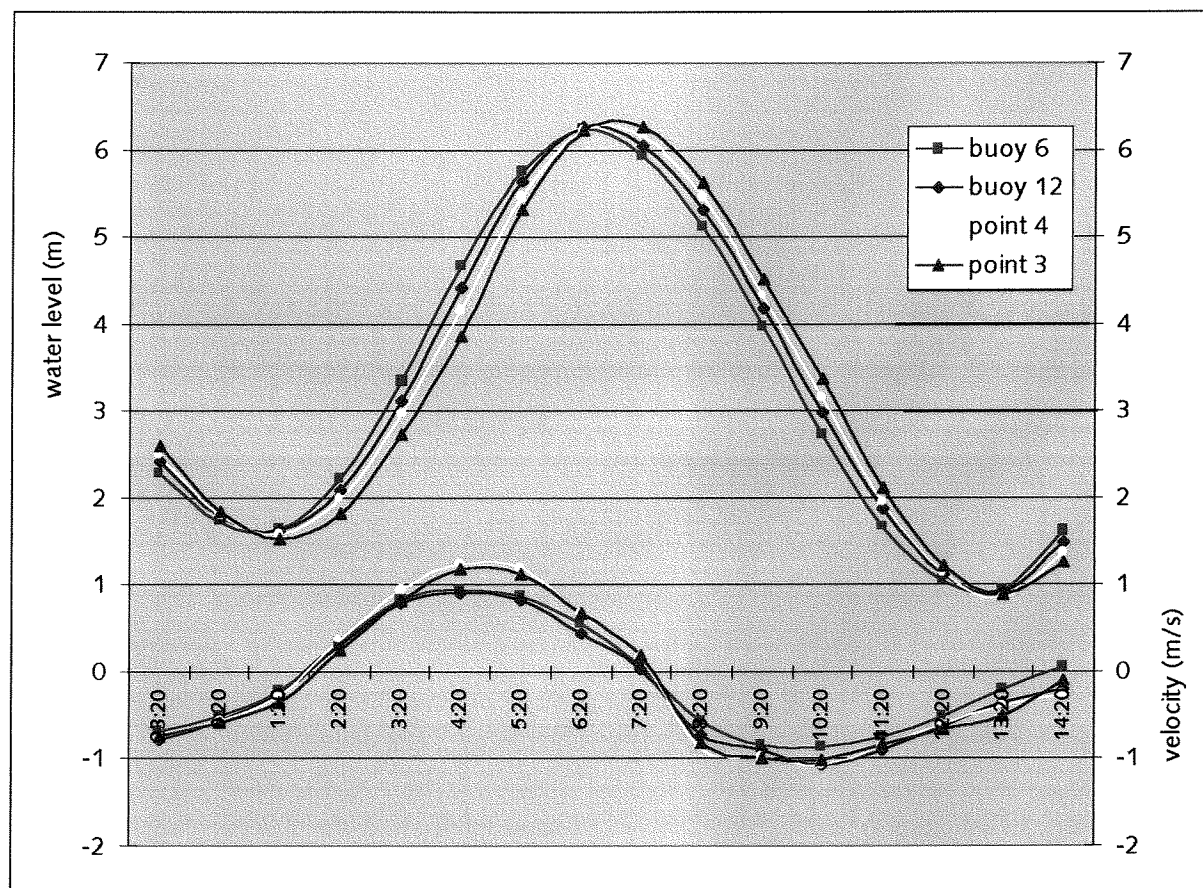
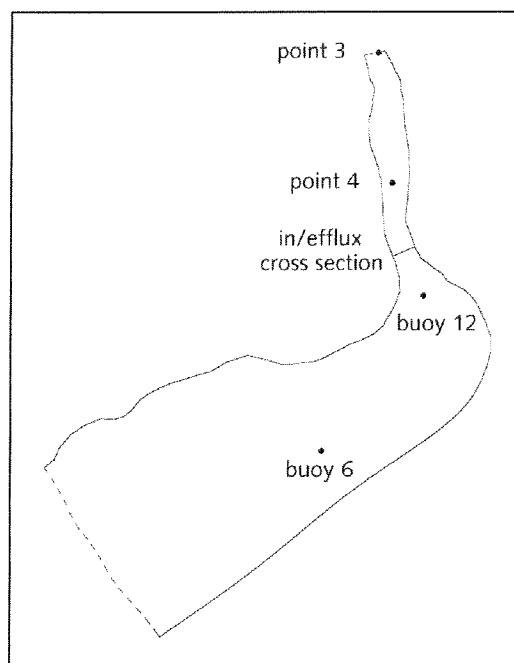
WL | DELFT HYDRAULICS

## Annex D

### Water level and flow velocity measurements

These measurements were taken on the first of December 1999.

	Buoy 6		Buoy 12		Point 4		Point 3	
	W.L.	Vel.	W.L.	Vel.	W.L.	Vel.	W.L.	Vel.
23:20	2,29	-0,68	2,42	-0,77	2,48	-0,75	2,59	-0,74
0:20	1,73	-0,50	1,79	-0,56	1,81	-0,56	1,84	-0,59
1:20	1,65	-0,22	1,63	-0,26	1,59	-0,28	1,53	-0,35
2:20	2,22	0,35	2,10	0,31	2,00	0,37	1,82	0,25
3:20	3,35	0,83	3,12	0,79	2,96	0,95	2,73	0,81
4:20	4,67	0,95	4,42	0,91	4,17	1,24	3,86	1,19
5:20	5,76	0,87	5,64	0,84	5,46	1,21	5,31	1,12
6:20	6,24	0,57	6,26	0,45	6,23	0,68	6,22	0,67
7:20	5,93	0,08	6,05	0,04	6,16	0,17	6,27	0,19
8:20	5,11	-0,57	5,31	-0,72	5,46	-0,87	5,63	-0,82
9:20	3,97	-0,83	4,18	-0,90	4,33	-0,97	4,52	-0,99
10:20	2,74	-0,85	2,98	-1,07	3,15	-1,06	3,38	-1,02
11:20	1,66	-0,74	1,87	-0,89	1,96	-0,85	2,11	-0,84
12:20	1,04	-0,50	1,12	-0,63	1,14	-0,61	1,22	-0,66
13:20	0,95	-0,19	0,90	-0,35	0,86	-0,39	0,89	-0,50
14:20	1,62	0,02	1,49	-0,19	1,38	-0,25	1,26	-0,10



# Annex E

## Input parameters

**Delft3D-FLOW**

Parameter	Value
Latitude	23 degrees N
Hydrodynamic time step	0.2 minutes (12 seconds)
Initial water level	6.5 m
Gravity	9.81 m/s <sup>2</sup>
Water density	1021 kg/m <sup>3</sup>
Water temperature	25 degrees Celsius
Salinity	32 ppt
Bottom roughness formula	
Horizontal eddy viscosity	50 m <sup>2</sup> /s
Threshold depth	0.1 m
Marginal depth	1.5 m
Smoothing time	60 minutes

**Boundary conditions**

	Frequency (degrees/hour)	Amplitude (m)	Phase (degrees)
Water level boundary	0	3.8	0
	14.4	0.4	-120.5
	28.8	2.535	0
Velocity boundary	0	-0.112	0
	28.8	1.11	294.1
	57.6	0.22	266.7
	86.4	0.053	34
	115.2	0.022	17.9
	144	0.034	57

**Delft3D-TRAN/BOTT**

Parameter		Value
Transport option		Suspended
Transport relation		Van Rijn
Coefficients for bed slope effect on		
Transport direction	Bed slope A	1.0
	Bed slope B	0.5
	Coefficient Shield number	1.0
Transport magnitude	Bed load	1.0
	Suspended load	1.0
Kinematic viscosity water		$1.00 \times 10^{-6} \text{ m}^2/\text{s}$
Density of sediment		$2650 \text{ kg/m}^3$
Porosity when settled		0.40
$D_{50}$		$60 \times 10^{-5} \text{ m}$
$D_{90}$		$75 \times 10^{-5} \text{ m}$
Bottom roughness height		0.03 m
Particle fall velocity		0.003 m/s
Coefficient ( $\alpha_1$ )		1.0
Suspended sediment boundary condition		
	Inflow condition	Equal to local equilibrium concentration
	Outflow condition	Upstream concentration
Bed level condition		Bed level unchanged
Initial sediment concentration		$0.001 \text{ m}^3/\text{m}^3$
Dispersion coefficient		Algebraic relation
	Coeff. A	0.1
	Coeff. B	$0.5 \text{ m}^2/\text{s}$
Bed level boundary	Absolute level	0.1 m
	Relative level	0.5
Transport time step		2 minutes
Initial adaptation time		60 minutes
Morphological time step		24 hours



# Annex F

## Calibration FLOW

The measured water levels and flow velocities have been compared with the model calculations. This has been done for a few locations (see annex D).

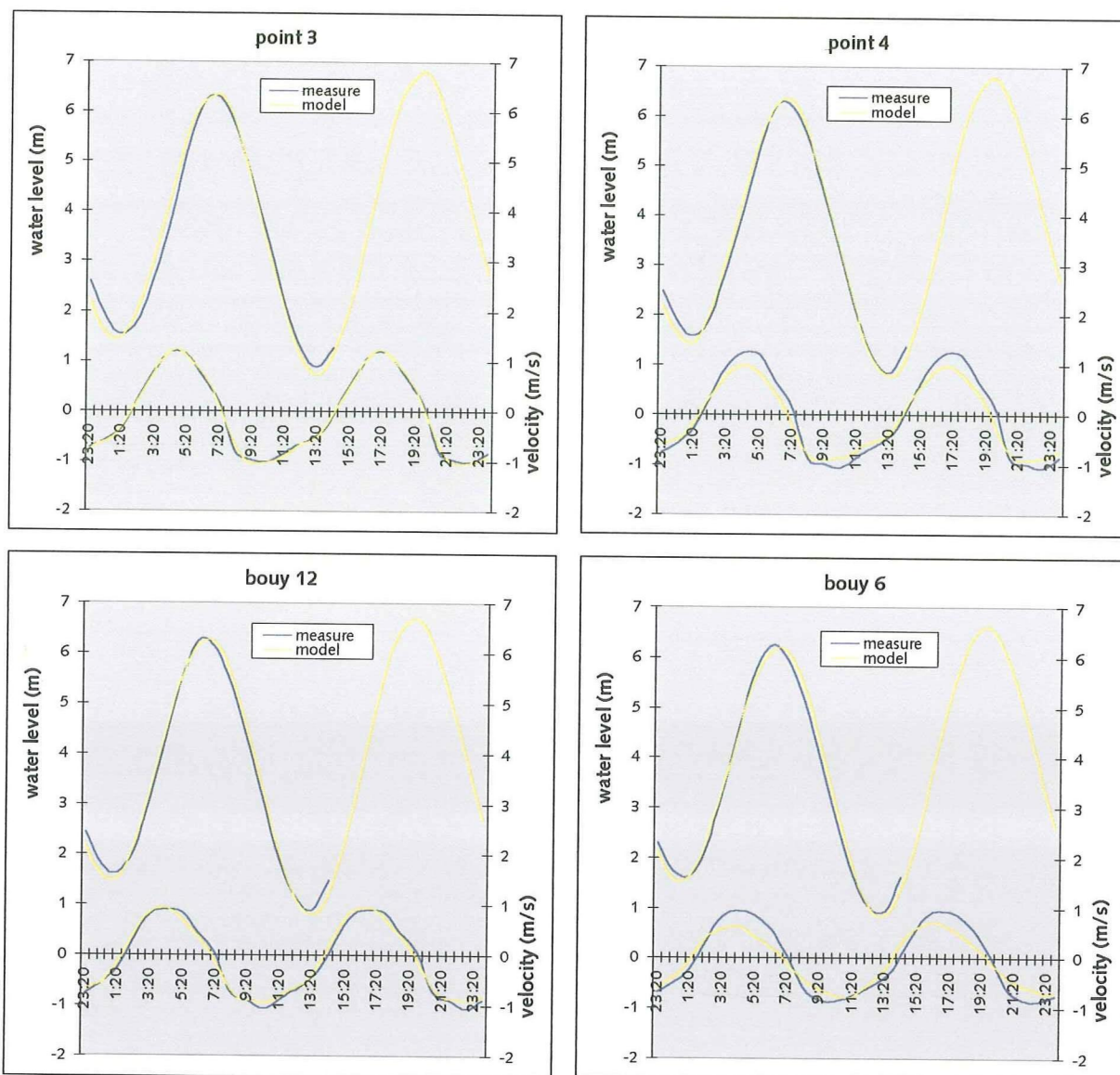
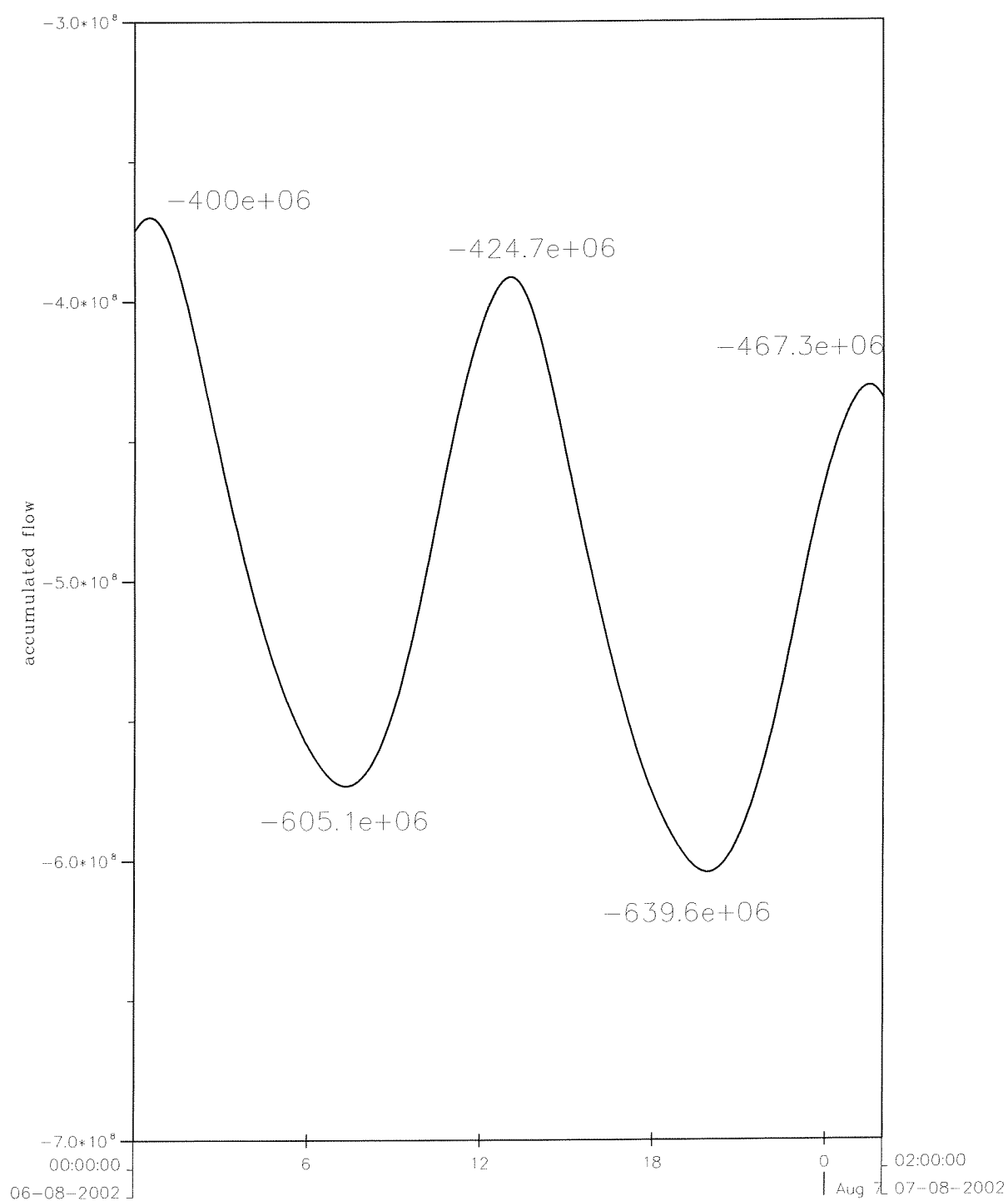


Figure F-1 Water level and flow velocity comparison

The calculated in- and efflux through the cross section are shown in figure F-2. Table 6-2 shows the added figures.



Accumulated flow through cross section

Figure F-2

## Annex G

Sedimentation/erosion quantities of calibration runs

D50/D90		80/100							
fall velocity		0,0053		Channel		Berths		Jetty	
INITIAL VALUES				2223870	6,01	2932134	12,22	4292014	8,87
DIFFERENCE				m^3 per month	cm per month	m^3 per month	cm per month	m^3 per month	cm per month
No.									
1	Chézy	60	0,01	7307	0,02	-42782	-0,18	59397	0,12
2			ξc 0,03	5340	0,01	-27208	-0,11	37259	0,08
3			0,05	4359	0,01	-21088	-0,09	28466	0,06
4		70	0,01	6502	0,02	-35639	-0,15	63528	0,13
5			ξc 0,03	4833	0,01	-22757	-0,09	39536	0,08
6			0,05	3965	0,01	-17685	-0,07	30115	0,06
7		80	0,01	6070	0,02	-30252	-0,13	66512	0,14
8			ξc 0,03	4537	0,01	-19422	-0,08	41152	0,09
9			0,05	3731	0,01	-15147	-0,06	31266	0,06
10	Manning	0,02	0,01	873	0,00	-46483	-0,19	55426	0,11
11			ξc 0,03	1348	0,00	-29567	-0,12	34712	0,07
12			0,05	1307	0,00	-22911	-0,10	26478	0,05
13		0,025	0,01	2382	0,01	-59655	-0,25	47846	0,10
14			ξc 0,03	2314	0,01	-37787	-0,16	30525	0,06
15			0,05	2053	0,01	-29194	-0,12	23448	0,05
16		0,03	0,01	5140	0,01	-72164	-0,30	40600	0,08
17			ξc 0,03	4034	0,01	-45621	-0,19	26499	0,05
18			0,05	3365	0,01	-35193	-0,15	20520	0,04

<b>D50/D90</b>		<b>60/75</b>							
<b>fall velocity</b>		<b>0,003</b>		<b>Channel</b>		<b>Berths</b>		<b>Jetty</b>	
<b>INITIAL VALUES</b>				2223870	6,01	2932134	12,22	4292014	8,87
<b>DIFFERENCE</b>				m^3 per month	cm per month	m^3 per month	cm per month	m^3 per month	cm per month
<b>No.</b>									
19	Chézy	60	0,01	26982	0,07	-70877	-0,30	108741	0,22
20			ξc 0,03	15189	0,04	-35864	-0,15	56898	0,12
21			0,05	11063	0,03	-25259	-0,11	40088	0,08
22		70	0,01	27861	0,08	-54783	-0,23	114075	0,24
23			ξc 0,03	15490	0,04	-27932	-0,12	59111	0,12
24			0,05	11243	0,03	-19744	-0,08	41538	0,09
25		80	0,01	29217	0,08	-41684	-0,17	117851	0,24
26			ξc 0,03	16037	0,04	-21529	-0,09	60633	0,13
27			0,05	11595	0,03	-15304	-0,06	42530	0,09
28	Manning	0,02	0,01	19145	0,05	-68712	-0,29	101813	0,21
29			ξc 0,03	11283	0,03	-34684	-0,14	53609	0,11
30			0,05	8328	0,02	-24416	-0,10	37815	0,08
31		0,025	0,01	17785	0,05	-96165	-0,40	90964	0,19
32			ξc 0,03	10858	0,03	-48279	-0,20	49053	0,10
33			0,05	8086	0,02	-33883	-0,14	34814	0,07
34		0,03	0,01	19743	0,05	-121044	-0,50	80440	0,17
35			ξc 0,03	12010	0,03	-60685	-0,25	44488	0,09
36			0,05	8930	0,02	-42540	-0,18	31777	0,07

## **Annex H**

Sedimentation/erosion patterns of calibration runs

Figure H-1 : runid 1 to 9

Figure H-2 : runid 10 to 18

Figure H-3 : runid 19 to 27

Figure H-4 : runid 28 to 36

# Annex I

## Residual sediment transport of calibration runs

Figure I-1 : Residual bed load transport, runid 1 to 9

Figure I-2 : Residual suspended transport, runid 1 to 9

Figure I-3 : Residual bed load transport, runid 10 to 18

Figure I-4 : Residual suspended transport, runid 10 to 18

Figure I-5 : Residual bed load transport, runid 19 to 27

Figure I-6 : Residual suspended transport, runid 19 to 27

Figure I-7 : Residual bed load transport, runid 28 to 36

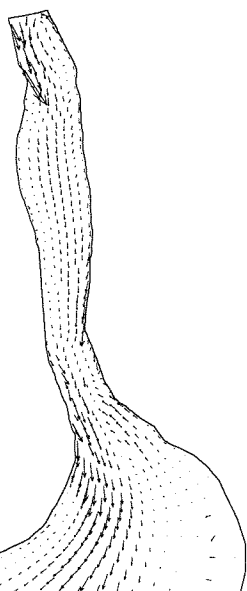
Figure I-8 : Residual suspended transport, runid 28 to 36



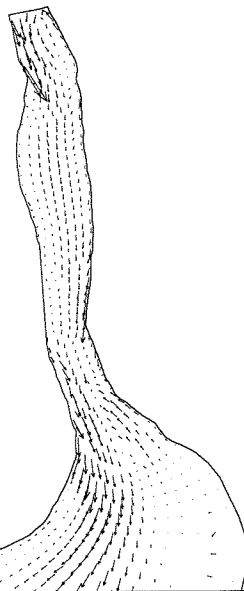
Residual bed load transport; run 1 to 9

→  $1.0 \cdot 10^{-6} \text{ m/s}$

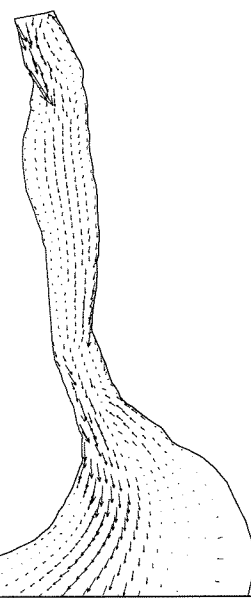
001



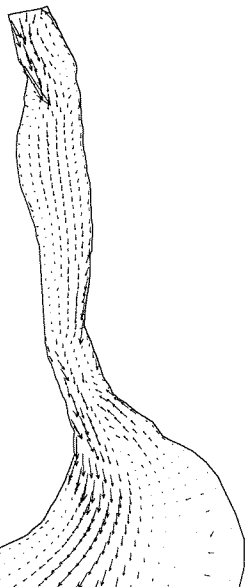
002



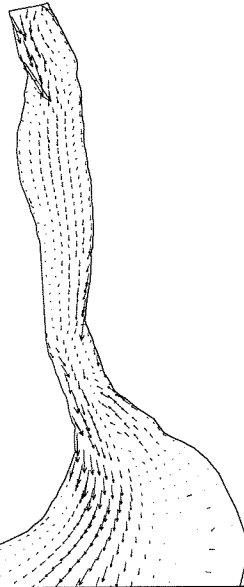
003



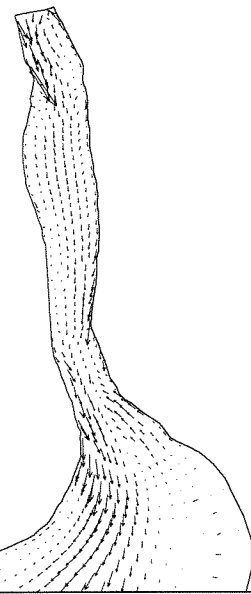
004



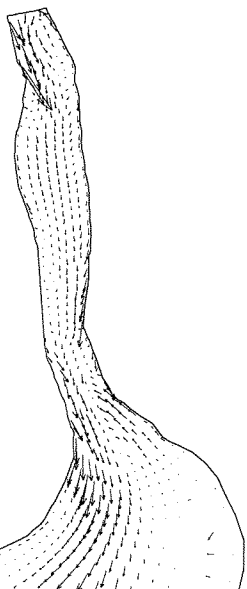
005



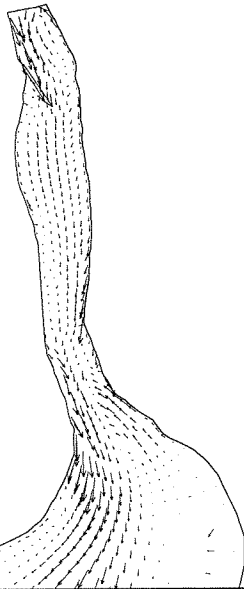
006



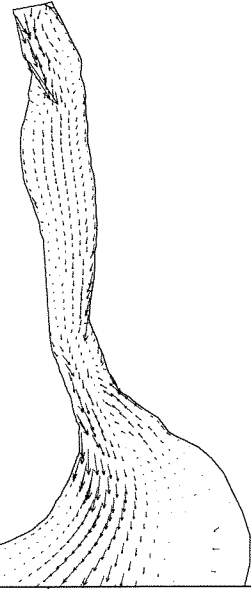
007



008



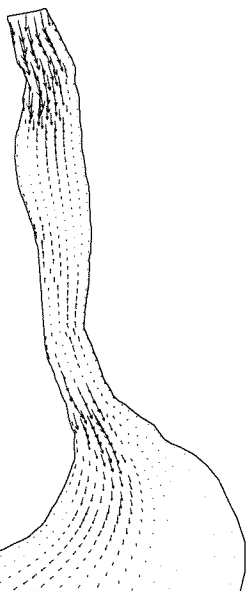
009



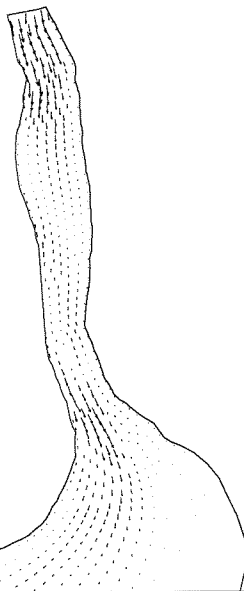
Residual suspended transport; run 1 to 9

→  $5.0 \cdot 10^{-4} \text{ m/s}$

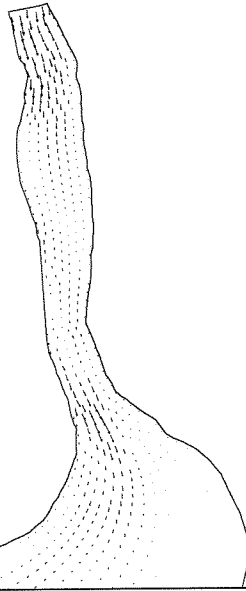
001



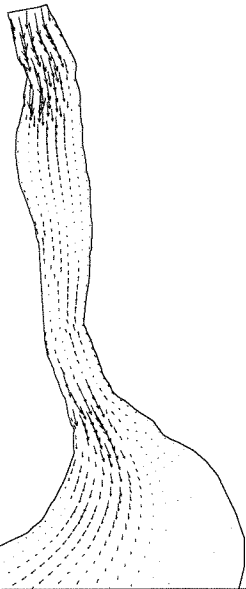
002



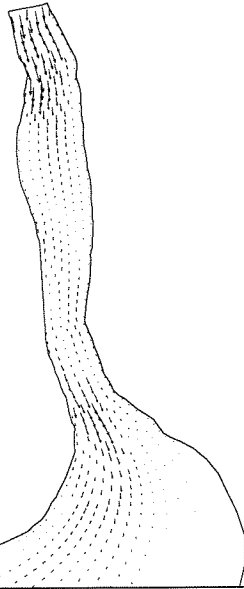
003



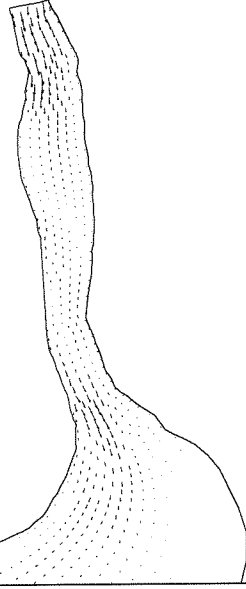
004



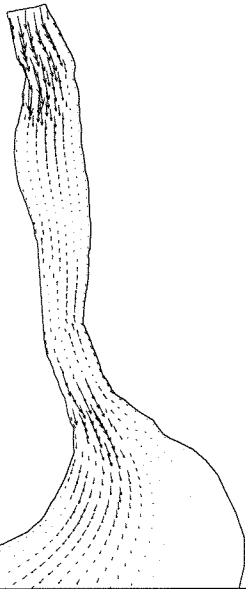
005



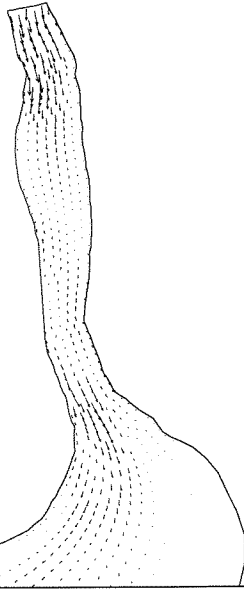
006



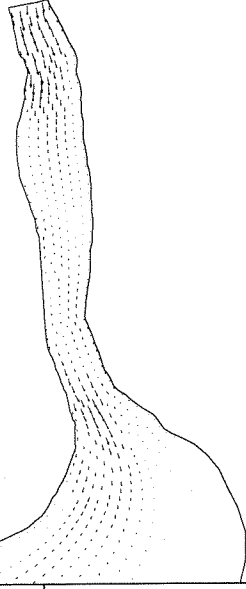
007



008



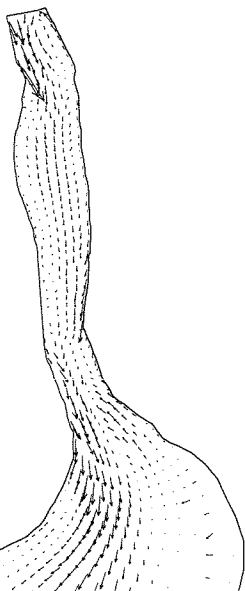
009



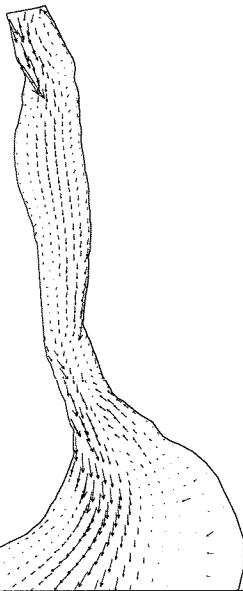
Residual bed load transport; run 10 to 18

→  $1.0 \cdot 10^{-6} \text{ m/s}$

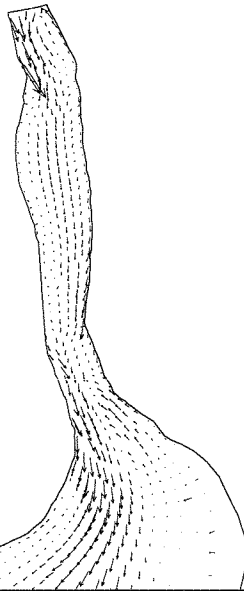
010



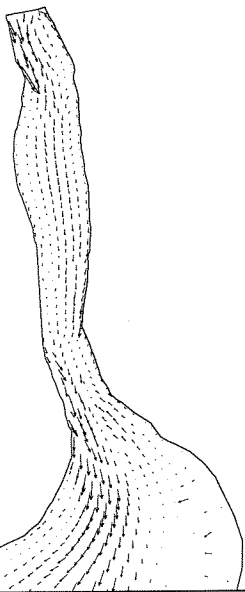
011



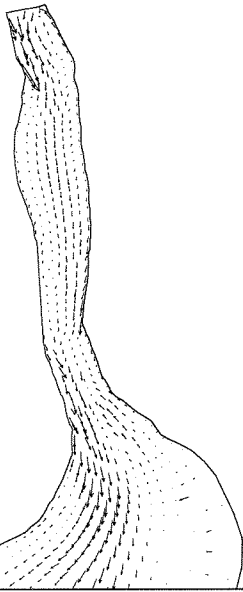
012



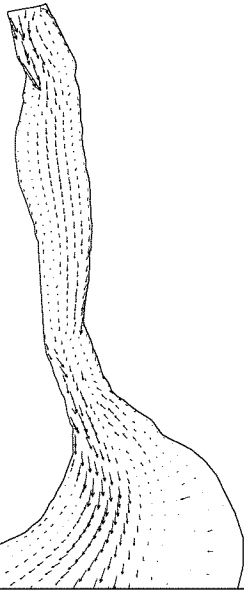
013



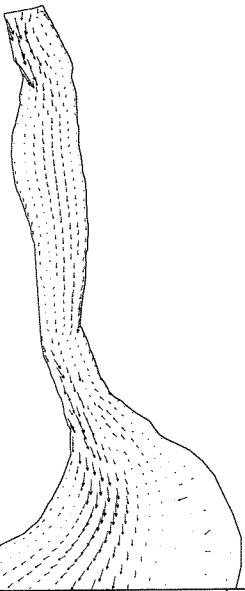
014



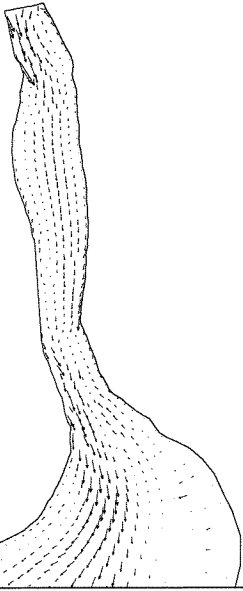
015



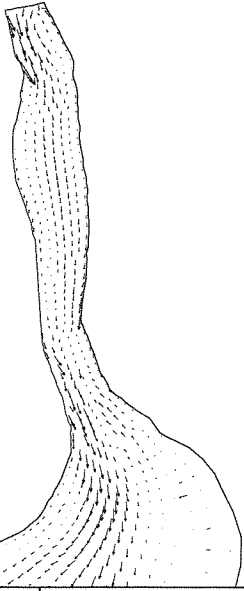
016



017

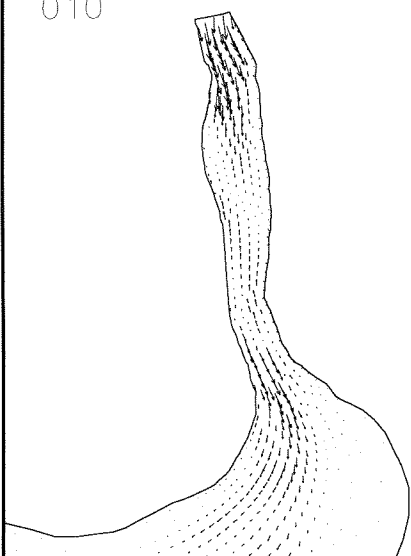


018

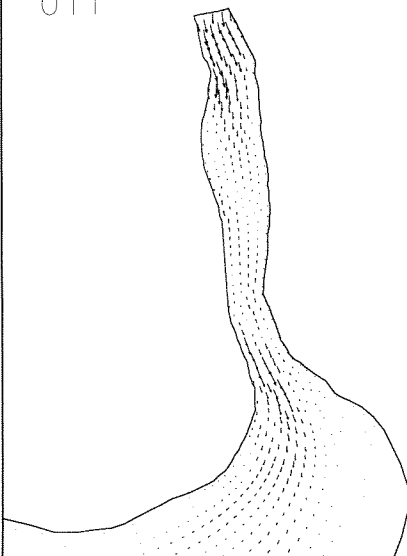


Residual suspended transport; run 10 to 18 →  $5.0 \cdot 10^{-4} \text{ m/s}$

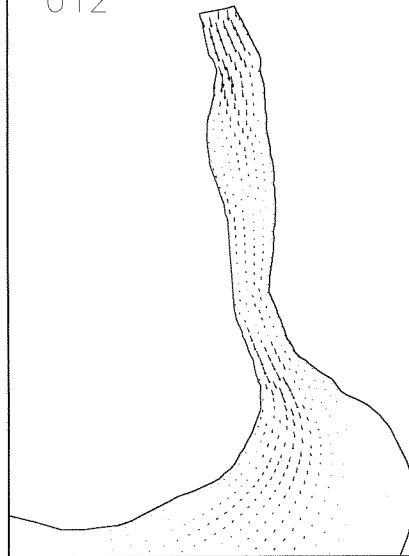
010



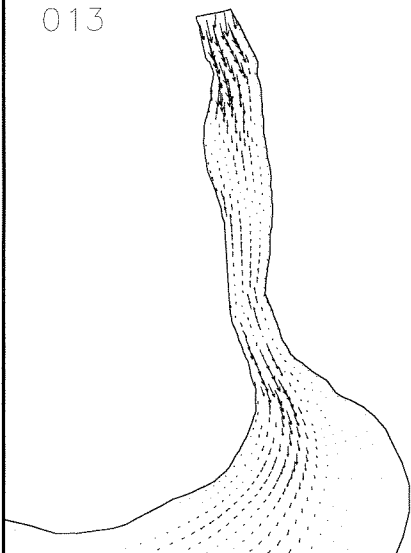
011



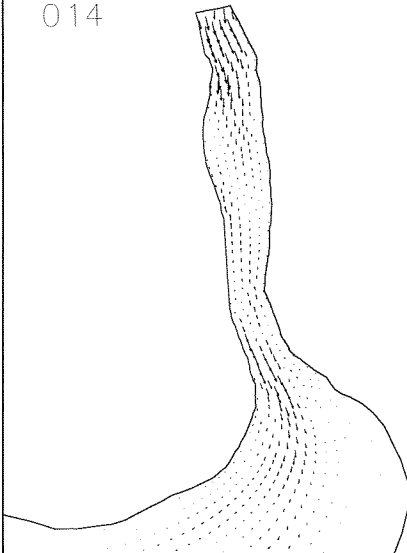
012



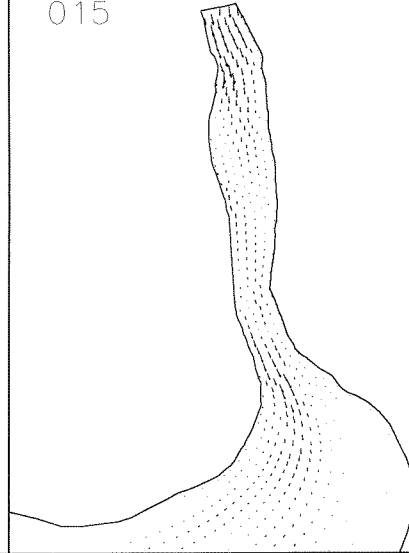
013



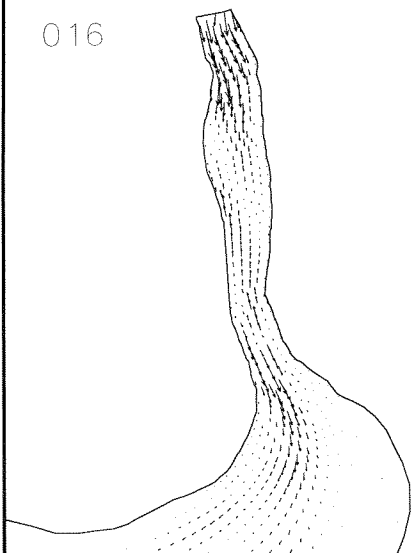
014



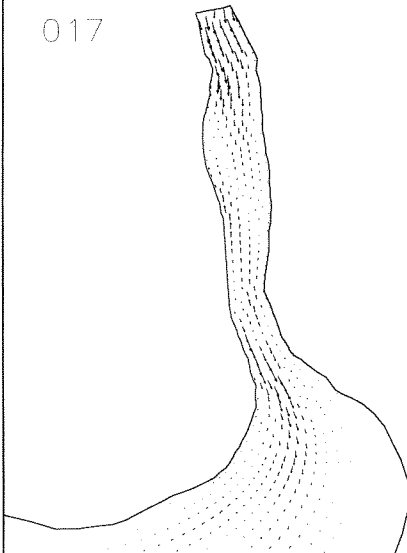
015



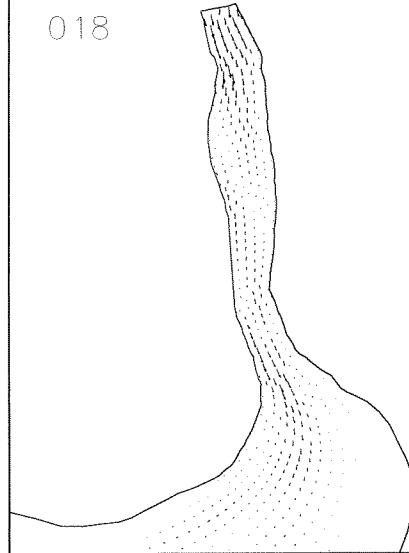
016



017

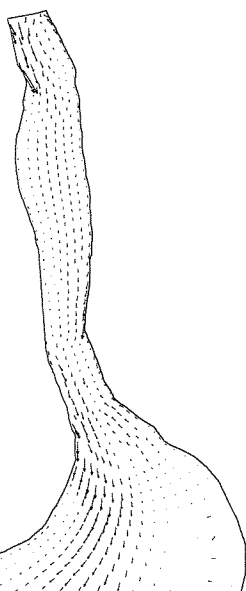


018

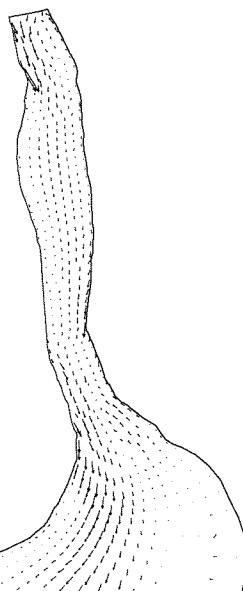


Residual bed load transport; run 19 to 27 →  $1.0 \cdot 10^{-6} \text{ m/s}$

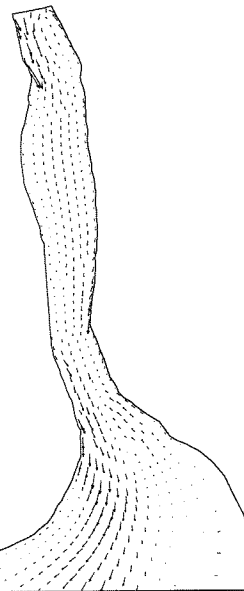
019



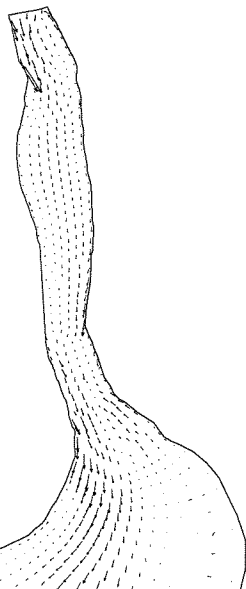
020



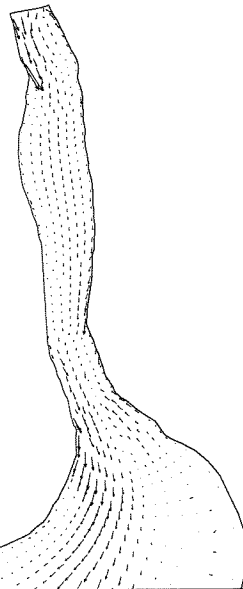
021



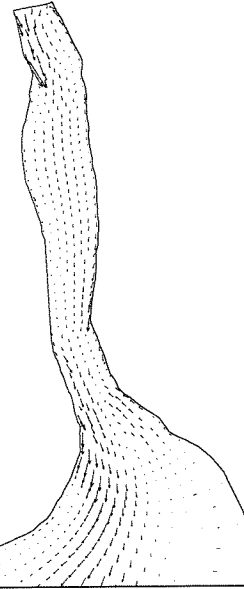
022



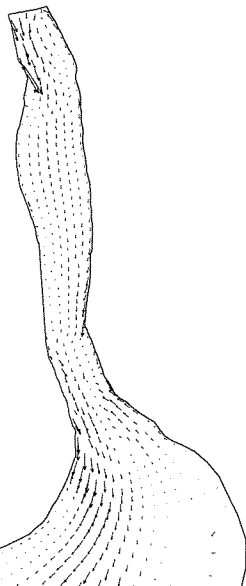
023



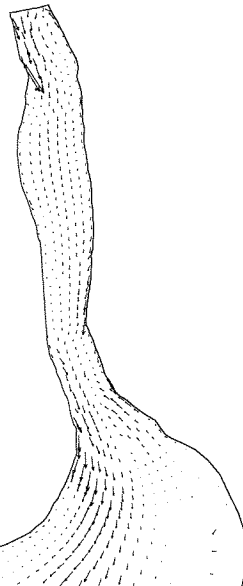
024



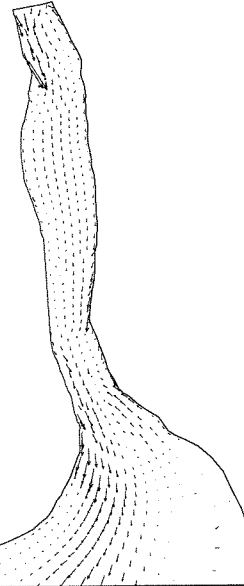
025



026

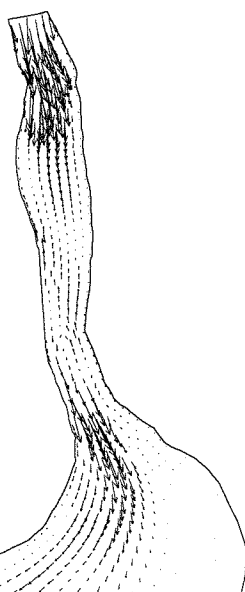


027

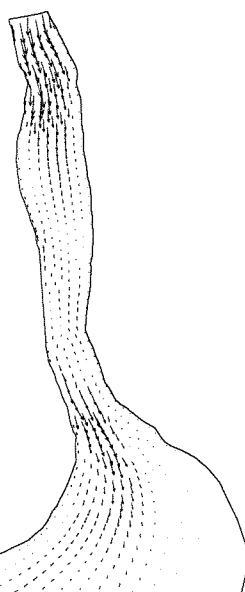


Residual suspended transport; run 19 to 27 →  $5.0 \cdot 10^{-4} \text{ m/s}$

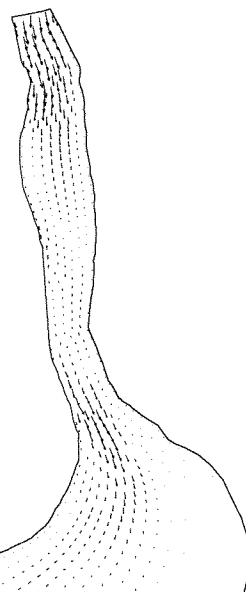
019



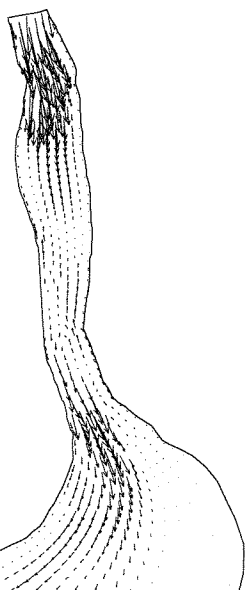
020



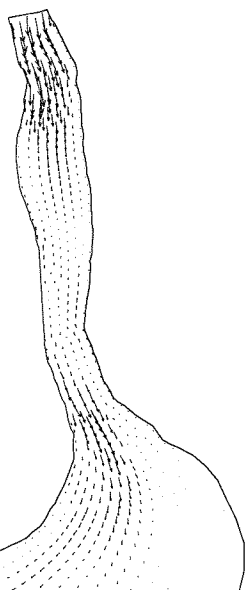
021



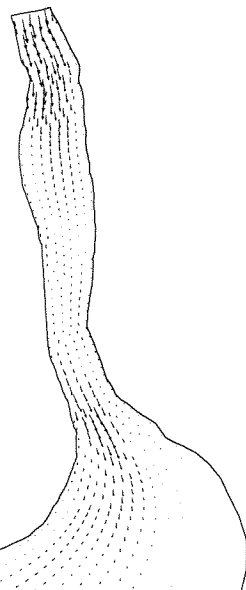
022



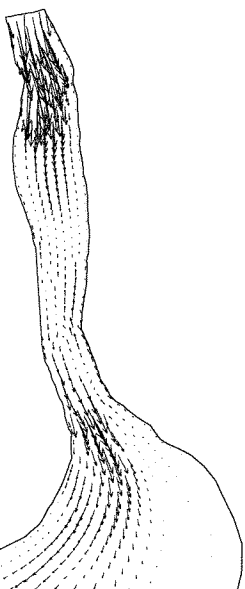
023



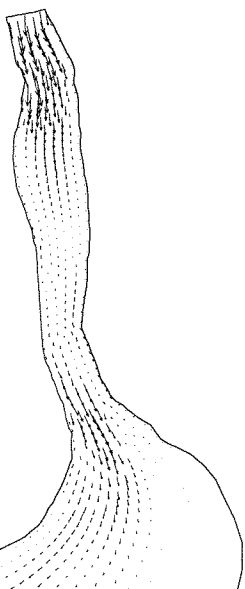
024



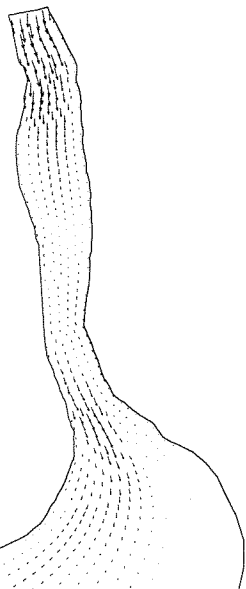
025



026



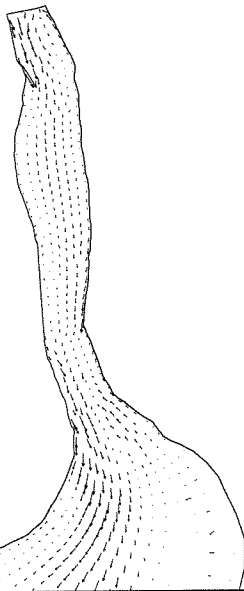
027



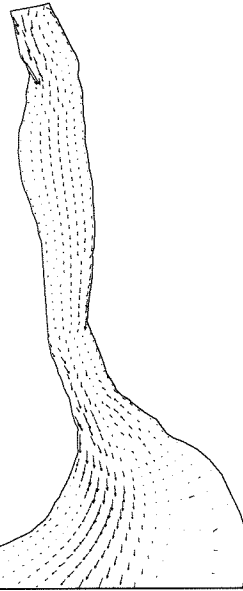
Residual bed load transport; run 28 to 36

→  $1.0 \cdot 10^{-6} \text{ m/s}$

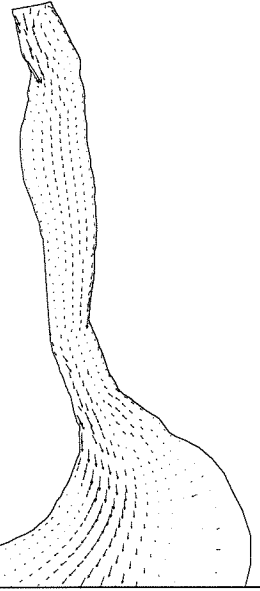
028



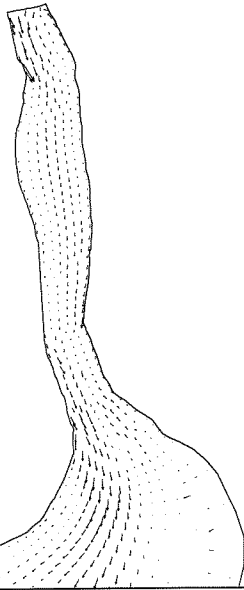
029



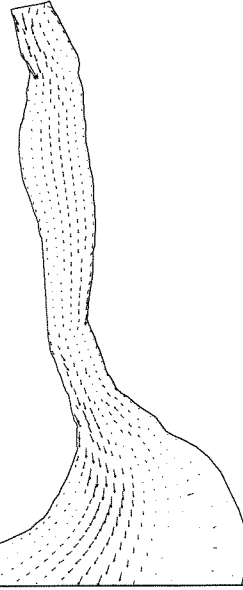
030



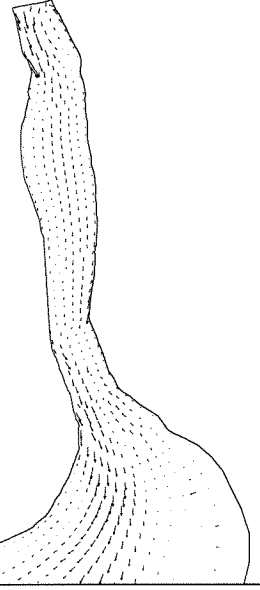
031



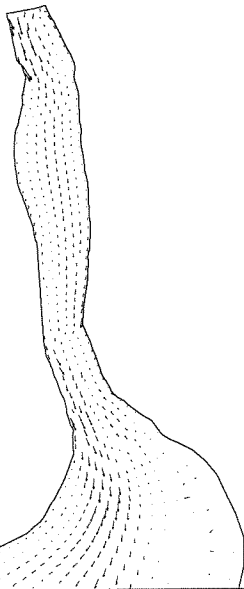
032



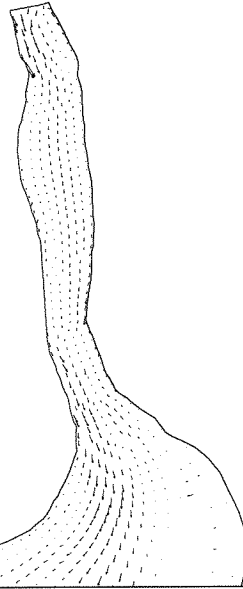
033



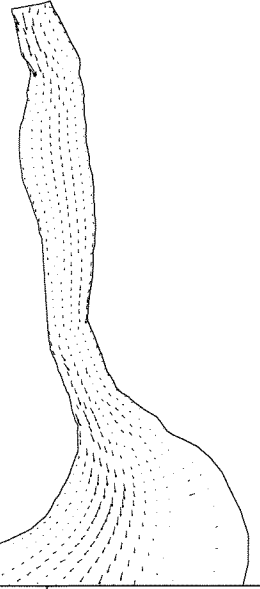
034



035

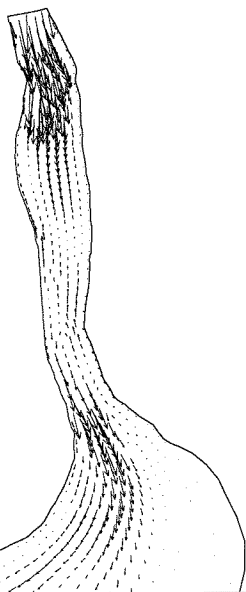


036

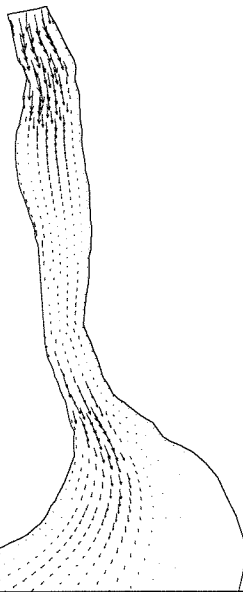


Residual suspended transport; run 28 to 36 →  $5.0 \cdot 10^{-4} \text{ m/s}$

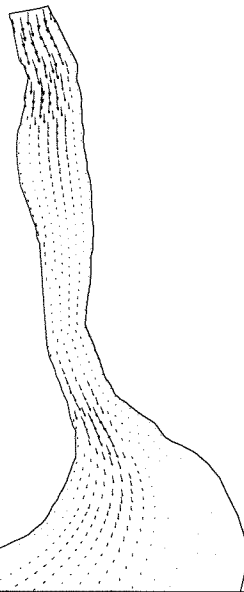
028



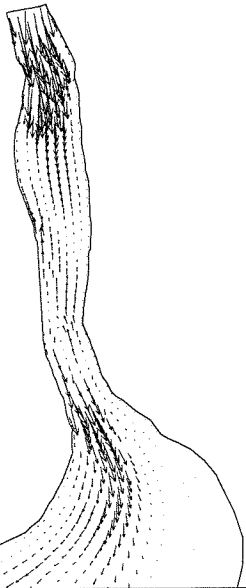
029



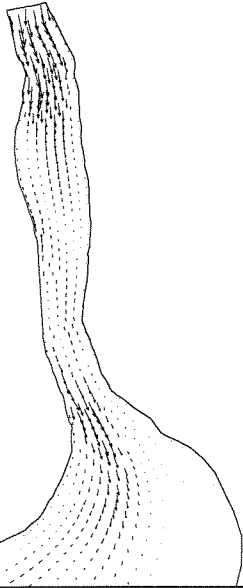
030



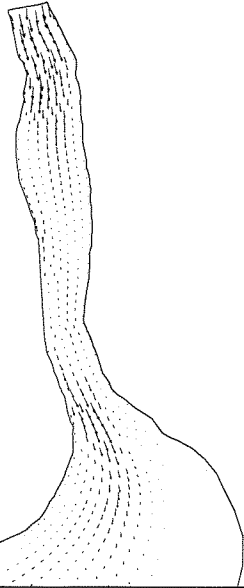
031



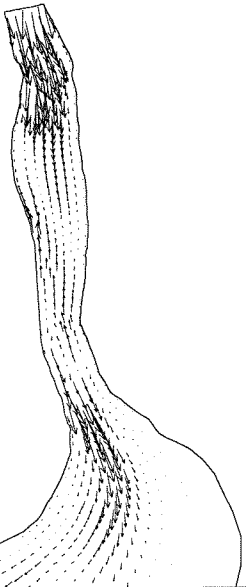
032



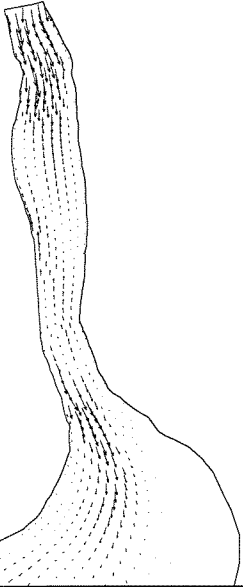
033



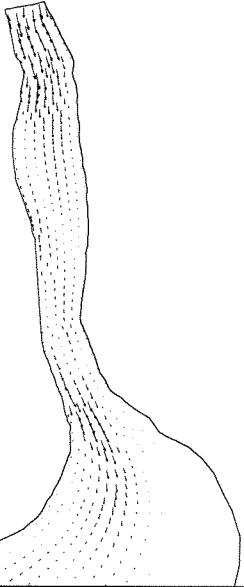
034



035



036





## Annex J

### Results of simulation runs

Figure J-1: Future required depth

Figure J-2 : Sedimentation/erosion pattern future situation

Figure J-3 : Residual bed load transport future situation

Figure J-4 : Residual suspended transport future situation

Figure J-5 : Model area and training wall

Figure J-6 : Sedimentation/erosion pattern

Figure J-7 : Residual bed load transport

Figure J-8 : Residual suspended transport

} concept 1

Figure J-9 : Model area and training wall

Figure J-10 : Sedimentation/erosion pattern

Figure J-11 : Residual bed load transport

Figure J-12 : Residual suspended transport

} concept 2

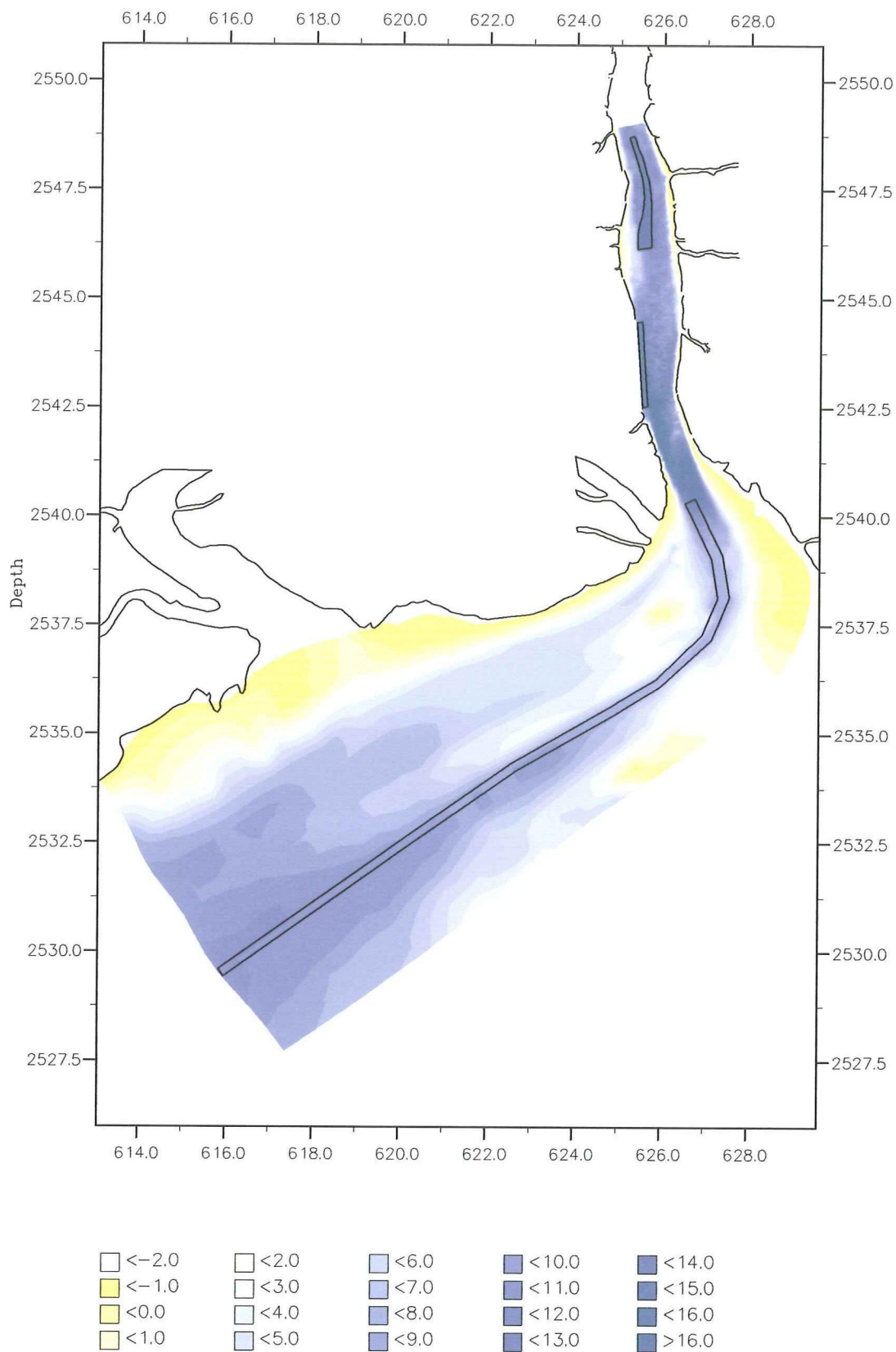
Figure J-13 : Model area and training wall

Figure J-14 : Sedimentation/erosion pattern

Figure J-15 : Residual bed load transport

Figure J-16 : Residual suspended transport

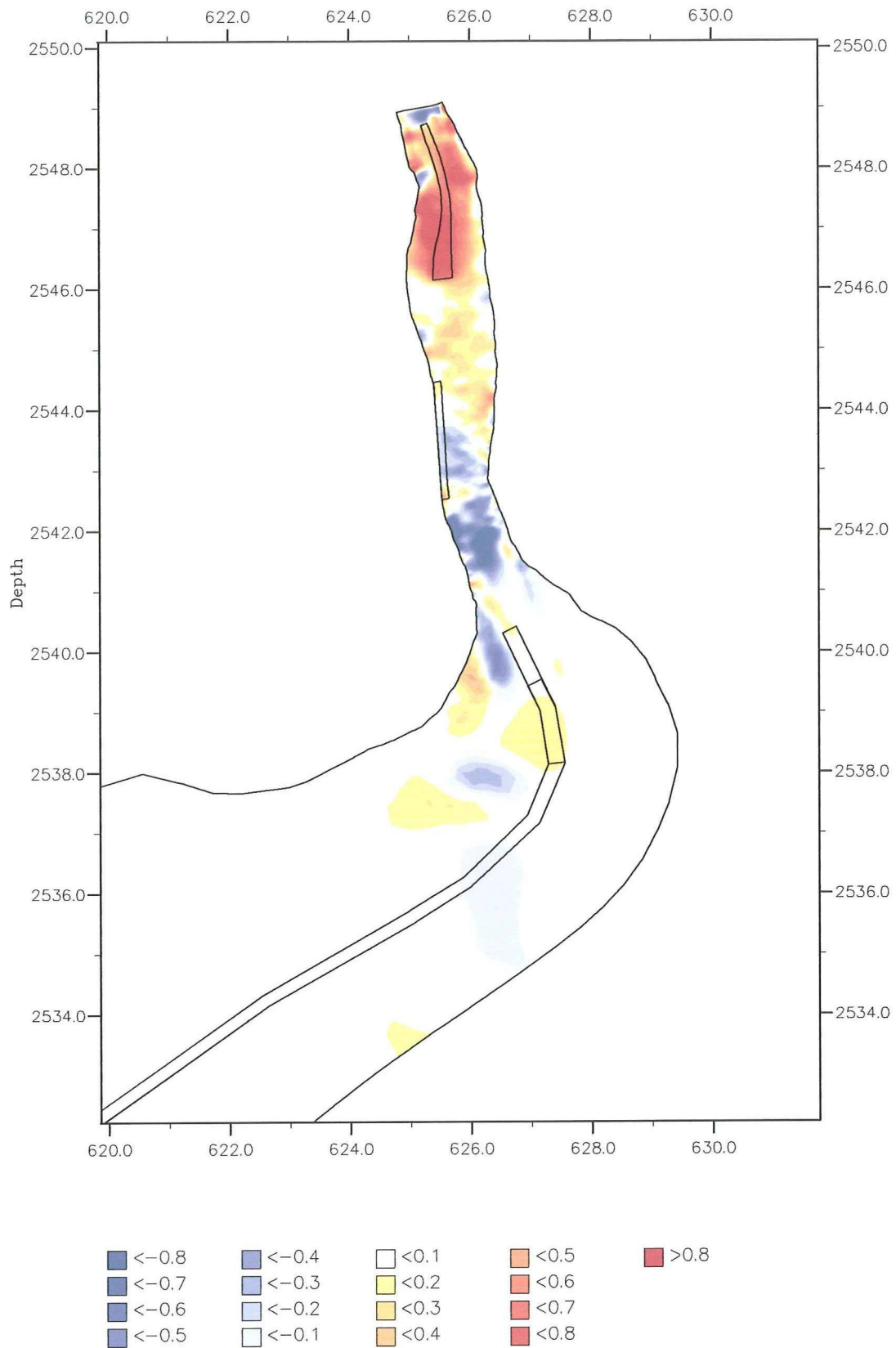
} concept 3



Future required depth  
Sogal Channel : CD - 8.0 m  
Berths and jetty area : CD - 14.2 m

Figure J-1

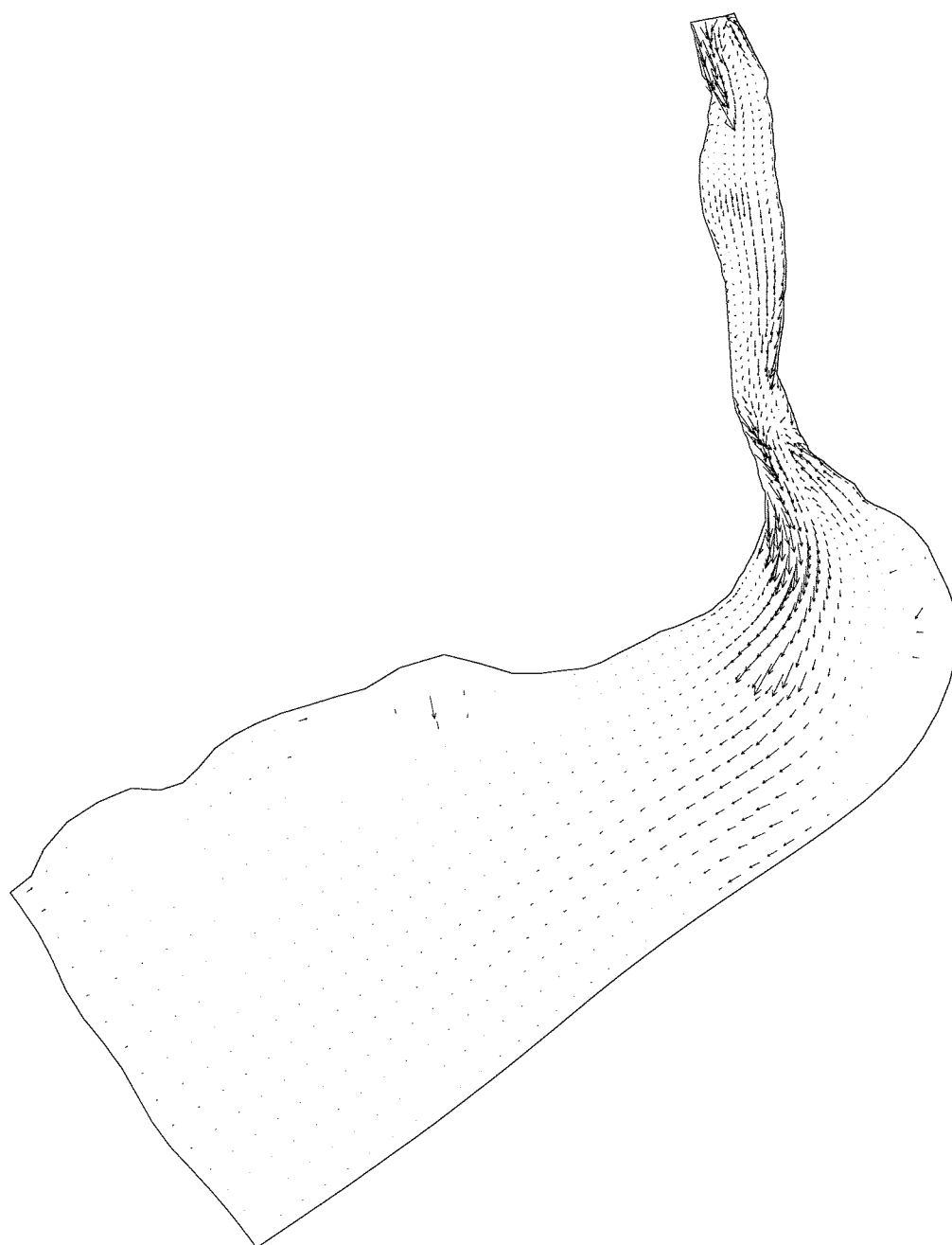
WL | DELFT HYDRAULICS



Sedimentation/erosion pattern of  
future deepened situation

Figure J-2

WL | DELFT HYDRAULICS

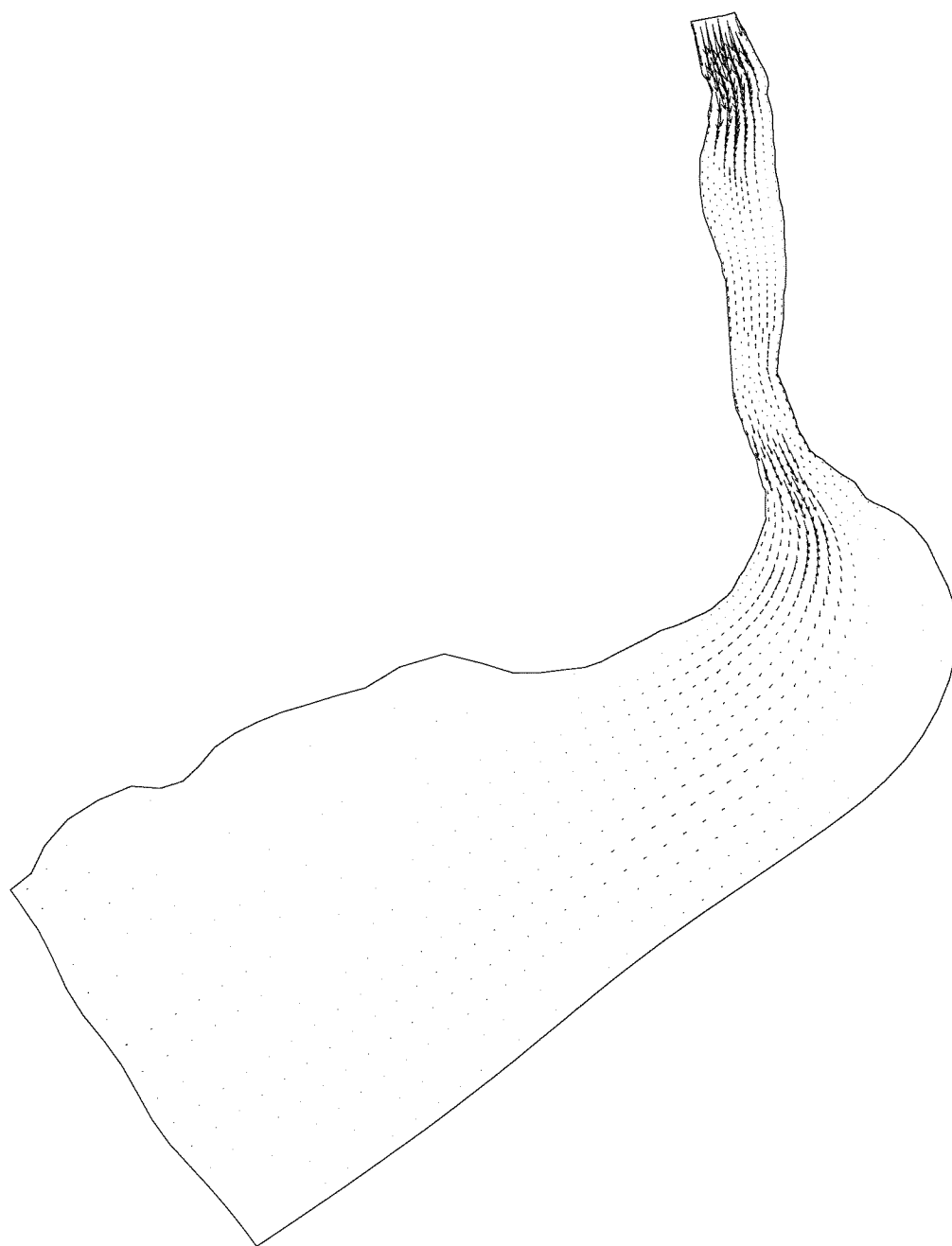


→  $5.0 \cdot 10^{-7} \text{ m/s}$

Residual bed load transport

Figure J-3

WL | DELFT HYDRAULICS

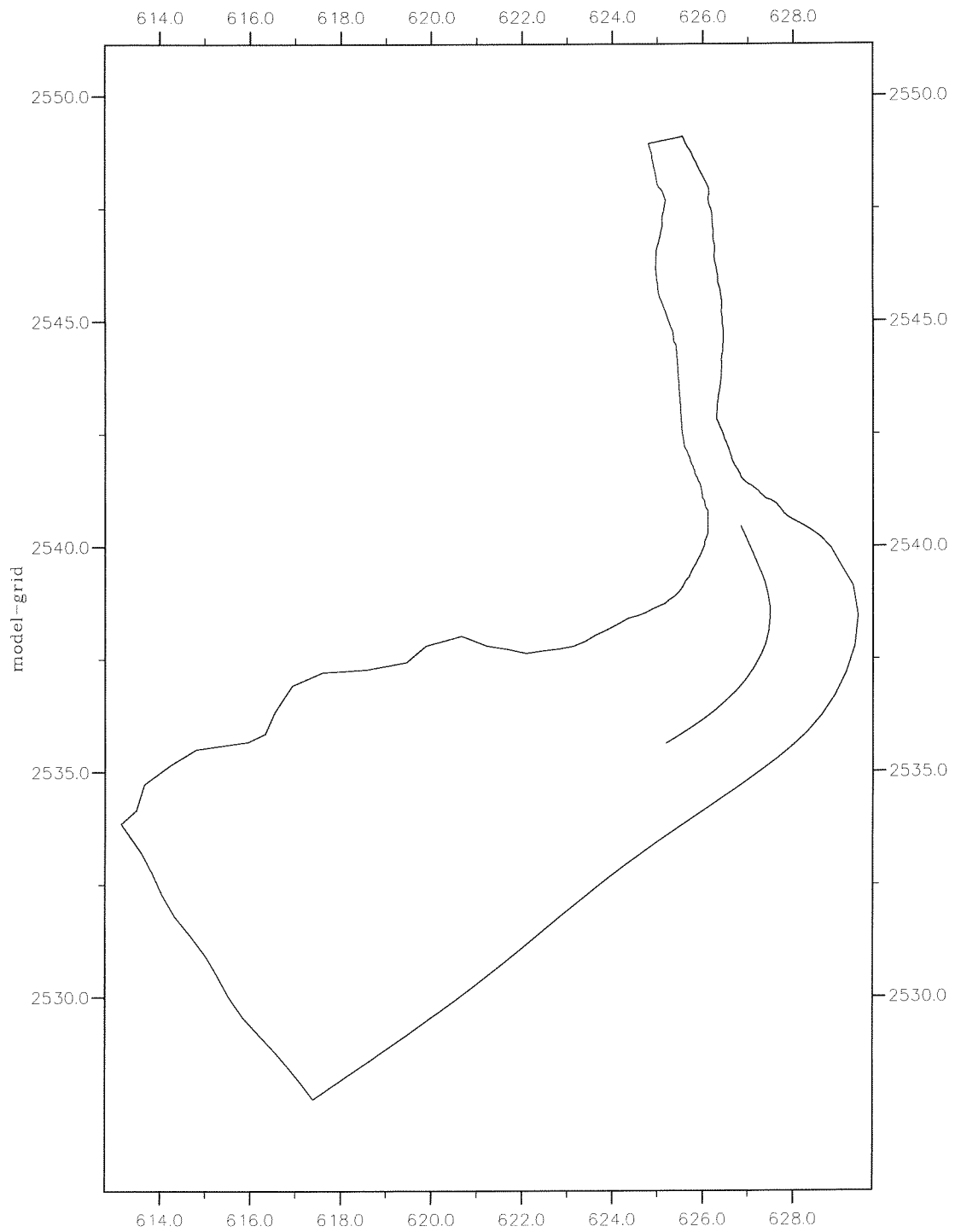


→ 0.001m/s

Residula suspended transport

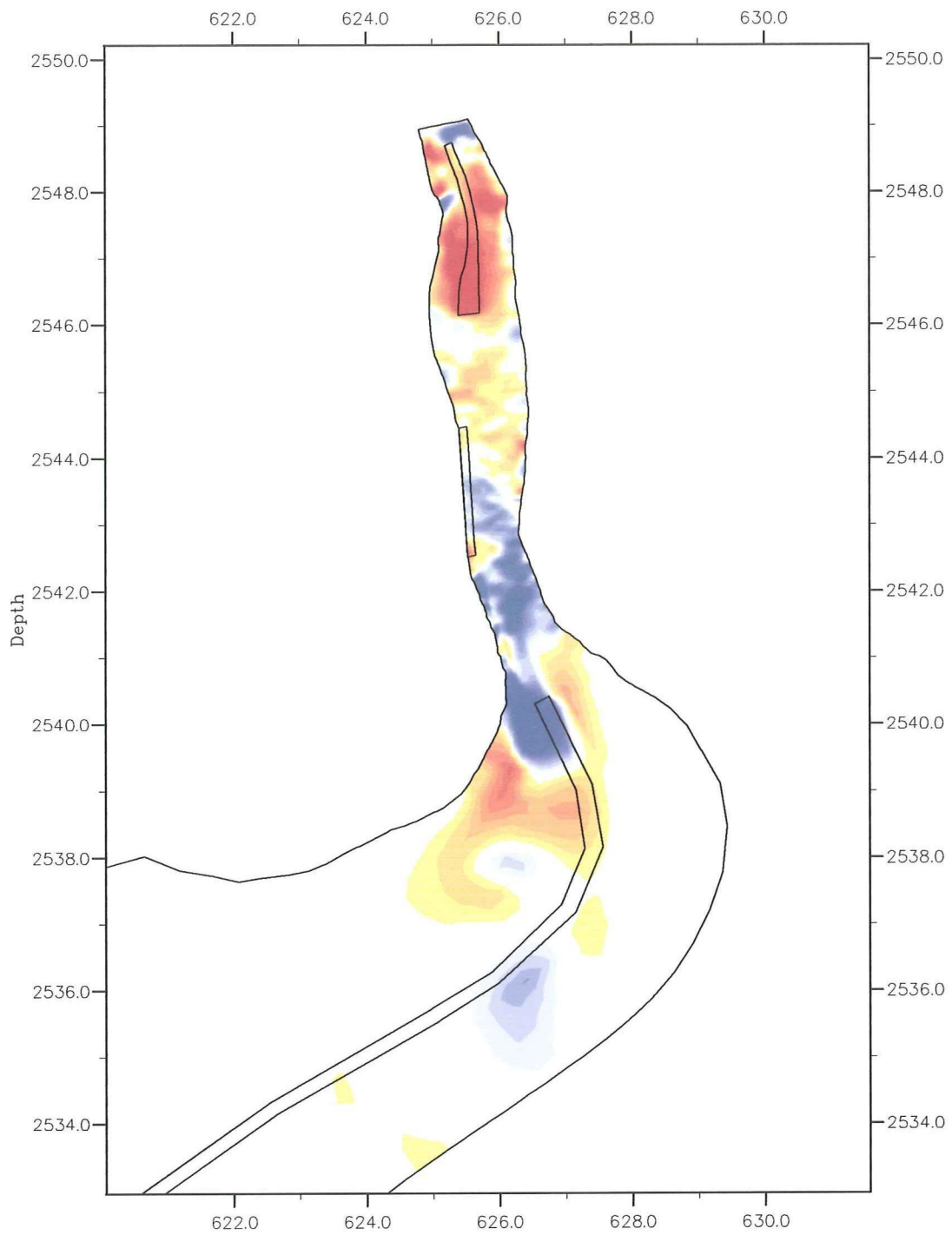
Figure J-4

WL | DELFT HYDRAULICS



Model area with training wall  
(concept 1)

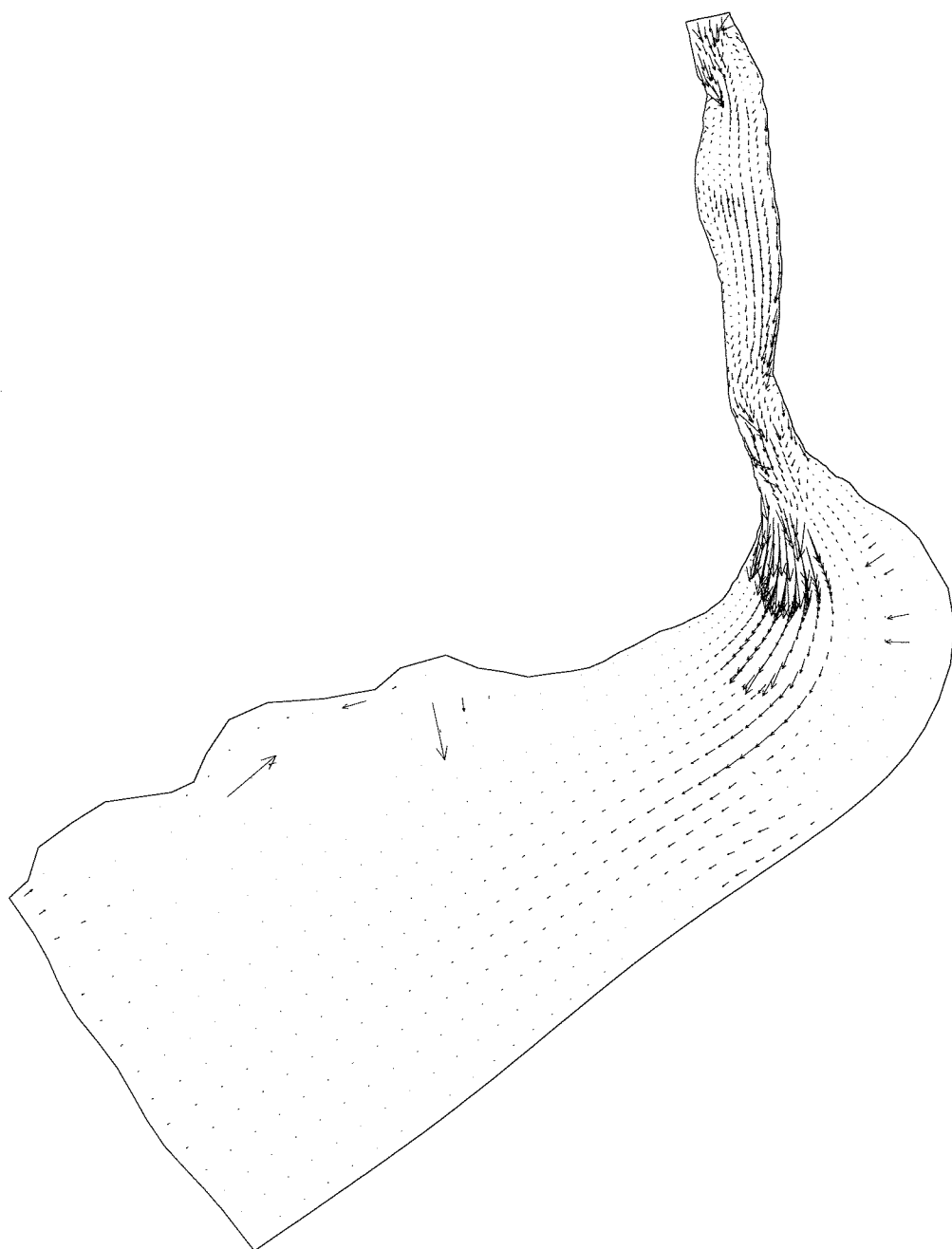
Figure J-5



Sedimentation/erosion pattern concept 1

Figure J-6

WL | DELFT HYDRAULICS



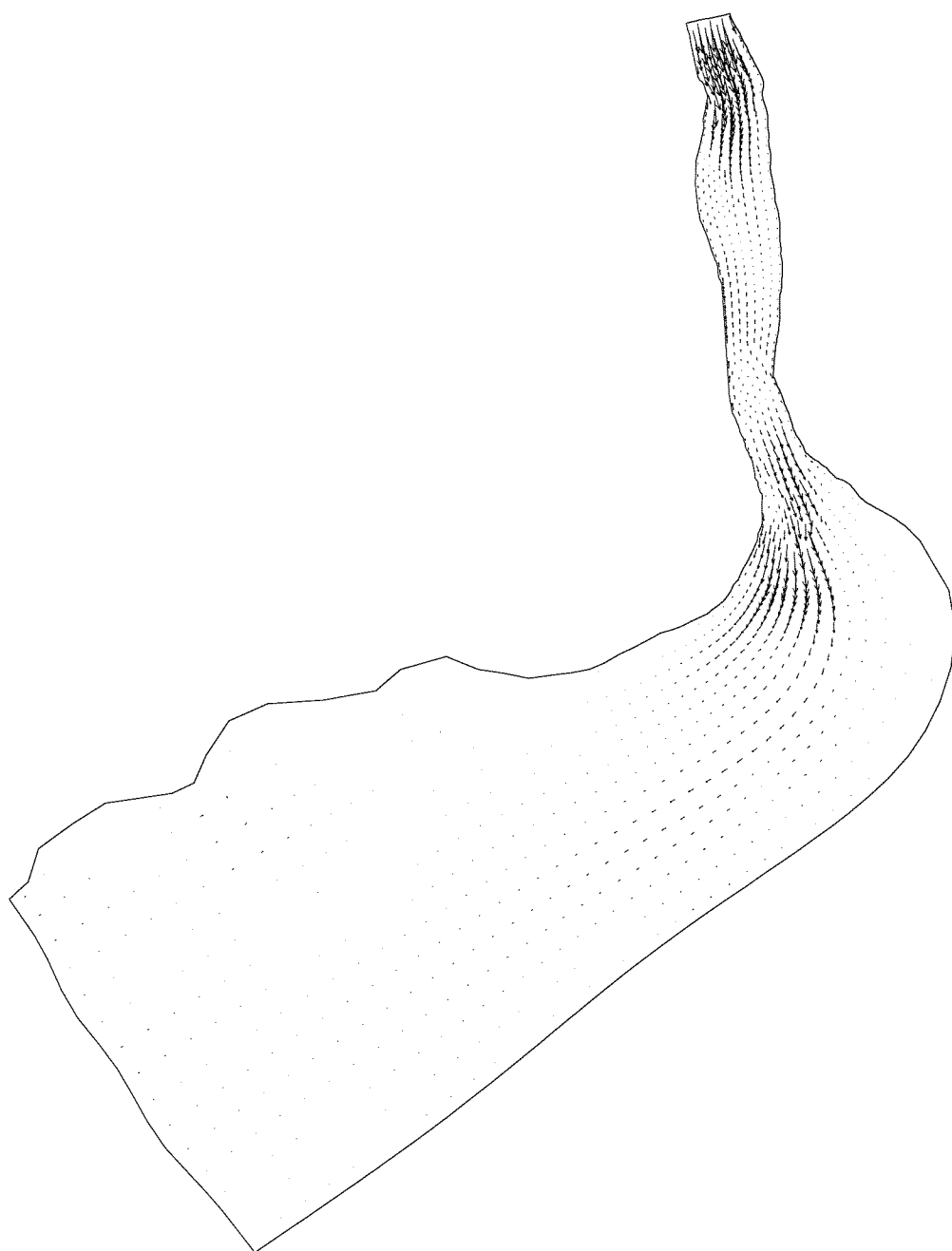
→  $5.0 \cdot 10^{-7} \text{ m/s}$

Residual bed load transport

Figure J-7

WL | DELFT HYDRAULICS



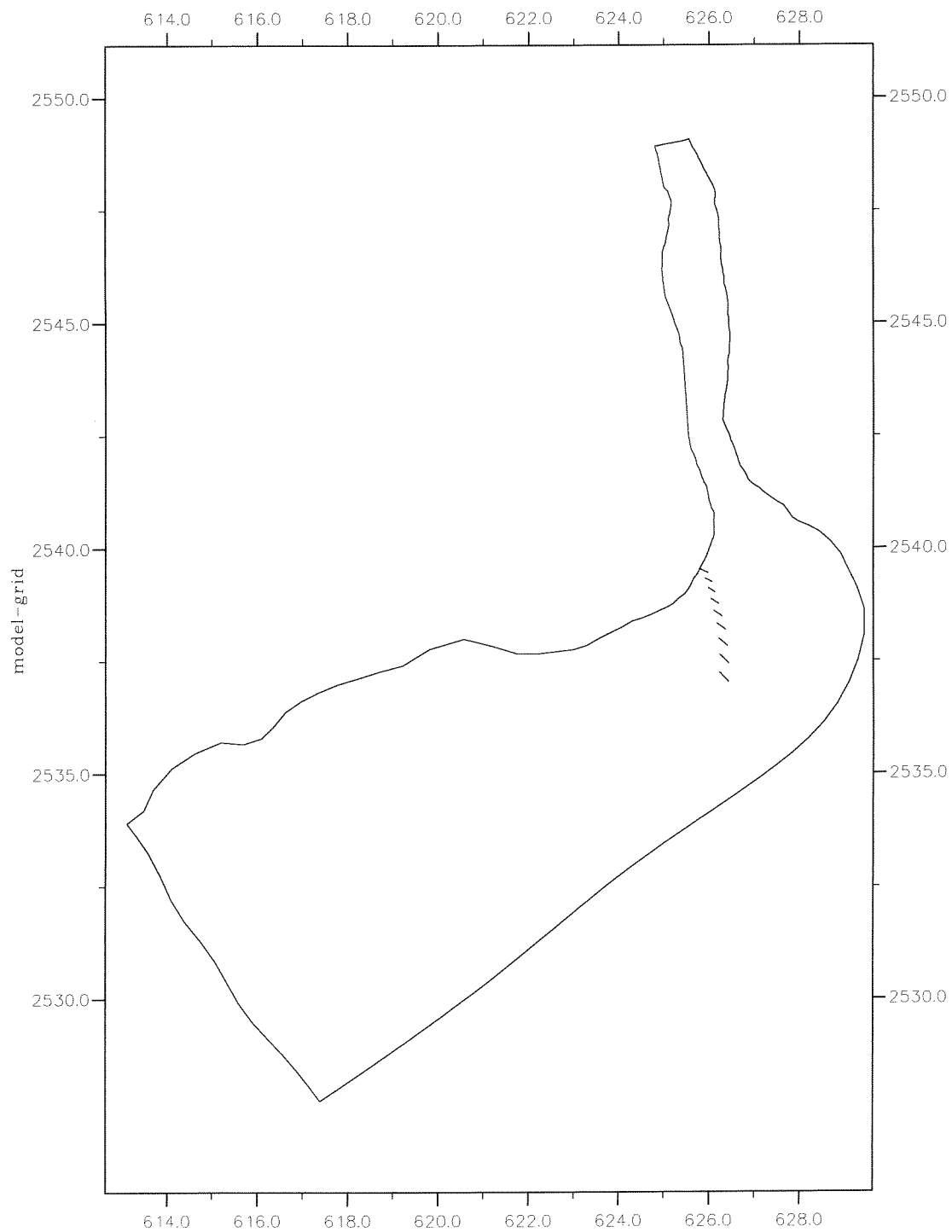


→ 0.001m/s

Residual suspended transport

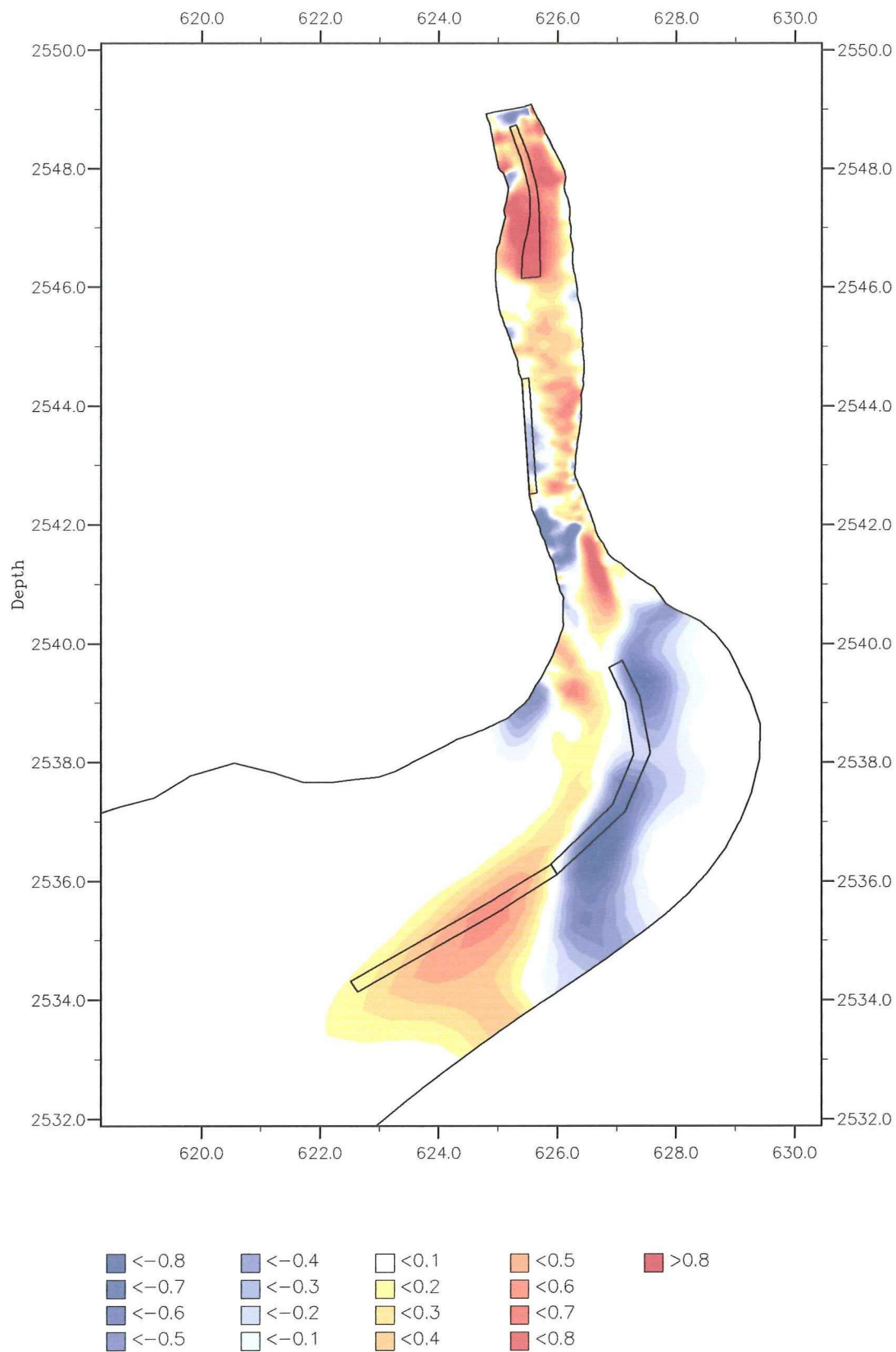
Figure J-8

WL | DELFT HYDRAULICS



Model area and staggered training wall  
(concept 2)

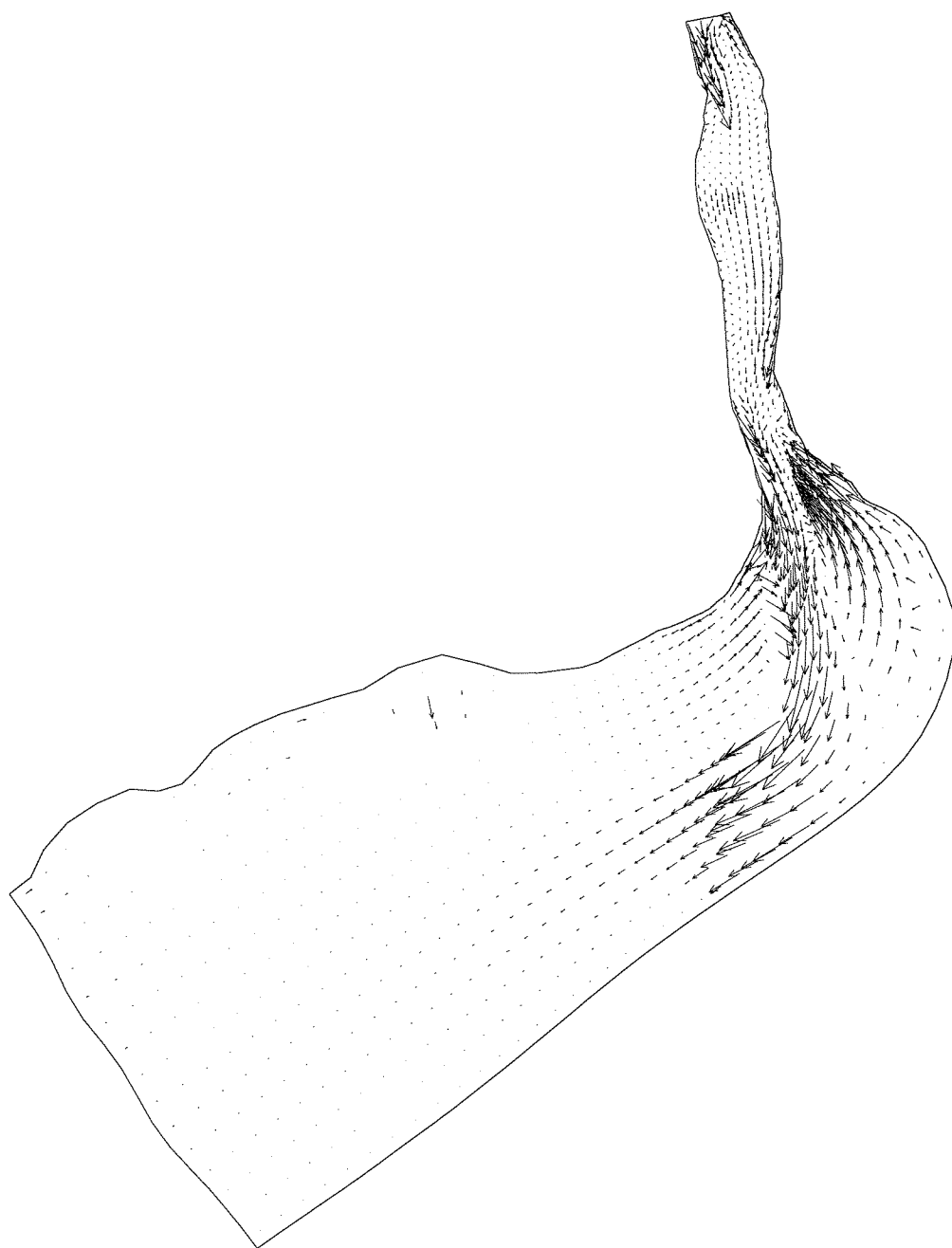
Figure J—9



Sedimentation/erosion pattern concept 2

Figure J-10

WL | DELFT HYDRAULICS

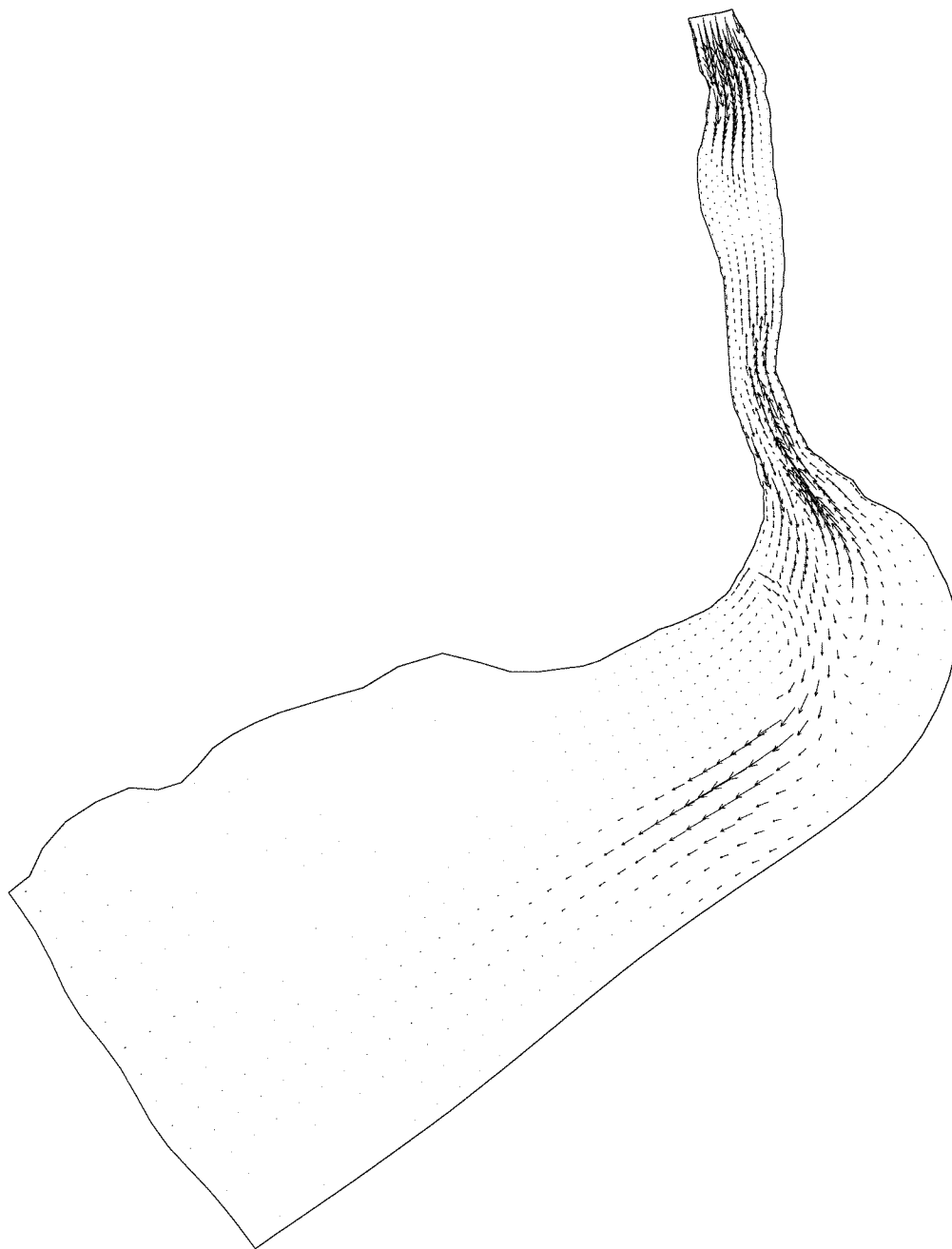


→  $5.0 \times 10^{-7} \text{ m/s}$

Residual bed load transport

Figure J-11

WL | DELFT HYDRAULICS

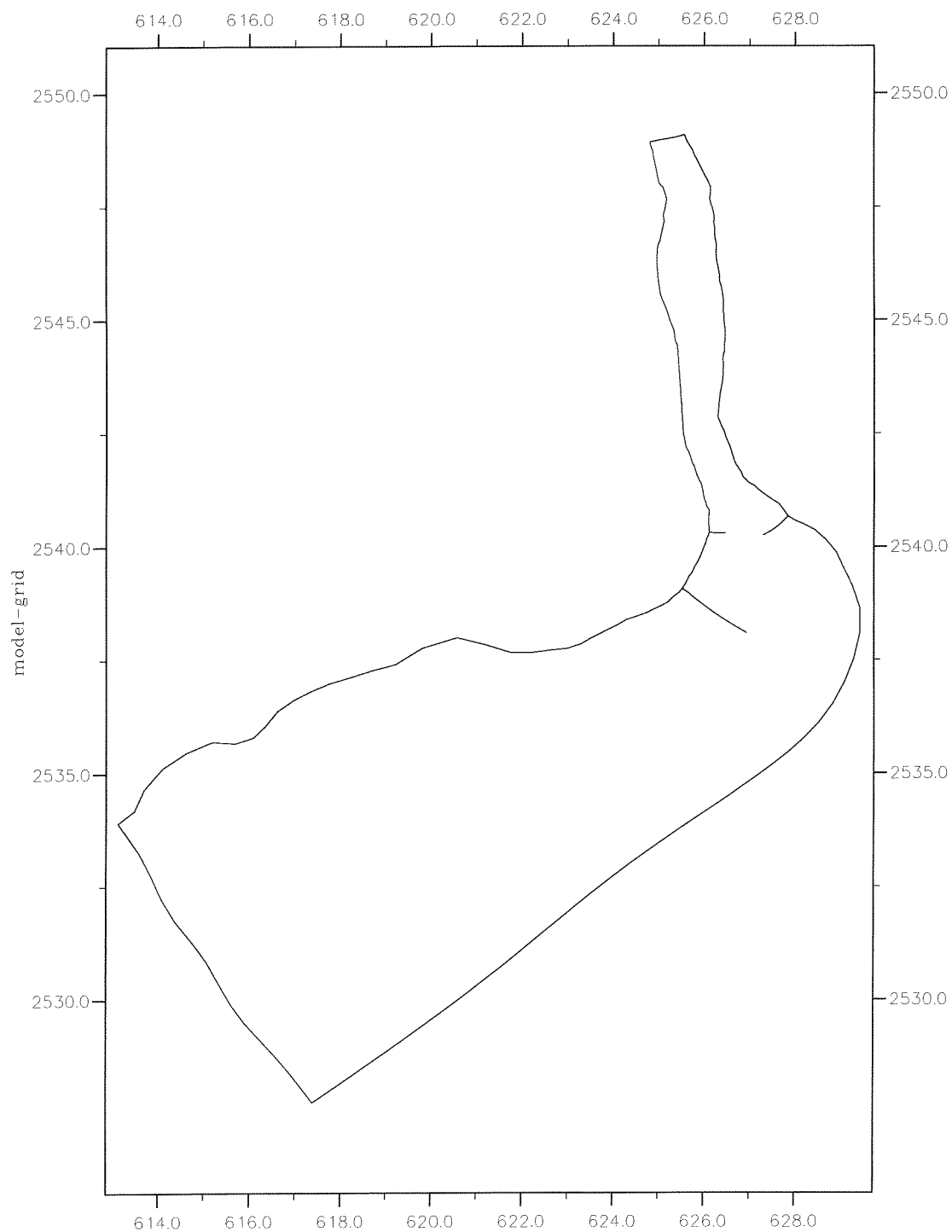


→ 0.001m/s

Residual suspended transport

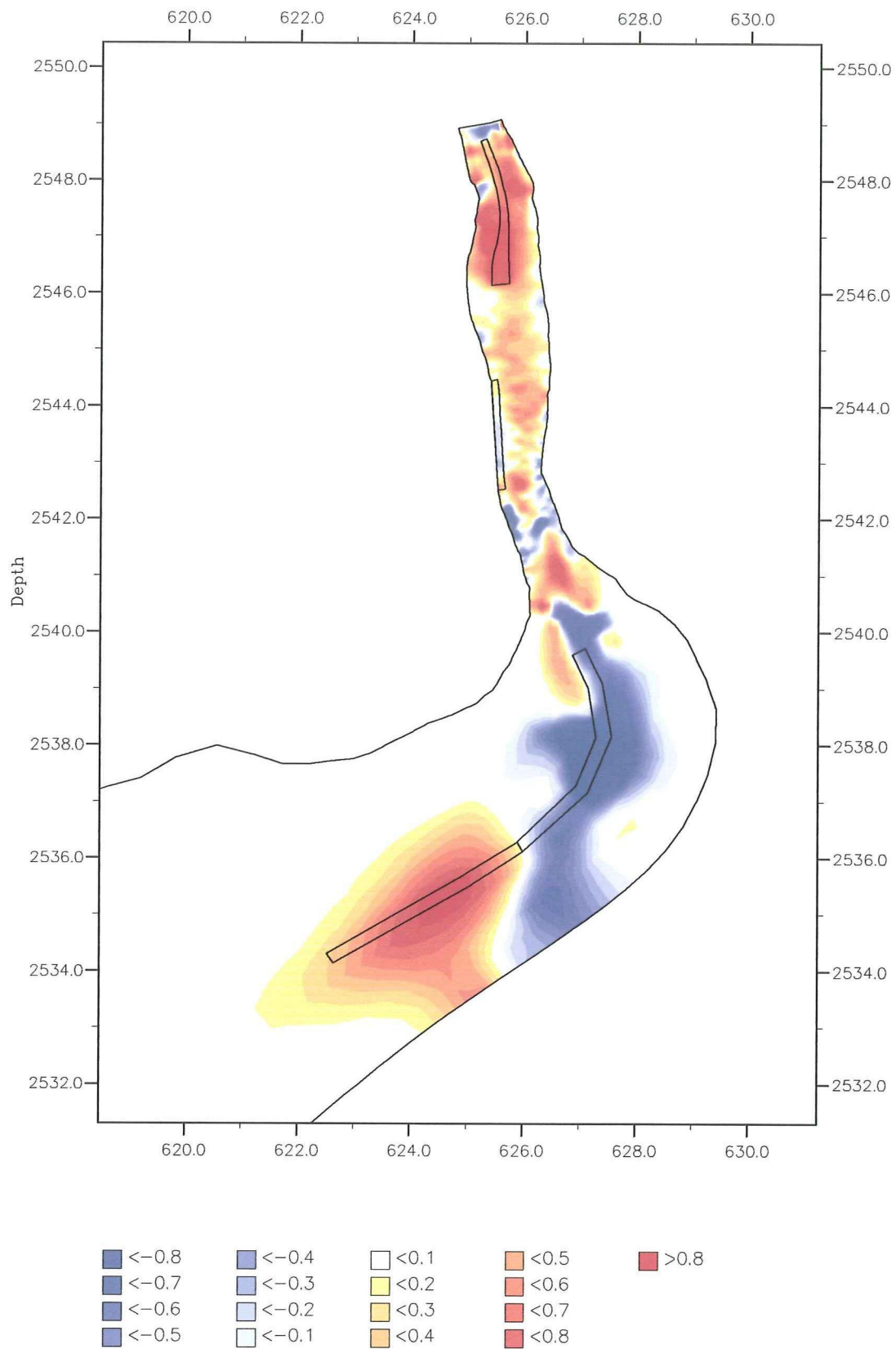
Figure J-12

WL | DELFT HYDRAULICS



Model area and training walls  
(concept 3)

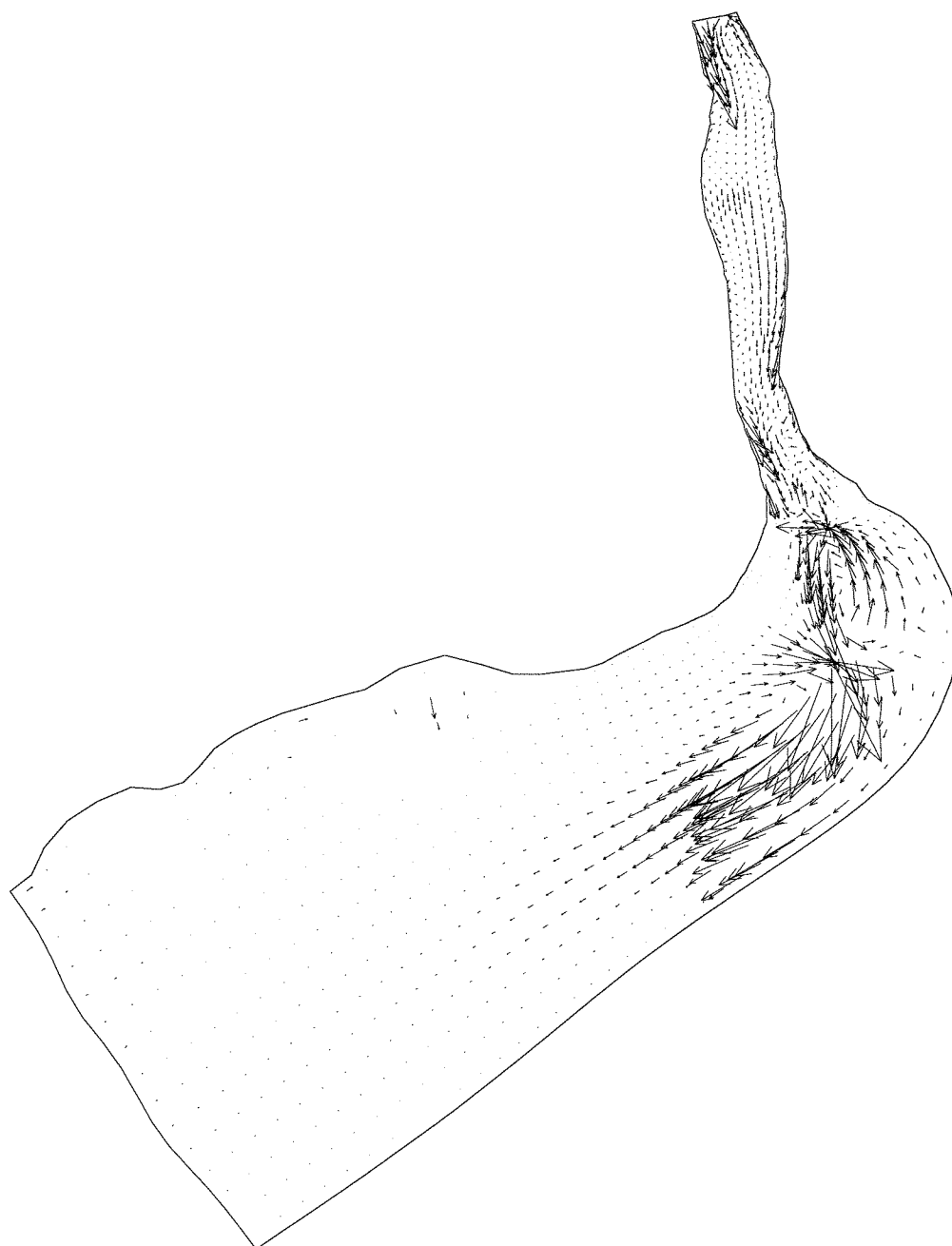
Figure J-13



Sedimentation/erosion pattern concept 3

Figure J-14

WL | DELFT HYDRAULICS



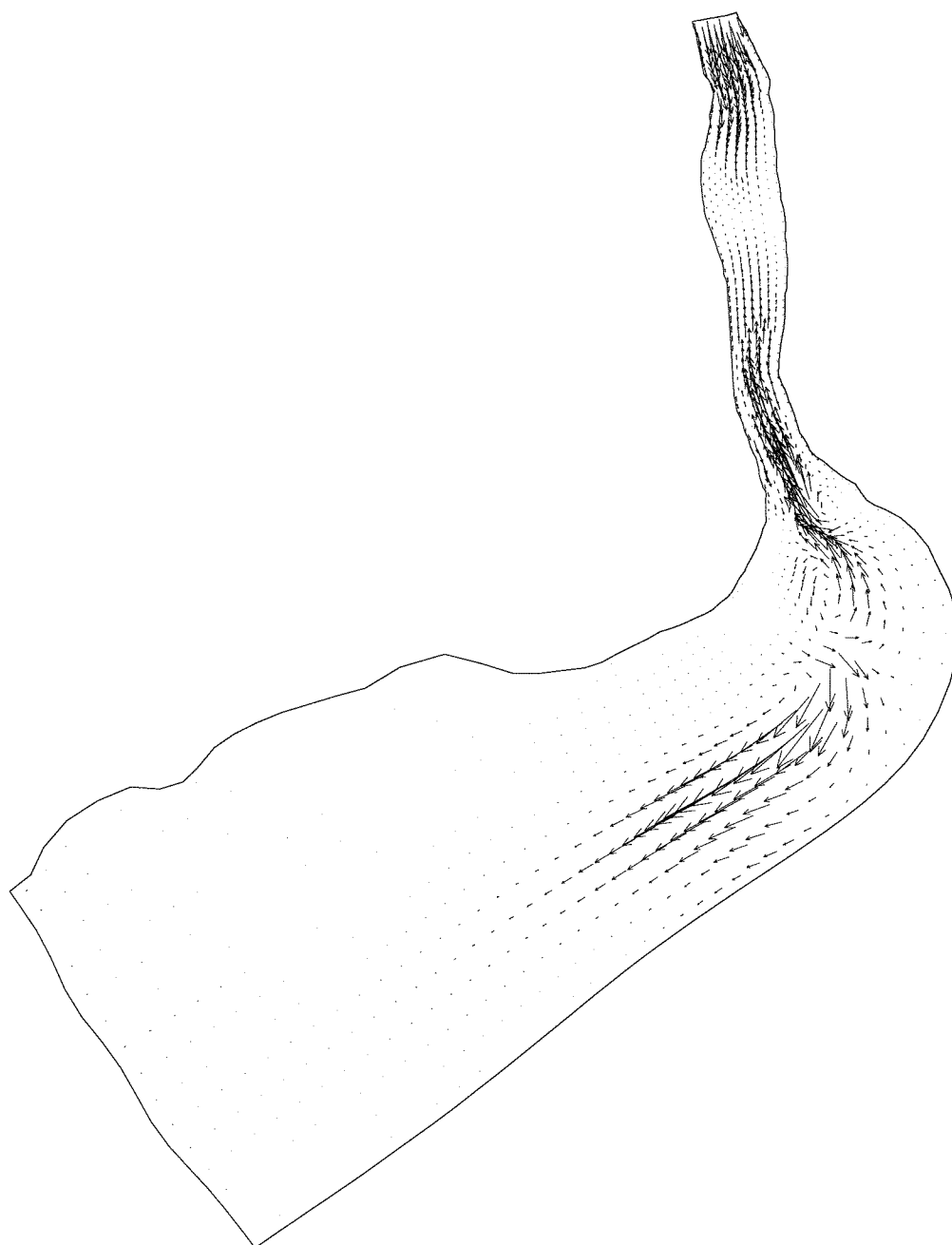
→  $5.0 \cdot 10^{-7} \text{ m/s}$

Residual bed load transport

Figure J-15

WL | DELFT HYDRAULICS





→ 0.001m/s

Residual suspended transport

Figure J-16

WL | DELFT HYDRAULICS